The Pennsylvania State University

The Graduate School

Department of Biology, Eberly College of Science

INSIGHTS FROM LONG-TERM MONITORING OF DEEP-SEA CORAL COMMUNITIES IMPACTED BY THE DEEPWATER HORIZON OIL SPILL

A Dissertation in

Biology

by

Fanny Girard

Submitted in Partial Fulfillment

of the Requirements

for the Degree of

Doctor of Philosophy

May 2018

The dissertation of Fanny Girard was reviewed and approved* by the following:

Charles R. Fisher
Professor of Biology
Distinguished Senior Scholar of Biology
Executive Director of the Millennium Scholars Program
Dissertation Advisor

Katriona Shea
Professor of Biology
Alumni Professor in the Biological Sciences
Chair of Committee

Todd C. LaJeunesse
Associate Professor of Biology

Keith Shapiro
Associate Professor of Art

Tracy Langkilde
Head of the Department of Biology

*Signatures are on file in the Graduate School

ABSTRACT

Deep-water corals form one of the most complex biological habitats in the deep sea, and house a high diversity of associated fauna. Yet, they are very vulnerable to anthropogenic impact due to their lack of mobility, exposed tissue, and generally low growth rates. In April 2010, the blowout of the Deepwater Horizon drilling platform in the northern Gulf of Mexico led to the largest oil spill in US history. The first impacted coral community was discovered three months after the well was capped. Corals there, were covered in a brown flocculent material (floc) that contained traces of oil, directly linking the observed damages to the spill. Eleven months later, two additional affected communities were discovered and, although corals were no longer covered in floc, the characteristic patchy impact distribution on the colonies, previously observed at the first site discovered, indicated that these corals had also been impacted by the spill. I quantified the impact and assessed the recovery of deep-sea corals using high-definition photographs of individual colonies. *Paramuricea* spp. colonies, well suited for visual monitoring due to their planar morphology, were imaged every year between 2011 and 2017 at five sites (three impacted and two reference sites). Images were then digitized to quantify impact and track recovery patterns. Overall recovery was slow. Although the health of lightly impacted corals improved, heavily impacted colonies showed little or no sign of recovery by 2017. The initial level of visible impact on corals had a significant effect on the improvements in the condition of individual branches between consecutive years. Furthermore, branch loss at two of the impacted sites was still significantly higher between 2016 and 2017 than at the reference sites. Even after seven years, the fate of the corals that were impacted by the Deepwater Horizon oil spill is still uncertain and the effects of the oil spill appear to be ongoing.

The high-resolution images collected between 2011 and 2014 were also used to investigate the relationship between *Paramuricea biscaya* and its ophiuroid associate *Asteroschema clavigerum*, based on the hypothesis that both species benefit from this association. Coral colonies associated with ophiuroids were on average less impacted than coral colonies that had no associates. After defining the area clearly under the influence of ophiuroids for each coral, I found that the level of visible impact to coral branches was lower in the area influenced by ophiuroids than outside that area, and that impacted branches within this area were

more likely to recover than branches outside the area of influence. These results suggest a mutualistic symbiosis between *P. biscaya* and *A. clavigerum*; Ophiuroids use corals to gain access to food particles brought by currents, and corals likely benefit through the physical action of ophiuroids removing particles deposited on polyps and perhaps inhibiting the settlement of hydroids. The beneficial role of ophiuroids was demonstrated on corals impacted by an oil spill, but these benefits could also extend to corals in environments exposed to natural sedimentation events, perhaps allowing corals to live in environments where heavy sedimentation would otherwise limit their survival.

In order to assess recovery over the long term and to plan for future monitoring, I developed an impact-dependent, state-structured matrix model. The model, parameterized using data collected as part of the long-term monitoring project, projected the dynamics of three-branch states: visibly healthy, unhealthy and hydroid-colonized. Although branch loss was implicitly included in the model, I focused on the return of extant damaged branches to a healthy state rather than on the slower re-growth of lost branches. The model estimated that, whereas most corals will recover to a visibly healthy state within a decade, the most impacted coral colonies will take up to three decades to visibly recover. Impact-related branch loss will lead to a 10% reduction in total biomass at the impacted sites by the time all coral colonies are projected to appear healthy. Given the very slow growth rates estimated for these corals, hundreds of years may be necessary for coral communities to re-grow to their original biomass.

Overall, even with the help of associated ophiuroids, the recovery of corals impacted by the oil spill is extremely slow, demonstrating the necessity to prevent impact to deep-sea corals rather than relying on restoration after the fact. Deep-sea corals are reliable indicators of anthropogenic impact in the deep sea because they are sessile, their skeleton is almost entirely covered with living tissue, making potential damage easily detectable, and natural mortality is an extremely rare event. The methods I employed allow the detection of small changes in the health of coral colonies that would not be visible with monitoring based on transects. Therefore, I suggest the establishment of photo-based coral-monitoring sites as part of protected areas to detect and limit future anthropogenic impact to vulnerable deep-sea ecosystems.

TABLE OF CONTENTS

LIST OF FIGURES

LIST OF TABLES

ACKNOWLEDGEMENTS

First, I am extremely thankful to my advisor for providing me with so many opportunities to improve my scientific skills, increase my experience, especially in the field, and grow as a scientist. Overall, I would like to thank all the members of the Fisher lab for their support. Arunima Sen, who immediately made me feel welcome and included me in her group of friends, for her friendship, her help at the beginning of my Ph.D. and her career advice. I am also grateful to Richard Dannenberg for always being so positive and for answering all my questions about graduate school when I had just arrived. I would like to thank Miles Saunders who taught me about GIS and how to use ArcMap and for his assistance anytime I had technical issues, as well as Cherisse Du Preez for our long discussions about data, career, but also personal life. Finally, I am really grateful to Sam Vohsen (even if I do not always show it!) for entertaining me, teaching me so many random facts, and for always being willing to discuss ideas and help whenever I was stuck on something. I am extremely grateful to all the undergraduate students who helped me digitize hundreds of corals; all this work would not have been possible without them. It would take too long to name all of them but I would like to give particular thanks to Bo Fu, Danielle McKean and Samantha Berlet who taught me the digitization method when I arrived and showed me how the Gulf of Mexico database was organized, as well as Taylor Boyer, Tim McElroy, Sarah Tabin, Rebecca Simpson, Tyler Harpster and Rafaelina Cruz who analyzed a significant part of the dataset used in this thesis. I would like to thank the members of my committee: Todd LaJeunesse, Keith Shapiro and, in particular Katriona Shea for guidance and insightful comments, as well as Stephen Schaeffer and Iliana Baums in the Biology Department for their advice.

I also thank the crew of the ships and deep submergence facilities for making data collection possible, as well as all the great scientists I have sailed with. In particular, I would like to thank Erik Cordes, Danielle DeLeo, Alexis Weinnig and Amanda Demopoulos for sharing their knowledge, and for their support.

During my time in State College, I have met several people who had a significant impact on my life and who, I am sure, will remain good friends in the future. In the Biology Department, I would like to especially express my gratitude to Tricia Goulding, Ana María González Angel and Monika Cechova, who all started in the program at the same time as me and were there throughout my Ph.D. adventure. I am really thankful to all of my State College friends for making my time here such a positive experience. More specifically, I would like to mention Prachi Joshi and Marcia Ortega Ramos because of their invaluable support and friendship; life here would not have been the same without them.

Finally, I thank my family and, more particularly, my parents Catherine and Philippe Girard who taught me the value of education and who always supported me.

This research was made possible by a grant from the Gulf of Mexico Research Initiative (GoMRI) as part of the Ecosystem Impacts of Oil and Gas Inputs to the Gulf (ECOGIG) consortium.

Chapter 1

Introduction

Early history of deep-sea coral research

Although the existence of deep-sea corals has been known since the mid-18th century, the extent of coral habitats around the world and their importance were not recognized until the 1970s. The first cold-water coral species, collected by dredge off Norway, was described by Carl Von Linné (Linnaeus) in 1758 (Linné & Salvius 1758) as *Madrepora pertusa* and is now known as *Lophelia pertusa*. Studies aimed at describing the Norwegian cold-water coral reefs started a decade later. These studies were conducted by the theologian and botanist Johan Ernst Gunnerus, who described the fauna commonly associated with *L. pertusa* (Gunnerus 1768), as well as other coral species including the octocoral *Gorgonia resedaeformis* (now *Primnoa resedaeformis*) (Gunnerus 1763). The number of cold-water scleractinians described significantly increased between 1848 and 1999 (Cairns 2001). Between 1848 and 1850 Henri Milne Edwards and Jules Haime re-described all known coral species, and 64 new azooxanthellate scleractinian species, more than doubling the number of species known at the time (Milne-Edwards & Haime 1857). From 1867 to 1881 scientists from the Museum of Comparative Zoology at Harvard conducted extensive dredging surveys in the deep sea, which led to the discovery and description of the first deep-sea coral species. During that time period, HMS *Lightning*, *Porcupine* and, later, *Challenger* collected thousands of deep-sea corals around the world. The number of species described significantly increased thanks to the work of Major Alfred Alcock between 1898 and 1907 based on samples collected in the Indo-Pacific region during various deep-water dredging programs (Cairns 2001). The history of octocoral taxonomy followed the same patterns as for scleractinians (Bayer 2001). The first published drawings of octocoral sclerites (*Corallium rubrum*) were published by John Ellis in 1755. Yet, sclerites were not recognized as a taxonomic characteristic until 1855 (Valenciennes 1855). As with scleractinians, the pioneering expeditions

of the nineteenth century significantly contributed to increase the number of known coral species (Bayer 2001).

Ecological importance and biology of deep-sea corals

Advances in technology, such as the development of survey sonars during the Second World War and, in the last few decades, advances in GPS technology and the use of manned research submersible and then Remotely Operated Vehicles (ROVs) and Automated Underwater Vehicles (AUVs), have revolutionized deep-sea research. These technologies not only allowed targeted sampling but also direct observations of deep-sea corals and their associates, providing essential information on the geographical distribution, ecology and biology of deep-sea corals.

At least 65% of all coral species worldwide occur in water deeper than 50 m (Cairns 2007). Deep-sea corals are found at all latitudes around the world (Roberts et al. 2006, Watling et al. 2011). They are most common between 200 and 1000 m, although many species are found at greater depths (down to 6000 m) (Grasshoff 1981, Roberts et al. 2006, Watling et al. 2011). With the exception of sea pens (Pennatulacea), corals require hard substrate to settle and grow (Wilson 1979). Additionally, deep-sea corals generally occur in areas of pronounced topographic relief where they are exposed to currents strong enough to provide them with food (particulate organic matter or zooplankton) and prevent sediment deposition (Bryan & Metaxas 2006, Roberts et al. 2009).

Whether they form reefs (e.g. scleractinians) or dense aggregations (e.g. octocorals), deep-water corals provide habitat to a variety of other species. They are thus associated with a higher diversity and abundance of megafaunal organisms than the surrounding deep-sea habitat (Jensen & Frederiksen 1992, Krieger & Wing 2002, Buhl-Mortensen & Mortensen 2005, Stone 2006, Quattrini et al. 2012). Hundreds of species live in tight association with deep-sea corals and many of these relationships have been described as symbiotic; mostly commensal or parasitic, and sometimes, mutualistic (Buhl-Mortensen 2004, Girard et al. 2016). Other organisms, including commercially valuable crustaceans and fishes, use corals as shelter, feeding grounds or nurseries (Etnoyer & Warrenchuk 2007, Mah et al. 2010, Du Preez & Tunnicliffe 2011, Baillon et al. 2012).

In general, deep-sea corals grow slowly and live a long time. Traditionally, growth rates were estimated by measuring the linear extension of scleractinian colonies growing on substrates of known age (generally man-made structures such as oil and gas platforms) (Gass & Roberts 2006). However, except for one recent study that estimated growth rates of the octocorals *Paragorgia arborea* and *Primnoa resedaeformis* from 3D models obtained via photogrammetric reconstruction (Bennecke et al. 2016), growth rates and ages of octocorals are measured by counting annual growth bands and validating these estimates with isotopic methods (commonly based on the isotopic decay of ^{14}C or ^{210}Pb) (Robinson et al. 2014). Studies using these methods have estimated extremely high longevities for several coral species, with some octocorals living for hundreds of years (Andrews et al. 2002, Prouty et al. 2014) and some black corals up to 4000 years (Roark et al. 2009). Because of their longevity, deep-sea corals have the potential to sustain stable and long-lasting high diversity habitats in the deep sea. Little is known about the reproductive biology of deep-water corals but several studies have suggested long reproductive cycles and low recruitment rates. Gamete development and oocyte maturation can take more than a year for the octocoral species *Ainigmaptilon antarcticum* (Orejas et al. 2002) and low number of recruits or high recruits mortality have been recorded for *Paragorgia arborea* and *Primnoa resedaeformis* respectively (Lacharité & Metaxas 2013). Slow recruitment rates combined with slow growth rates recorded for several coral species suggest a low recovery potential and high vulnerability of deep-sea corals to both natural and anthropogenic impacts.

Anthropogenic impacts

While recent advances in technology have contributed to significantly increase our knowledge of deep-sea coral biology, they have also facilitated anthropogenic activities in the deep ocean, increasing the possibility of impacting all vulnerable deep-sea ecosystems (Ramirez-Llodra et al. 2011). Bottom trawling, dragging a large net over the sea floor to gather commercially valuable bottom-living animals (primarily fishes), is currently the main threat to deep-water corals (Ramirez-Llodra et al. 2011). Extensive damage from bottom trawling to coral communities have been documented throughout the world (Hall-Spencer et al. 2002, Gass & Willison 2005, Clark & Koslow 2008). For instance, Fosså et al. (2002) estimated that 30 to 50% of *Lophelia pertusa* reefs off Norway had been damaged by trawling. In addition to direct

physical damage, trawling generally re-suspends sediment (Palanques et al. 2001), increasing water turbidity and potentially smothering nearby coral colonies. Although not as damaging as bottom trawling, other fishing activities, such as the use of longlines, also have the potential to impact deep-sea coral communities (Fisher et al. 2014).

In addition to being collected as bycatch, some deep-water corals have been harvested for hundreds of years to make jewelry. Most fisheries target the octocotal *Corallium*, but other corals such as black corals, bamboo corals and the zoanthid *Gerardia* are also commonly collected (Roberts et al. 2009). Studies have shown that collecting corals for jewelry could have an impact on both the size (decrease in the number of large colonies) and genetic structure (inbreeding depression) of coral populations (Baco & Shank 2005, Tsounis et al. 2006).

Impacts from fisheries have been studied for years and the consequences of fishing activities on deep-sea corals are well documented. However, the consequences of threats such as deep-sea mining, climate change and oil and gas activities are still poorly understood. Although deep-sea mining has not started yet, it has the potential to lead to significant biodiversity loss (Van Dover et al. 2017). Three types of deposit are currently of interest for mining; polymetallic nodules in abyssal plains, polymetallic sulfides on hydrothermal vents and cobalt-rich crusts on seamounts (Ecorys 2014). Mining activities, especially mining of cobalt crusts, have the potential to significantly impact coral communities, which are often abundant and diverse on seamounts.

Although the effects of climate change have been extensively studied in shallow water, little is known about its effects in the deep ocean. Yet, models project an increase in temperature as well as a decrease in pH and oxygen concentration in the deep sea (Chen et al. 2017, Schmidtko et al. 2017, Sweetman et al. 2017), all of which will likely affect coral physiology.

There is a growing concern that the expansion of oil and gas exploration activities may have significant impacts on deep-sea coral communities. The extent of these impacts is still unclear, but routine oil and gas activities can have detrimental effects. More specifically, direct physical disturbance associated with the placement of infrastructures on the sea floor, production of sediment plumes during the drilling process, and the discharge of drill cutting, drilling muds, produced water or chemicals have been shown to affect benthic communities (Cordes et al. 2016). Additionally, deep-water coral communities have the potential to be affected by accidental oil spills. Anderson et al. (2012) have estimated that large spills (more than 1000

barrels) happened on average once every 21 months on the US continental shelf between 1971 and 2010, and once every 2.5 months between 1974 and 2008 on a global scale. Moreover, the likelihood of an accidental spill increases with the depth of operations (Muehlenbachs et al. 2013). The effect of oil exposure on corals has been studied in shallow water, and has been shown to impact all coral life stages (Turner & Renegar 2017). For instance, the 1986 Panama oil spill had a negative impact on both the growth and reproduction of corals due the reallocation of energy toward tissue regeneration (Guzmán et al. 1991, Guzmán 1994). Moreover, even after 5 years, no recovery from injuries was observed at one of the impacted sites (Guzmán 1994). However, very little was known about the effect of oil spills on deep-sea corals until the 2010 Deepwater Horizon oil spill in the northern Gulf of Mexico.

Coral communities in the deep Gulf of Mexico and consequences of the Deepwater Horizon oil spill

A total of 258 deep-sea coral species have been documented in the northern Gulf of Mexico, octocorals being the most diverse. In the deep Gulf of Mexico (> 200 m) corals generally settle and grow on authigenic carbonate precipitates that formed as a by-product of the microbial alteration of hydrocarbons and anaerobic methane oxidation in areas of active seepage (Cordes et al. 2008). Hydrocarbon seeps are found throughout the continental slope of the northern Gulf of Mexico and are a result of its complex geology (Fisher et al. 2007). Areas of active seepage are initially dominated by microbial mats and chemosynthetic clams or mussels. As carbonates precipitate, seepage generally slows down, allowing the settlement of vestimentiferan tubeworms, and later, of deep-sea corals (Fisher et al. 2007). Because of its massive hydrocarbon reserves, the Gulf of Mexico is one of the most active regions in the world for the oil and gas industry, and reserves deeper than 3000 m are being exploited (Cordes et al. 2016).

On 20 April 2010, the blowout of the Deepwater Horizon oil platform in lease block Mississippi Canyon (MC) 252, 65 km off the Louisiana coast, lead to the largest oil spill in recorded history. Approximately 4.9 million barrels (780 million liters) of crude oil were released at a depth of 1500 m during the 87 days before the Macondo well was capped on 15 July 2010 (McNutt et al. 2011). As a response to the spill seven million liters of dispersant were

used; the majority was released from airplanes at the surface, but three million liters were directly injected at the well on the sea floor. During and following the discharge, a large deep-water oil plume formed and persisted for months centered at an approximate depth of 1100 m (Camilli et al. 2010). Moreover, about half of the oil reached the surface and contributed to a large marine snow formation event (Passow et al. 2012, Passow 2014). The presence of large marine snow floating in the vicinity of oil layers was documented in May 2010 (Passow et al. 2012). All the marine snow had vanished a month later, suggesting a rapid sedimentation to the deep sea (Passow 2014).

The first impacted coral community was discovered in November 2010 during a Natural Resource Damage Assessment (NRDA) expedition that was investigating potential damage to deep-sea corals (White et al. 2012a). This community was located in MC 294, 13 km from the Macondo well at a depth of 1370 m, and was dominated by the octocoral *Paramuricea biscaya* (although a few other species such as a *Paragorgia regalis* colony and three *Swiftia* spp. colonies also showed signs of impact) (White et al. 2012a). Corals at this site were covered in a brown flocculent material ("floc") that contained traces of oil from the Macondo well and dioctyl sodium sulfosuccinate, a surfactant present in the dispersant corexit used during the spill (White et al. 2012a, White et al. 2014). Two additional coral communities dominated by *P. biscaya* were discovered almost a year later in October 2011 (Fisher et al. 2014). These two communities were in lease blocks MC 297 and MC 344, 6 and 22 km from the spill at depths of 1560 and 1850 m, respectively. Corals at these sites were not covered in floc at that time, but displayed the characteristic patchy hydroid colonization and damage pattern that was observed at MC 294 at this point in time (after the floc had dispersed).

Because *P. biscaya* has a planar morphology and all branches can be seen in the same two-dimensional image, it is an excellent candidate for image analysis. Therefore, an image-based, long-term monitoring study was initiated in 2010 in order to assess the recovery of corals that were impacted by the Deepwater Horizon oil spill. Early results showed that the median level of impact at MC 294 decreased between 2010 and 2012 (mostly due to the floc falling off coral branches) but that corals that were impacted to over 20% of the colony still displayed significant injury in 2012 (Hsing et al. 2013). Colonization of damaged branches by hydroids was observed for the first time in 2011 and was still expanding on some colonies in 2012. This

study found that the recovery of individual branches from damage and hydroid colonization was negatively correlated with the initial level of impact (Hsing et al. 2013).

In this thesis, data collected between 2011 and 2017 as part of the monitoring project that started after the Deepwater Horizon oil spill are used to evaluate the long-term impact of the spill on deep-sea coral communities. The main goals are to show the value of repetitive high-resolution imagery (a non-destructive method) to 1) assess the long-term impact of the spill on corals (Chapter 2), 2) characterize the relationship between corals and their associates as well as the role played by associates in coral recovery (Chapter 3), 3) parameterize a population model in order to estimate the time necessary for the recovery of impacted coral communities and optimize monitoring strategies (Chapter 4), and 4) collect baseline data on the biology of deep-sea corals and establish long-term monitoring stations to detect future anthropogenic impact to deep-sea communities.

References

Anderson CM, Mayes M, LaBelle RP (2012) Oil Spill Occurrence Rates for Offshore Spills. Bureau of Ocean Energy Management, Herndon, V A

Andrews AH, Cordes EE, Mahoney MM, Munk K, Coale KH, Cailliet GM, Heifetz J (2002) Age, growth and radiometric age validation of a deep-sea, habitat-forming gorgonian (*Primnoa resedaeformis*) from the Gulf of Alaska. Hydrobiologia 471:101-110

Baco AR, Shank TM (2005) Population genetic structure of the Hawaiian precious coral *Corallium lauuense* (Octocorallia: Coralliidae) using microsatellites. In: Freiwald A, Roberts JM (eds) Cold-Water Corals and Ecosystems. Springer Berlin Heidelberg, Berlin, Heidelberg

Baillon S, Hamel J-F, Wareham VE, Mercier A (2012) Deep cold-water corals as nurseries for fish larvae. Frontiers in Ecology and the Environment 10:351-356

Bayer FM (2001) Octocoral research-past, present and future. Atoll research bulletin 494:81

Bennecke S, Kwasnitschka T, Metaxas A, Dullo W-C (2016) In situ growth rates of deep-water octocorals determined from 3D photogrammetric reconstructions. Coral Reefs:1-13

Bryan TL, Metaxas A (2006) Distribution of deep-water corals along the North American continental margins: Relationships with environmental factors. Deep Sea Research Part I: Oceanographic Research Papers 53:1865-1879

Buhl-Mortensen L (2004) Symbiosis in Deep-Water Corals. Symbiosis 37:33-61

Buhl-Mortensen L, Mortensen PB (2005) Distribution and diversity of species associated with deep-sea gorgonian corals off Atlantic Canada. In: Freiwald A, Roberts JM (eds) Cold-Water Corals and Ecosystems, Berlin

Cairns SD (2001) A Brief History of Taxonomic Research on Azooxanthellate Scleractinia (Cnidaria: Anthozoa). Bulletin of the Biological Society of Washington 10:191-203

Cairns SD (2007) Deep-water corals: an overview with special reference to diversity and distribution of deep-water scleractinian corals. Bulletin of Marine Science 81:311-322

Camilli R, Reddy CM, Yoerger DR, Van Mooy BAS, Jakuba MV, Kinsey JC, McIntyre CP, Sylva SP, Maloney JV (2010) Tracking Hydrocarbon Plume Transport and Biodegradation at Deepwater Horizon. Science 330:201-204

Chen C-TA, Lui H-K, Hsieh C-H, Yanagi T, Kosugi N, Ishii M, Gong G-C (2017) Deep oceans may acidify faster than anticipated due to global warming. Nature Climate Change 7:890-894

Clark MR, Koslow JA (2008) Impacts of fisheries on seamounts. In: Pitcher TJ, Morato T, Hart PJB, Clark MR, Haggan N, Santos RS (eds) Seamounts: Ecology, Fisheries & Conservation. John Wiley & Sons, Oxford

Cordes EE, Jones DOB, Schlacher TA, Amon DJ, Bernardino AF, Brooke S, Carney R, DeLeo DM, Dunlop KM, Escobar-Briones EG, Gates AR, Génio L, Gobin J, Henry L-A, Herrera S, Hoyt S, Joye M, Kark S, Mestre NC, Metaxas A, Pfeifer S, Sink K, Sweetman AK, Witte U (2016) Environmental Impacts of the Deep-Water Oil and Gas Industry: A Review to Guide Management Strategies. Frontiers in Environmental Science 4

Cordes EE, McGinley MP, Podowski EL, Becker EL, Lessard-Pilon S, Viada ST, Fisher CR (2008) Coral communities of the deep Gulf of Mexico. Deep Sea Research Part I: Oceanographic Research Papers 55:777-787

Du Preez C, Tunnicliffe V (2011) Shortspine thornyhead and rockfish (Scorpaenidae) distribution in response to substratum, biogenic structures and trawling. Marine Ecology Progress Series 425:217-231

Ecorys (2014) Study to investigate state of knowledge of Deep Sea Mining. Interim report under FWC MARE/2012/06 - SC E1/2013/04

Etnoyer P, Warrenchuk J (2007) A catshark nursery in a deep gorgonian field in the Mississippi Canyon, Gulf of Mexico. Bulletin of Marine Science 81:553-559

Fisher C, Roberts H, Cordes E, Bernard B (2007) Cold Seeps and Associated Communities of the Gulf of Mexico. Oceanography 20:118-129

Fisher CR, Hsing P-Y, Kaiser CL, Yoerger DR, Roberts HH, Shedd WW, Cordes EE, Shank TM, Berlet SP, Saunders MG, Larcom EA, Brooks JM (2014) Footprint of *Deepwater Horizon* blowout impact to deep-water coral communities. Proceedings of the National Academy of Sciences 111:11744-11749

Fosså JH, Mortensen PB, Furevik DM (2002) The deep-water coral *Lophelia pertusa* in Norwegian waters: distribution and fishery impacts. Hydrobiologia 471:1-12

Gass SE, Roberts JM (2006) The occurrence of the cold-water coral *Lophelia pertusa* (Scleractinia) on oil and gas platforms in the North Sea: Colony growth, recruitment and environmental controls on distribution. Marine Pollution Bulletin 52:549-559

Gass SE, Willison JHM (2005) An assessment of the distribution of deep-sea corals in Atlantic Canada by using both scientific and local forms of knowledge. In: Freiwald A, Roberts JM (eds), Berlin

Girard F, Fu B, Fisher CR (2016) Mutualistic symbiosis with ophiuroids limited the impact of the Deepwater Horizon oil spill on deep-sea octocorals. Marine Ecology Progress Series 549:89-98

Grasshoff M (1981) Die Gorgonaria, Pennatularia und Antipatharia des Tiefwassers der Biskaya (Cnidaria, Anthozoa). Ergebnisse der franzosischen Expeditionen Biogas, Polygas, Géomanche, Incal, Noratlante und Fahrten der Thalassa 1. Allgemeiner Teil. Bulletin du Museum National d'Histoire Naturelle 4:732-766

Gunnerus JE (1763) Om en søevext, allevegne ligesom besat med frøehuuse, Gorgonia resedæformis. Det Kongelige Norske Videnskabers Selskabs Skrifter, Book 2

Gunnerus JE (1768) Om nogle Norske Coraller. Det Kongelige Norske Videnskabers Selskabs Skrifter, Book 4

Guzmán HM (1994) Injury, regeneration and growth of Caribbean reef corals after a major oil spill in Panama. Marine ecology Progress series (Halstenbek) 105:231

Guzmán HM, Jackson JBC, Weil E (1991) Short-term ecological consequences of a major oil spill on Panamanian subtidal reef corals. Coral Reefs 10:1-12

Hall-Spencer J, Allain V, Fosså JH (2002) Trawling damage to Northeast Atlantic ancient coral reefs. Proceedings of The Royal Society B 269:507-511

Hsing P-Y, Fu B, Larcom Ea, Berlet SP, Shank TM, Govindarajan AF, Lukasiewicz AJ, Dixon PM, Fisher CR (2013) Evidence of lasting impact of the Deepwater Horizon oil spill on a deep Gulf of Mexico coral community. Elementa: Science of the Anthropocene 1:000012

Jensen A, Frederiksen R (1992) The fauna associated with the bank-forming deepwater coral *Lophelia pertusa* (Scleractinaria) on the Faroe shelf. Sarsia 77:53-69

Krieger KJ, Wing BL (2002) Megafauna associations with deepwater corals (*Primnoa* spp.) in the Gulf of Alaska. Hydrobiologia 471:83-90

Lacharité M, Metaxas A (2013) Early life history of deep-water gorgonian corals may limit their abundance. PloS one 8:1-10

Linné Cv, Salvius L (1758) Systema Naturae per regna tria naturae, secundum classes, ordines, genera, species, cum characteribus, differentiis, synonymis, locis, Vol v.1. Impensis Direct. Laurentii Salvii, Holmiae

Mah C, Nizinski M, Lundsten L (2010) Phylogenetic revision of the Hippasterinae (Goniasteridae; Asteroidea): systematics of deep sea corallivores, including one new genus and three new species. Zoological Journal of the Linnean Society 160:266-301

McNutt M, Camilli R, Guthrie G, Hsieh P, Labson V, Lehr B, Maclay D, Ratzel A, Sogge MK (2011) Assessment of Flow Rate Estimates for the Deepwater Horizon / Macondo Well Oil Spill. Washington DC, United States

Milne-Edwards H, Haime J (1857) Histoire naturelle des coralliaires, ou polypes proprement dits, Vol 1857-60. Roret, Paris

Muehlenbachs L, Cohen MA, Gerarden T (2013) The impact of water depth on safety and environmental performance in offshore oil and gas production. Energy Policy 55:699-705

Orejas C, López-González PJ, Gili NT, J. M. , Gutt J, Arntz WE (2002) Distribution and reproductive ecology of the Antarctic octocoral *Ainigmaptilon antarcticum* in the Weddell Sea. Marine Ecology Progress Series 231:101-114

Palanques A, Guillén J, Puig P (2001) Impact of bottom trawling on water turbidity and muddy sediment of an unfished continental shelf. Limnology and Oceanography 46:1100-1110

Passow U (2014) Formation of rapidly-sinking, oil-associated marine snow. Deep Sea Research Part II: Topical Studies in Oceanography 129:232-240

Passow U, Ziervogel K, Asper V, Diercks a (2012) Marine snow formation in the aftermath of the Deepwater Horizon oil spill in the Gulf of Mexico. Environmental Research Letters 7:035301-035301

Prouty NG, Fisher CR, Demopoulos AWJ, Druffel ERM (2014) Growth rates and ages of deep-sea corals impacted by the Deepwater Horizon oil spill. Deep Sea Research Part II: Topical Studies in Oceanography 129:196-212

Quattrini AM, Ross SW, Carlson MCT, Nizinski MS (2012) Megafaunal-habitat associations at a deep-sea coral mound off North Carolina, USA. Marine Biology 159:1079-1094

Ramirez-Llodra E, Tyler PA, Baker MC, Bergstad OA, Clark MR, Escobar E, Levin LA, Menot L, Rowden AA, Smith CR, van Dover CL (2011) Man and the last great wilderness: Human impact on the deep sea. PLoS ONE 6:e22588

Roark EB, Guilderson TP, Dunbar RB, Fallon SJ, Mucciarone Da (2009) Extreme longevity in proteinaceous deep-sea corals. Proceedings of the National Academy of Sciences 106:5204-5208

Roberts JM, Wheeler AJ, Freiwald A (2006) Reefs of the deep: the biology and geology of cold-water coral ecosystems. Science 312:543-547

Roberts JM, Wheeler AJ, Freiwald A, Cairns SD (2009) Cold-Water Corals: The Biology and Geology of Deep-Sea Coral Habitats. Cambridge University Press, Cambridge

Robinson LF, Adkins JF, Frank N, Gagnon AC, Prouty NG, Brendan Roark E, de Flierdt Tv (2014) The geochemistry of deep-sea coral skeletons: A review of vital effects and applications for palaeoceanography. Deep Sea Research Part II: Topical Studies in Oceanography 99:184-198

Schmidtko S, Stramma L, Visbeck M (2017) Decline in global oceanic oxygen content during the past five decades. Nature 542:335

Stone RP (2006) Coral habitat in the Aleutian Islands of Alaska: depth distribution, fine-scale species associations, and fisheries interactions. Coral Reefs 25:229-238

Sweetman AK, Thurber AR, Smith CR, Levin LA, Mora C, Wei C-L, Gooday AJ, Jones DOB, Rex M, Yasuhara M, Ingels J, Ruhl HA, Frieder CA, Danovaro R, Würzberg L, Baco A, Grupe BM, Pasulka A, Meyer KS, Dunlop KM, Henry L-A, Roberts JM (2017) Major

impacts of climate change on deep-sea benthic ecosystems. Elementa: Science of the Anthropocene 5:4

Tsounis G, Rossi S, Gili J-M, Arntz W (2006) Population structure of an exploited benthic cnidarian: the case study of red coral (*Corallium rubrum* L.). Marine Biology 149:1059-1070

Turner NR, Renegar DA (2017) Petroleum hydrocarbon toxicity to corals: A review. Marine Pollution Bulletin

Valenciennes A (1855) Extrait d'une Monographie de la famille des Gorgonodées de la classe des polypes. Les Comptes Rendus de l'Académie des Sciences 41:7-15

Van Dover CL, Ardron JA, Escobar E, Gianni M, Gjerde KM, Jaeckel A, Jones DOB, Levin LA, Niner HJ, Pendleton L, Smith CR, Thiele T, Turner PJ, Watling L, Weaver PPE (2017) Biodiversity loss from deep-sea mining. Nature Geosci 10:464-465

Watling L, France SC, Pante E, Simpson A (2011) Biology of deep-water octocorals. In: Lesser M (ed) Advances in Marine Biology, Book 60

White HK, Hsing PY, Cho W, Shank TM, Cordes EE, Quattrini AM, Nelson RK, Camilli R, Demopoulos AW, German CR, Brooks JM, Roberts HH, Shedd W, Reddy CM, Fisher CR (2012a) Impact of the *Deepwater Horizon* oil spill on a deep-water coral community in the Gulf of Mexico. Proceedings of the National Academy of Sciences 109:20303-20308

White HK, Lyons SL, Harrison SJ, Findley DM, Liu Y, Kujawinski EB (2014) Long-Term Persistence of Dispersants following the Deepwater Horizon Oil Spill. Environmental Science & Technology Letters 1:295-299

Wilson JB (1979) 'Patch' development of the deep-water coral *Lophelia Pertusa* (L.) on Rockall Bank. Journal of the Marine Biological Association of the United Kingdom 59:165-177

Chapter 2

Long-term impact of the Deepwater Horizon oil spill on deep-sea corals detected after seven years of monitoring

Fanny Girard, Charles R. Fisher

Department of Biology, The Pennsylvania State University, 208 Mueller Laboratory, University Park, Pennsylvania 16802, USA

In review

Abstract

Cold-water corals form high biodiversity habitats in the deep sea. They are generally long-lived, slow-growing, and thus particularly vulnerable to anthropogenic impact. We used high-definition imagery to quantify the impact and assess the recovery of deep-sea corals that were affected by the 2010 Deepwater Horizon oil spill in the Gulf of Mexico. Over three hundred *Paramuricea spp.* colonies were imaged yearly between 2011 and 2017 at five sites, and the images were digitized to quantify health, hydroid overgrowth, identify branch loss, and track recovery patterns. Although the median level of impact decreased after 2011 at all impacted sites, it has been stable since then and remained higher than at the reference sites. Recovery depended on the initial level of impact to the colonies, which negatively affected the ability of individual branches to recover or remain healthy. The effect of initial impact on recovery between consecutive years was still visible seven years after the spill, indicating a long-term, non-acute, impact on the colonies. Impacted corals were also more likely to lose branches, and branch loss was still significantly higher at some of the impacted sites between 2016 and 2017, indicating an ongoing effect of the spill, which may eventually lead to delayed mortality. The methodology we employed allows us to successfully detect small changes in the health of corals. We suggest the establishment of image-based coral-monitoring sites to collect baseline data on coral biology, assess the efficacy of Marine Protected Areas, and detect future anthropogenic impact to these vulnerable deep-sea ecosystems.

Introduction

Cold-water corals are widespread around the world and can be found over a wide range of latitudes and depths (Watling et al. 2011). A large number of mobile animals, including commercially valuable species, use corals as feeding grounds, refuges from predators, or nurseries (Krieger & Wing 2002, Etnoyer & Warrenchuk 2007, Du Preez & Tunnicliffe 2011, Baillon et al. 2012). As a result, whether they form reefs or occur in dense assemblages, deep-sea coral communities contribute to the formation of high biodiversity habitats (Jensen & Frederiksen 1992, Buhl-Mortensen & Mortensen 2005, Buhl-Mortensen et al. 2010). Additionally, deep-water coral communities have been characterized as hotspots of carbon cycling in the deep ocean (Oevelen et al. 2009, Cathalot et al. 2015) and appear to play a role in nitrogen cycling as well (Middelburg et al. 2015).

As it is often the case with deep-sea fauna, most cold-water corals are long-lived. Based on isotope studies, several octocoral species can live for hundreds of years and a colony of the black coral *Leipathes* sp. was determined to be over 4000 years old (Andrews et al. 2002, Roark et al. 2009, Prouty et al. 2014). In association with this longevity, deep-sea corals generally have low metabolic and growth rates, making them more vulnerable to impact and slow to recover (Cordes et al. 2001, Andrews et al. 2002, Risk et al. 2002).

Deep-sea corals are facing a number of threats from human activities. Fishing, and bottom trawling in particular, have been shown to inflict considerable damage on deep-sea coral communities (Koslow et al. 2001, Fosså et al. 2002, Hall-Spencer et al. 2002, Clark & Koslow 2008). There is a growing concern that the potential for mining cobalt-rich crusts on seamounts, as well as offshore oil and gas extraction could also have a significant impact on deep-sea coral communities. Although less well documented, the direct physical disturbance and sediment plumes produced by these activities could be as detrimental as trawling (Van Dover 2007, Clark et al. 2010, Cordes et al. 2016).

The oil and gas industry is particularly active in the northern Gulf of Mexico, where reserves at depths over 3000 m are being extracted (Cordes et al. 2016). Deep-sea corals are abundant and diverse in the northern Gulf of Mexico with 258 species documented, including 132 species of octocorals (Etnoyer & Cairns 2016). Although the deep sea floor in the Gulf of Mexico consists mostly of fine-grained sediment, exposed carbonate hardgrounds that form as a

byproduct of microbial activity at seeps can provide the hard substrate necessary for the attachment of deep-water corals (Fisher et al. 2007).

The 2010 Deepwater Horizon blowout in the northern Gulf of Mexico led to the release of approximately 4.9 million barrels (780 million liters) of crude oil at a depth of 1500 m over an 87-day period (McNutt et al. 2011). In addition, a total of 7 million liters of dispersant were applied at the surface or at the wellhead on the sea floor. Due to both the use of dispersant and the physics of the release, much of the oil remained at depth, forming a deep-water plume that persisted for months (Camilli et al. 2010). The oil that did reach the surface contributed to a large marine snow formation event, which may have also been affected by the presence of dispersant (Passow et al. 2012, Passow 2014, Passow et al. 2017). Both the deep-water plume and sinking of oil-contaminated marine snow had the potential to affect vulnerable deep-sea communities.

Three months after the well was capped, an impacted coral community was discovered 13 km away from the Macondo well in the US Bureau of Ocean Energy Management (BOEM) lease block Mississippi Canyon (MC) 294 at a depth of 1370 m. At this time, the majority of coral colonies at this site were covered, at least in part, by a brown flocculent material (floc) that contained traces of oil from the Macondo well, as a well as dioctyl sodium sulfosuccinate, a surfactant contained in the dispersant deployed during the spill (White et al. 2012a, White et al. 2014). This suggests that the corals at this site were exposed to both oil and dispersant. Toxicity experiments conducted on deep-sea and mesophotic octocorals from the northern Gulf of Mexico showed that these corals were particularly vulnerable to mixtures of oil and dispersant (DeLeo et al. 2015, Frometa et al. 2017).

Two additional impacted sites were documented in October 2011 in lease blocks MC 297 and MC 344, 6 and 22 km away from the spill site (Fisher et al. 2014b). By this time, the corals at these two sites were no longer covered in floc, but did display a characteristic patchy covering of hydroids on exposed skeleton that was also observed at MC 294 at this point in time. The level of visible impact at MC 297 (1560 m depth) was comparable to MC 294, while it was less severe at MC 344 (1850 m depth) at this point in time. All three coral communities were dominated by the octocoral species *Paramuricea biscaya* (Grasshoff, 1977) (Fisher et al. 2014b).

A monitoring study was initiated in 2010 at MC 294 and in 2011 at MC 297 and MC 344 to assess the recovery of corals that were impacted by the spill. A temporal study following impacted corals at MC 294 between 2010 and 2012 showed that, even though the median level

of impact decreased during that period, corals that were impacted over 20% or more of their colony still showed signs of injury in 2012 (Hsing et al. 2013). Recovery from impact was negatively correlated to the initial level of impact in 2010, and hydroid overgrowth, which started in 2011, was still expanding on some colonies. Another study found that coral recovery was also affected by the presence of the brittle star *Asteroschema clavigerum* commonly associated with *Paramuricea biscaya* (Girard et al. 2016 - Chapter 3). Corals associated with ophuroids were on average less impacted than corals without associates and branches in the vicinity of ophiuroids were more likely to recover from impact and hydroid colonization.

Here we used data collected from 2011 to 2017 at the three impacted sites to characterize the long-term effect of the Deepwater Horizon oil spill on deep-sea corals.

Materials and methods

Study sites

Individual coral colonies were imaged every year from 2011 to 2017 at three impacted sites (MC 294, MC 297 and MC 344). Two reference sites (Atwater Valley (AT) 357 and Green Canyon (GC) 852 located 183 and 325 km away from the Macondo well, respectively), where there was no visual evidence of recent impact, were also monitored at points during this time period. One of the reference sites, AT 357 (1050 m depth), was shallower than the impacted sites and dominated by a different *Paramuricea* species, *Paramuricea* sp. B3. For logistical reasons, AT 357 was monitored from 2011 to 2016 but not in 2017. The other reference site, GC 852 (1400 m depth), was dominated by *Paramuricea biscaya*, the species that was the most impacted by the oil spill. Corals at this site were monitored for the first time in 2016, and again in 2017. Although data were available at MC 294 prior to 2011, we chose 2011 as the baseline for this study for two reasons. The first was that 2011 was the first complete, high-quality, image dataset collected at all impacted sites and the AT 357 reference site. The second was that much of the impact detected in 2010 at MC 294 consisted of branches covered with floc, many of which were not visibly impacted when next imaged in 2011. Plexaurid corals, such as *P. biscaya* and *P.* sp. B3, have a planar morphology and thus make excellent candidates for image analysis, as all branches are generally visible in the same image.

Monitoring and image analysis

A total of 326 coral colonies were monitored between 2011 and 2017 (49 at MC 294, 56 at MC 297, 61 at MC 344, 100 at AT 357 and 60 at GC 852). Coral colonies were imaged every year with a digital still camera using the same headings and camera settings. Images taken in 2011 (or the year a colony was discovered if it was after 2011) were digitized using Inkscape 0.48.5 (The Inkscape Team 2011), and branches coded based on four categories: healthy, unhealthy (covered in floc, excess mucous or exposed skeleton), colonized by hydroids, and unclassified (branch obscured or image quality not sufficient to determine the condition of the branch) (Fig. 2-1A&H). Branches were coded conservatively; whenever it was not clear whether a branch was unhealthy it was coded as healthy, and when the presence of hydroids was not obvious the branch was coded as unhealthy. To determine the condition of coral colonies after 2011, we used the 2011 image as a template, and re-coded branches every year based on their new state. Two colonies at MC 297 were partially colonized by a stoloniferan species. However, colonization by stoloniferans was not added as a category and these colonies were excluded from the analyses due to the small sample size. To track changes in coral condition over time, the 2011 images were used as templates, and branches were re-coded every year based on their new state (Fig. 2-1B to N). After 2011, a new coding category was added to follow branches that were lost between consecutive years. The proportion of branches in each category was measured every year, and changes in the state of individual branches were followed to estimate the proportion of branches that transitioned from one category to another as well as the number of branches that broke off between each consecutive year. Each coral colony was digitized independently by two observers. After ensuring that there was no significant difference between observers using the Student's t-test, the arithmetic mean of the digitized values was calculated and used for all analyses. In the case of branch loss, the images digitized by both observers were compared and the number of branches that broke was estimated once a consensus was reached.

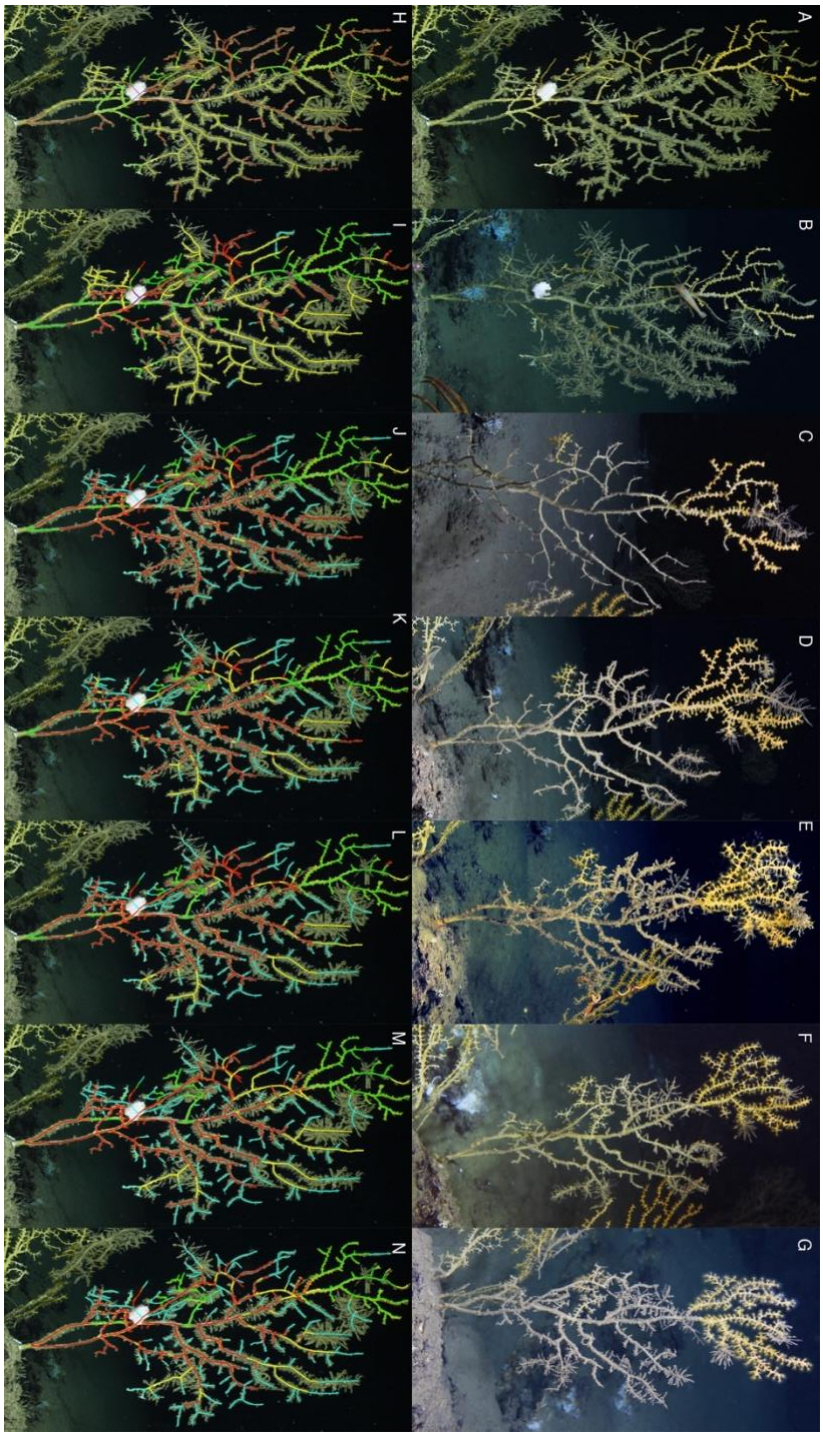

Figure 2-1. Changes in an impacted coral colony at MC 294 between 2011 and 2017. The 2011 image (A) was digitized (H) and branches coded as healthy (green), unhealthy (red), colonized by hydroids (yellow) or unclassified (purple). To quantify changes over time, branches were re-coded based on their new condition in 2012 (B, I), 2013 (C, J), 2014 (D, K), 2015 (E, L), 2016 (F, M), and 2017 (G, N). A new category was added after 2011 to account for branches that broke between consecutive years (blue).

The total number of internodes in 2011 (segment that separates two branches) on each coral colony was quantified using the Cell Counter tool in ImageJ 1.48. This number was adjusted each following year by subtracting the number of branches that fell off. The number of internodes per colony was used as a proxy for the number of branches.

Coral colonies were excluded from the analyses when the image quality was not sufficient to distinguish between different branch states or when the colony was sampled as part of other research projects.

Recovery and effect of the initial level of total visible impact on changes in the state of individual branches

The median level of total visible impact was calculated two ways for each year; the sum of unhealthy and hydroid-colonized branches, including lost branches and not including lost branches. The difference in the proportion of visibly impacted branches between the impacted and reference sites was tested for each year with Generalized Linear Models (GLMs). The effect of site on the ratio between the number of visibly impacted branches and total number of branches was tested using a binomial error distribution with a logit link function. When overdispersion was detected (the residual deviance is greater than the residual degree of freedom, indicating that the variability in the data is larger than the variability expected under the assumed binomial distribution) a quasibinomial, instead of a binomial family, was used in the model.

The correlation between the initial level of total visible impact in 2011 and the total visible impact (sum of unhealthy, hydroid-colonized and lost branches) in 2017 was tested using Spearman's rank correlation.

Changes in the state of individual branches were quantified between every consecutive year. GLMs were used to test the effect of the initial total visible impact proportion (2011) on the proportion of healthy branches that remained healthy, the proportion of unhealthy branches that recovered to a healthy state and the proportion of branches colonized by hydroids that became healthy between each consecutive year. These transitions were treated as binomial or quasibinomial (if overdispersion was detected) responses and were modeled using proportion data (counts of branches that did or did not stay/become healthy) using a logit link function. The relevant subset of the data was used for each model (for instance, only healthy branches were used when modeling the transition from healthy to healthy).

Total branch loss

The number of breaking events (number of times a portion of the colony disappeared between years) was measured for each coral colony. In order to quantify changes in branch loss over time, the ratio between the total number of breakpoints per month (the number of months separating data collection varied from one year to another) and the combined total number of

branches of all corals was calculated between each consecutive year at each site. Every year, the difference between the number of breaking events at the reference and impacted sites was tested using GLMs. The effect of site on the ratio between the number of breaking events and total number of branches was tested using a binomial or quasibinomial (if overdispersion was detected) error distribution. To assess changes in branch loss over time, the differences in branch loss between different pairs of consecutive year were tested with the pairwise Wilcoxon Signed Rank test. A Bonferroni correction was applied to account for multiple comparisons.

State of lost branches

Breakpoints were sorted depending on whether breakage occurred in healthy, unhealthy or hydroid-colonized areas of the colonies. At each site, the null hypothesis that breakage was random was tested with Fisher's exact test, and expected values under that hypothesis were estimated based on the total number of branches in each category (healthy, unhealthy or hydroid-colonized) observed in 2011. The proportions of breaking events in unhealthy and hydroid-colonized areas of the colonies were compared with a two-proportion z-test. Additionally, the number of breaking events that occurred in unhealthy parts that were previously colonized by hydroids was recorded.

The effect of the initial total visible impact proportion (2011) on the proportion of both all branches (ratio between the number of breakpoints and combined total number of branches) and healthy branches (ratio between the number of breakpoints in healthy areas of the colonies and combined total number of healthy branches) that broke between 2011 and 2017 was tested with GLMs. GLMs were fitted with a logit link function using a binomial or quasibinomial (if overdispersion was detected) error structure (branches either did or did not break).

Rank of lost branches

For each colony, branches were classified using the branch ordering system developed by Brazeau and Lasker (1988). In this system, distal branches are considered first order branches. When two first order branches join, a second order branch arises. Similarly, when two second order branches join, a third order branch arises, and so on. Higher order branches only arise when branches of equal lower order join. As a result of this ordering system, branches with similar functional aspects will have the same rank. Each branch was assigned a rank based on the 2011 images, and the proportion of branches that broke in each rank was followed over time. Temporal changes in the proportion of branches of each rank that broke between every

consecutive year were tested at each site using GLMs. The effect of year on the proportion of branches that broke in each rank was tested for each contrast (first vs second order, first vs third order and second vs third order) with a logit link function using a binomial or quasibinomial (in case of overdispersion) error distribution. Only three levels were considered, as no branches with a rank higher that three broke during the study period.

All statistical analyses were performed in R (R Core Team 2014).

Results

Changes in total visible impact between 2011 and 2017

No obvious signs of impact were detected at any time at either reference site; between 2011 and 2016 at AT 357 or in 2016 or 2017 at GC 852. The median level of background "total visible impact" varied between 0 and 0.67% in different years at AT 357 and was equal to 0.15% in both 2016 and 2017 at GC 852. While some coral colonies at these sites had a few unhealthy branches, these were generally at the bottom edge of the colony in close proximity to the sediment. Hydroid colonization was rare at the reference sites (the median proportion of branches colonized by hydroids was always 0 and the maximum observed average in a year was 0.4%).

Overall, the range of impact to individual corals at MC 294 and MC 344 was wider than that at MC 297 (Fig. 2-2A). The median level of total visible impact in 2011 was higher at MC 294 (14 %) and MC 297 (13%) than at MC 344 (5 %) (Fig. 2-2A). Although the median level of total visible impact decreased after 2011 and has been stable ever since (between 4 and 6 % at MC 294, 6 and 7 % at MC 297, and 3 and 4 % at MC 344), the level of total visible impact remained higher than at the reference sites every year (GLM: branch loss included: the total visible impact proportion was significantly higher than at the reference sites every year except for 2011 at MC 344, 2015 at MC 297 and 2016 at MC 297 and MC 344; Table A), even when branch loss was not included in the total visible impact calculation (GLM: branch loss excluded: the total visible impact proportion was significantly higher than at the reference sites every year except for 2011 at MC 344 and 2016 at MC 297; Table B).

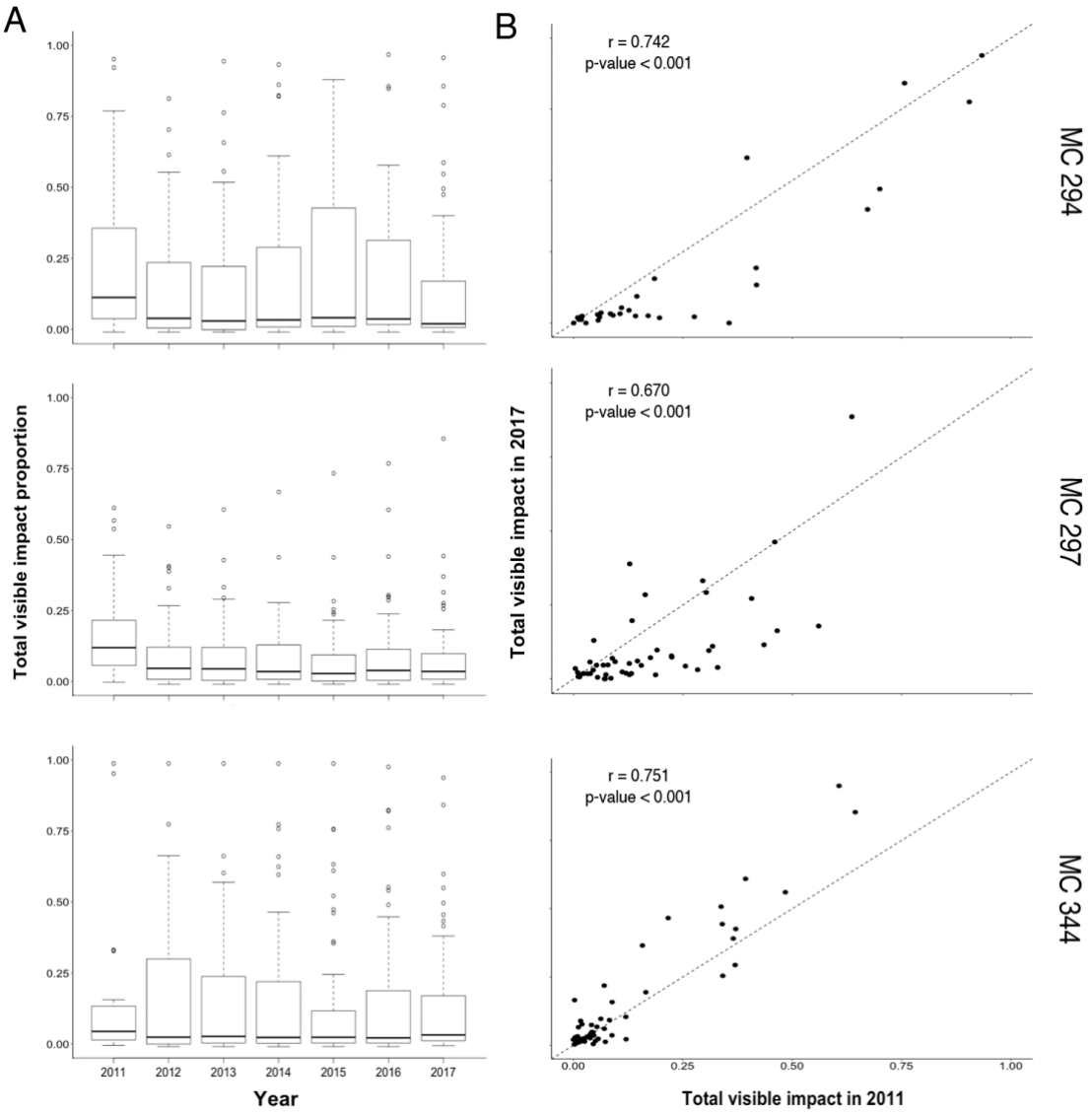

Figure 2-2. Changes in total visible impact over time at the three impacted sites: MC 294, MC 297 and MC 344. (A) Boxplot representing changes in the median level of total visible impact (branch loss included) between 2011 and 2017 and (B) Total visible impact in 2017 as a function of total visible impact in 2011. The dotted line represents the 1:1 line separating corals that recovered from corals whose health deteriorated. The Spearman's correlation coefficients and their associated p-values are indicated.

Long-term effect of the initial total visible impact on coral recovery and changes in the state of individual branches

The level of total visible impact on coral colonies in 2017 was significantly positively correlated with the level of total visible impact on these same colonies in 2011 (Fig. 2-2B). The health of the majority of coral colonies at MC 294 and MC 297 improved between 2011 and 2017, with an average increase in the proportion of healthy branches of 6% per colony. However, the condition of most corals deteriorated at MC 344 where, on average, the proportion of healthy branches decreased by 3% per colony.

The initial (2011) level of total visible impact had a significant negative effect on the proportion of branches that remained healthy between every consecutive year except for 2016-2017 at MC 294 and MC 297, and 2013-2014 at MC 344 (Fig. 2-3; Table C). The initial level of total visible impact also had a significant negative effect on the proportion of unhealthy branches that recovered between each consecutive year except between 2013-2014, 2015-2016 and 2016-2017 at MC 297, and 2012-2013 and 2013-2014 at MC 344. The proportion of branches colonized by hydroids that recovered between consecutive years was also significantly negatively affected by the initial level of total visible impact, except between 2015 and 2016 at MC 294 and 2013-2014 at MC 297. This transition was not significantly affected by the initial level of total visible impact at MC 344.

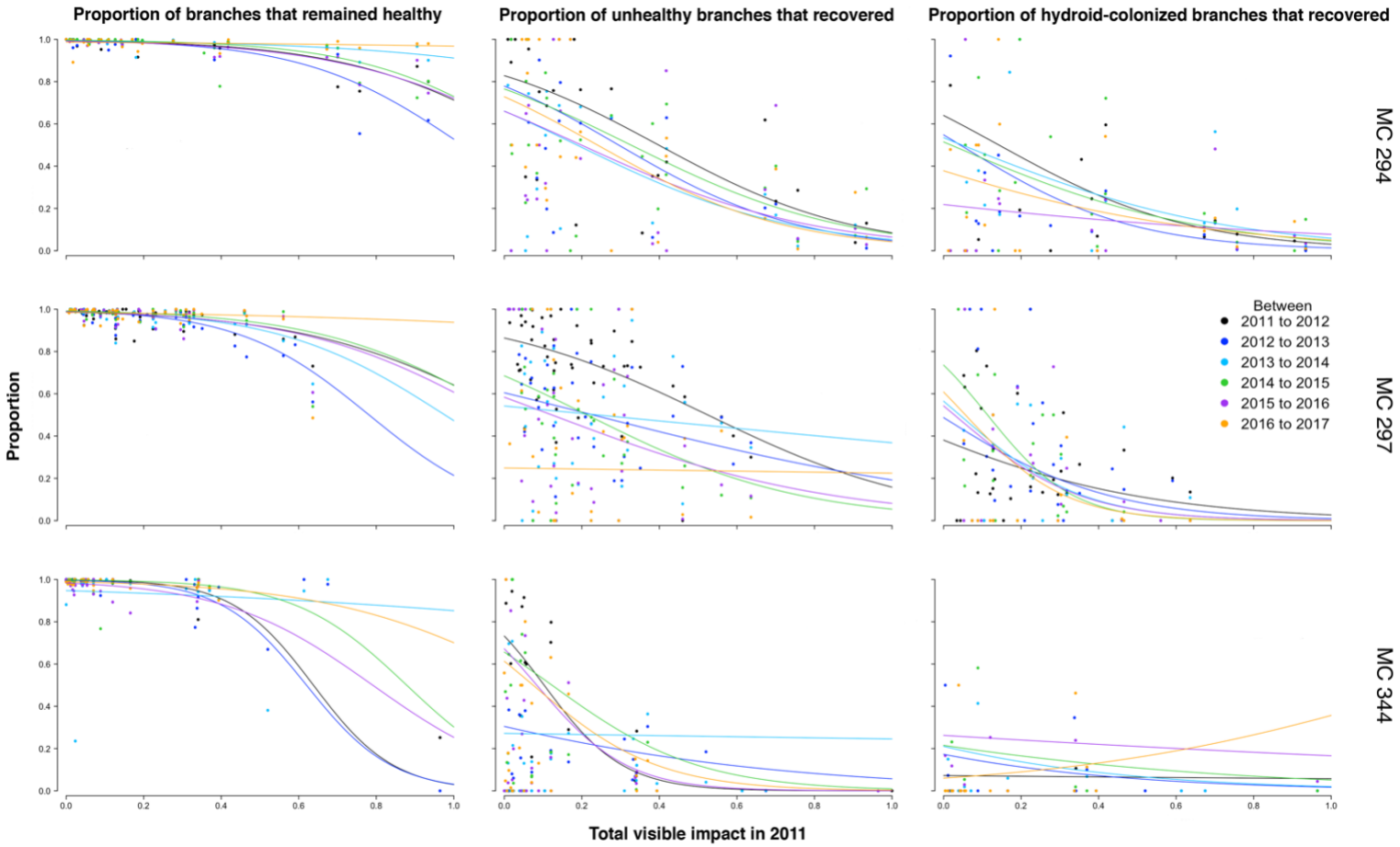

Figure 2-3. Proportion of branches that remained healthy and that were unhealthy or colonized by hydroids and recovered between each consecutive year as a function of the initial level of total visible impact. Predictions from the Generalized Linear models were fitted to the dataset.

Branch loss comparisons between years and sites

Branch loss was observed at all sites, even the reference sites, throughout the study period. Branch loss was significantly higher at MC 294 than at the reference sites (AT 357 or GC 852) between every consecutive year (Fig. 2-4; Table D). Branch loss at MC 294 was the highest between 2011-2012 and 2012-2013, it then decreased after 2013 and did not significantly change afterward (Fig. 2-4; Table E). Branch loss at MC 297 was only significantly higher than at the reference sites between 2013 and 2014 and did not change significantly over time. Branch loss at MC 344 was significantly higher than at the reference sites between 2015-2016 and 2016-2017 but did not change significantly over time (Fig. 2-4; Table D&E).

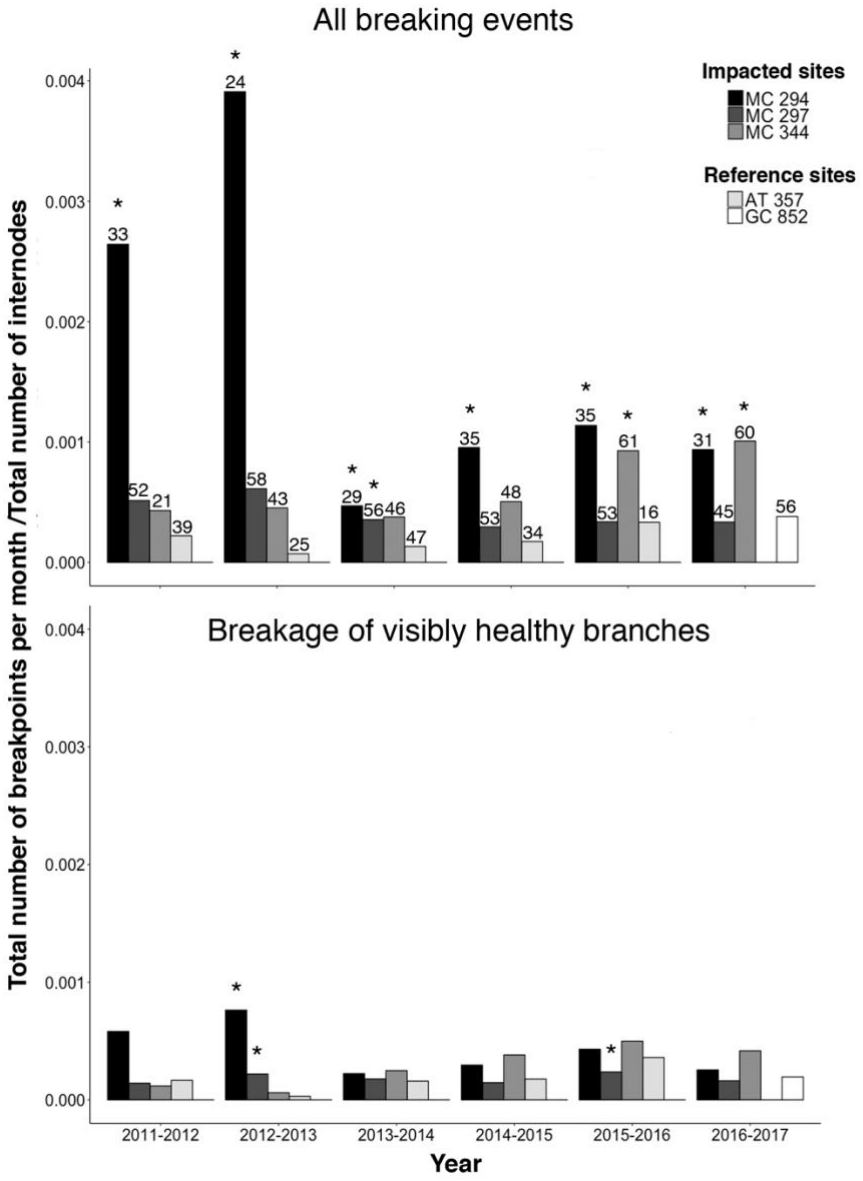

Figure 2-4. Changes in the ratio between the total number of breakpoints per month and total number of branches between 2011 and 2017. The number of colonies used in the GLM models is indicated above each bar. The stars (*) indicate impacted sites for which branch loss was significantly different from the reference site (AT 357 between 2011 and 2016 and GC 852 between 2016 and 2017)

Breakage location and effect of impact on branch loss

Although the majority of branches were healthy in 2011, breakage between 2011 and 2017 occurred significantly more often in areas of the colonies that were unhealthy or colonized by hydroids (Fisher's exact test: p-value < 0.001 at all sites; Fig. 2-5). The proportion of branches that broke in areas colonized by hydroids was significantly higher than the proportion of branches that broke in unhealthy parts of the colonies at MC 294 and MC 297 (two-proportion z-test: p-value < 0.001 at both MC 294 and MC 297), but not at MC 344 (two-proportion z-test: p-value = 0.433). Moreover, 42, 28 and 9% of the unhealthy branches that broke at MC 294, MC 297 and MC 344, respectively, were previously colonized by hydroids.

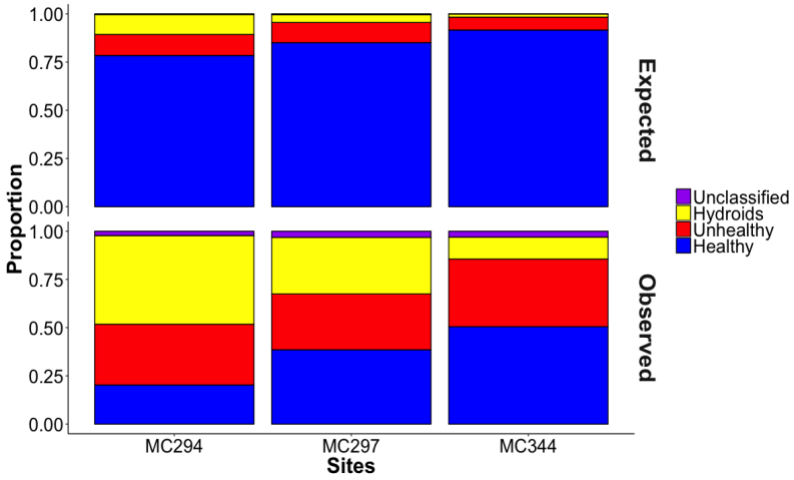

Figure 2-5. Proportion of branches in each state in 2011 (Expected probabilities used for the proportion test) and observed proportion of branches that broke in each state between 2011 and 2017 at MC 294, MC 297 and MC 344 (impacted sites).

Branches breaking in visibly healthy parts of the colony were observed at all sites throughout the study period. The number of branches breaking in healthy areas was not significantly different between the impacted and reference sites, except at MC 294 and MC 297 between 2012-2013 (Fig. 2-4; Table F). Moreover, no significant changes in healthy branch loss were observed over time at any of the impacted sites (Fig. 2-4; Table G).

Overall, the initial total visible impact proportion had a significant effect on the total normalized number of breakpoints (total number of breakpoints divided by the total number of branches) between 2011 and 2017 at all three impacted sites (Table 2-1). The initial level of total visible impact also had a significant positive effect on the number of branches that broke in visibly healthy parts of the colonies between 2011 and 2017 at MC 294 and MC 297, but not MC 344 (Table 2-1).

Table 2-1. GLM results for the effect of the initial proportion of total visible impact on the total normalized number of breakpoints (number of breakpoint divided by the total number of branches) and on the normalized number of breakpoints in visibly healthy parts of the colonies (number of breakpoints in healthy areas divided by the total number of visibly healthy branches) at all three impacted sites between 2011 and 2017.

Site	All breakpoints		Healthy breakpoints	
	Estimate	Standard error	Estimate	Standard error
MC 294	5.11 **	0.256	4.18 **	0.437
MC 297	5.75 **	0.897	3.30 *	1.15
MC 344	4.38 **	0.703	1.62	1.60

*p-value < 0.05; **p-value < 0.001

The majority of breaking events occurred on first order branches (terminal branches) (Fig. 2-6).

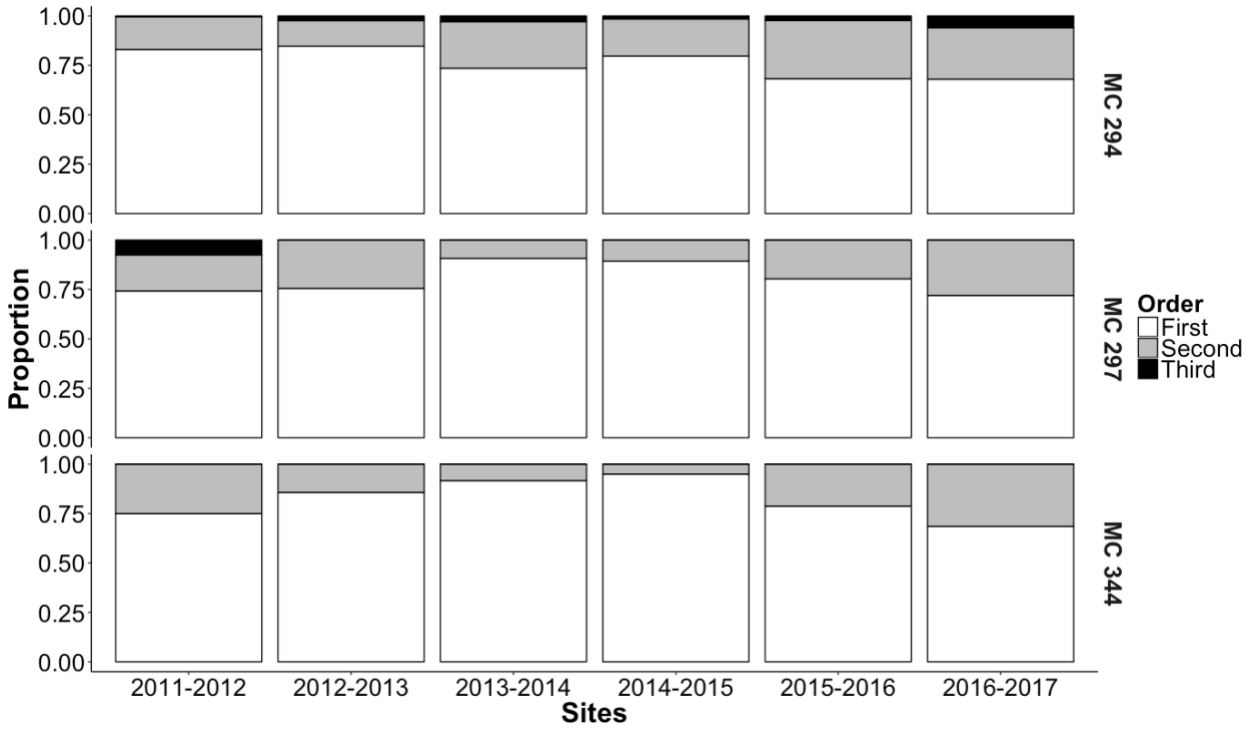

Figure 2-6. Changes in the proportion of first, second and third order branches that broke between 2011 and 2017 at all three impacted sites (MC 294, MC 297 and MC 344).

Second order branches broke every year at all three sites, while breakage of third order branches was observed every year at MC 294, and only between 2011 and 2012 at MC 297. The relative proportion of first, second and third order branches that broke did not significantly change between 2011 and 2017 at any of the impacted sites with the exception of MC 297 due to a few

third order branches breaking in the first year (MC 294: first vs second: p-value = 0.0923, first vs third: p-value = 0.229, second vs third: p-value = 0.485; MC 297: first vs second: p-value = 0.448, first vs third: 0.0157, second vs third: 0.0306; MC 344: first vs second: 0.158; Results were considered significant for a p-value < 0.0167 after Bonferroni correction of $\alpha = 0.05$). No breakage of branches with an order higher than three was observed.

Discussion

Overall, recovery was slow and the level of visible impact at all three impacted sites remained significantly higher than at the reference sites through 2017. The positive correlation between the level of total visible impact in 2011 and 2017, as well as the negative effect of initial impact (2011) on the recovery of unhealthy and hydroid-colonized branches explain both the decrease in the median level of total visible impact after 2011 (lightly impacted corals recovered) and the following stabilization of this median (heavily impacted corals are not recovering). These observations align with early results showing that corals that were initially only lightly impacted with floc were more likely to show early signs of recovery (Hsing et al. 2013). However, even seven years after the spill, a negative effect of the initial total visible impact on the proportion of healthy branches that remain healthy between consecutive years and on the proportion of unhealthy or hydroid-colonized branches that recover between subsequent years remains. This long-term non-acute effect of initial impact on the condition of individual branches suggests that many more years will be necessary for coral recovery and that colonies with more extensive injury may never recover. Other studies have documented slow to no recovery for other octocoral species. The extent of injury on *Paramuricea clavata* colonies affected by the 1999 heat wave in the Mediterranean decreased significantly during the first two years and then stabilized to a level that was still higher than what was observed before the event (Linares et al. 2005). In contrast, the condition of mesophotic corals impacted by the Deepwater Horizon oil spill was still declining after four years, suggesting recovery for these corals is unlikely (Etnoyer et al. 2015, Silva et al. 2015).

Although the median level of impact at both MC 294 and MC 297 was still higher than at the reference sites in 2017, there was a general trend toward recovery at these sites. Interestingly, the health of the majority of the coral colonies at MC 344, which was less visibly impacted in

2011 (Fisher et al. 2014b), deteriorated through 2017. MC 344 is deeper, corals are smaller and occur in lower density than at the other two impacted sites (Doughty et al. 2014). Furthermore, the ages determined from two specimens recovered from this site were both in excess of 600 years, suggesting much lower growth rates than at the other two impacted sites (Prouty et al. 2014). Deep-sea fauna, such as corals, living in non-chemosynthetic environments depend mostly on surface primary productivity, of which both quantity and quality decreases with depth (Suess 1980). Further, not all locations at any depth will be equally favorable for corals due to differences in substrate availability, local current regimes etc. Therefore, we suggest that the lower resilience observed for corals at MC 344 may be due to food limitation, or some other site specific factor making these corals less robust, and therefore less resilient to anthropogenic impact.

Tissue regeneration is a complex process that can be influenced by a combination of intrinsic (size, age, morphology, genotype) and extrinsic (environment, predation, competition) factors (Henry & Hart 2005). In our study the overall level of impact on coral colonies in 2011 had a significant influence on the recovery of individual impacted branches (unhealthy or hydroid-colonized branches) as well as on the ability of healthy branches to remain healthy over time. Corals are modular organisms, all replicated modules (polyps) are capable of all physiological functions but are interconnected, meaning that a change in a part of the colony is likely to affect the entire colony (Sánchez & Lasker 2003). Colony integration likely explains the influence of the level of total visible impact on changes in individual branches also previously observed by Hsing et al. (2013). Moreover, several studies found that the presence of healthy tissue surrounding wounds facilitated recovery (Meesters et al. 1997, Lirman 2000, Cerrano et al. 2005). Conversely, the presence of wounds on the colony may have disconnected and isolated visibly healthy branches from the rest of the colony, reducing their ability to remain healthy. Similarly, the level of initial total visible impact had a significant effect on the breakage of visibly healthy branches at both MC 294 and MC 297 between 2011 and 2017. These visibly healthy branches could have been less resistant to breakage due to being isolated from the rest of the colony, or could have been branches that were previously impacted and visibly (but not fully) recovered.

The level of initial total visible impact also had a significant effect on total branch loss, and impacted branches were more likely to break than healthy branches, particularly when they

were colonized by hydroids. The presence of epibionts on a coral's skeleton has been suggested to weaken the skeleton by increasing branch resistance to water movement due to the added epibiont mass (Bavestrello et al. 1997). The extensive hydroid colonization observed at MC 294 could explain the high level of branch loss observed at this site throughout the study period. Surprisingly, branch loss at MC 297 was not significantly higher than at the reference sites. Hydroid colonization was less extensive at this site compared to MC 294, and although the majority of coral colonies showed signs of impact, the number of corals impacted over 50% of the colony in 2011 was also smaller (5% of the corals at MC 297 compared to 13% at MC 294). Branch loss at MC 344 was similar to the reference sites until 2015, but was significantly higher after 2015. Several heavily impacted colonies discovered, and added to our study, in 2014 and 2015 contributed to the increase in the recorded number of breaking events.

Branch loss at MC 294 was the highest during the first three years that followed the spill. Even though it decreased and stabilized after that, the fact that branch loss at both MC 294 and MC 344 was still higher than at the reference sites between 2016 and 2017 also indicates an ongoing effect of the spill on these corals. Although the rank of the branches that broke did not significantly change between 2011 and 2017, with the majority of branches breaking so far being first order terminal branches, breakage of higher order branches is likely to increase in the future. For several heavily impacted coral colonies such as the one represented in Fig. 1, the fracture of the axial skeleton near the base, a major source of mortality in octocorals (Yoshioka & Yoshioka 1991), is expected. Linares et al. (2005) documented a delayed mortality of *P. clavata* colonies that were heavily impacted during a mass mortality event in the Mediterranean. We suggest that a similar delayed mortality of impacted *P. biscaya* may occur in the next few years.

The high branch loss combined with the slow growth rates previously estimated for *Paramuricea biscaya* in the Gulf of Mexico (Prouty et al. 2014) will lead to an overall decrease in colony size at the impacted sites, especially if corals keep losing branches at these rates in the next few years. A direct link between colony size and fecundity has been demonstrated for several octocoral species, sexual maturity occurring only once colonies reach a certain size and smaller colonies being less fecund (Coma et al. 1995, Page & Lasker 2012). A decrease in coral sizes at the impacted sites could thus lead to a decrease in fecundity. Moreover, several studies found that the presence of wounds affected both growth and sexual reproduction in corals due to energy being reallocated for regeneration (Guzmán et al. 1991, Brazeau & Lasker 1992,

Meesters et al. 1997, Linares et al. 2007, Page & Lasker 2012). A decrease in growth and fecundity at these sites could have long-term consequences for the regional coral metapopulation.

A limited amount of branch loss was observed at both reference sites, pointing out the need for a better understanding of deep sea coral's biology and their interaction with their environment. Damaged branches were observed on relatively few colonies at these sites, generally at the bottom edge of the colony at the sediment-water interface. These branches were likely damaged by repeated exposure to sediment due to localized hydrodynamic effects, and could have broken off for the same reason. However, about half of the branches that broke at the reference sites were visibly healthy, suggesting that a certain level of branch loss occurs naturally in the apparent absence of anthropogenic impact. A greater diversity and abundance of associates was also observed at the reference sites as compared to the impacted sites. At the impacted sites, the only coral associates documented were the ophiuroid *Asteroschema clavigerum* and, occasionally, hormatiid anemones. At GC 852, a species of hermit crab and aplacophorans were commonly observed on *P. biscaya* in addition to *Asteroschema clavigerum* and hormatiid anemones. Whether the lower diversity and abundance of associates on *P. biscaya* at the impacted sites post spill was a result of the exposure of the communities to oil and dispersant, or some other factor inherent in the different sites, is not known.

Although we only analyzed three coral communities that were impacted by the Deepwater Horizon oil spill, we did collect data on another apparently impacted coral community. This coral community was discovered in June 2014, at a depth of 1700 m in lease block MC 258 located 25 km west of the Macondo well. Thirteen coral colonies (eight *Stichopathes* sp., one *Bathypathes* sp., two *Paramuricea* sp., one *Keratoisis* sp. and one unidentified bamboo coral) were found at this site, two of which (one *Paramuricea* sp. and *Keratoisis* sp.) showed light, but notable, patchy impact, characteristic of corals that were impacted by the spill. Considering this discovery, as well as the large geographical area that was affected by the spill (Valentine et al. 2014, Chanton et al. 2015), it is likely that more impacted coral communities still remain to be discovered.

Conclusions

The analyses of high-definition images of individual coral colonies, collected during seven years of monitoring following the Deepwater Horizon oil spill, allowed us to detect relatively small changes in the state of individual branches between years and to precisely quantify branch loss over time. Overall recovery was slow. The ability of individual impacted branches to recover, as well as branch loss, were still dependent on the initial impact to the colonies after seven years, indicating a long-term non-acute effect of the spill. Furthermore, there are trends in the data suggesting that subacute effects are increasing over time at the deepest site. These results indicate that many more years will be necessary for moderately to heavily impacted corals to recover, and that some coral colonies will likely never recover. Deep-sea corals, and plexaurid corals in particular, are excellent biomonitors (sentinels) for anthropogenic impact (Fisher et al. 2014a). Establishing image-based coral-monitoring sites at a variety of depths and locations in the Gulf of Mexico would provide critical regional baseline data, significantly improve our understanding of the biology of these ecosystem engineers, and, if implemented as part of a Marine Protected Area, provide a tool to evaluate the efficiency of conservation measures. It would also provide a powerful tool to detect anthropogenic impact in the deep sea in general. With ever increasing energy extraction and the deepening impacts from fishing, ocean acidification and increasing water temperature due to climate change, the need for baseline data and monitoring is becoming acute.

Acknowledgements

We would like to thank the crews of the ships and deep submergence facilities for their assistance with data collection. Special thanks to all the undergraduate students involved in the digitization of coral images because this study would not have been possible without them. Specifically, we would like to thank B. Fu, T. Boyer, R. Cruz, T. Harpster, S. Vohsen, C. Du Preez, R. Dannenberg, J. Mentch, M. Kurmann, D. McKean, S. Berlet, S. Smith, A. Weinheimer, C. Bashaw, A. Yang, K. Anderson, and M. McGuigan for their assistance with data collection and analysis. This research was made possible by a grant from the Gulf of Mexico Research Initiative. Data are publicly available through the Gulf of Mexico Research Initiative Information

and Data Cooperative (GRIIDC) at https://data.gulfresearchinitiative.org (doi: <10.7266/N7NG4NJP>, <10.7266/N7HQ3WVD>, <10.7266/N7D21VJQ>, <10.7266/N78913TC>, <10.7266/N74J0C2M>). This is contribution no. 490 from the Ecosystem Impacts of Oil and Gas Inputs to the Gulf (ECOGIG) consortium.

Role of the funding source

This work was funded by the Gulf of Mexico Research Initiative to support the ECOGIG consortium administered by the University of Georgia. Some of the data collected in 2011 were funded by NOAA and BP as part of the Deepwater Horizon oil spill Natural Resource Damage Assessment (NRDA). The funding sources had no role in data collection, the preparation of the manuscript or decision to publish.

References

Andrews AH, Cordes EE, Mahoney MM, Munk K, Coale KH, Cailliet GM, Heifetz J (2002) Age, growth and radiometric age validation of a deep-sea, habitat-forming gorgonian (*Primnoa resedaeformis*) from the Gulf of Alaska. Hydrobiologia 471:101-110

Baillon S, Hamel J-F, Wareham VE, Mercier A (2012) Deep cold-water corals as nurseries for fish larvae. Frontiers in Ecology and the Environment 10:351-356

Bavestrello G, Cerrano C, Zanzi D, Cattaneo-Vietti R (1997) Damage by fishing activities to the Gorgonian coral *Paramuricea clavata* in the Ligurian Sea. Aquatic Conservation: Marine and Freshwater Ecosystems 7:253-262

Brazeau DA, Lasker HR (1992) Growth Rates and Growth Strategy in a Clonal Marine Invertebrate, the Caribbean Octocoral *Briareum asbestinum*. The Biological Bulletin 183:269-277

Buhl-Mortensen L, Mortensen PB (2005) Distribution and diversity of species associated with deep-sea gorgonian corals off Atlantic Canada. In: Freiwald A, Roberts JM (eds) Cold-Water Corals and Ecosystems, Berlin

Buhl-Mortensen L, Vanreusel A, Gooday AJ, Levin La, Priede IG, Buhl-Mortensen P, Gheerardyn H, King NJ, Raes M (2010) Biological structures as a source of habitat heterogeneity and biodiversity on the deep ocean margins. Marine Ecology 31:21-50

Camilli R, Reddy CM, Yoerger DR, Van Mooy BAS, Jakuba MV, Kinsey JC, McIntyre CP, Sylva SP, Maloney JV (2010) Tracking Hydrocarbon Plume Transport and Biodegradation at Deepwater Horizon. Science 330:201-204

Cathalot C, Van Oevelen D, Cox TJS, Kutti T, Lavaleye M, Duineveld G, Meysman FJR (2015) Cold-water coral reefs and adjacent sponge grounds: Hotspots of benthic respiration and organic carbon cycling in the deep sea. Frontiers in Marine Science 2:37

Cerrano C, Arillo a, Azzini F, Calcinai B, Castellano L, Muti C, Valisano L, Zega G, Bavestrello G (2005) Gorgonian population recovery after a mass mortality event. Aquatic Conservation: Marine and Freshwater Ecosystems 15:147-157

Chanton J, Zhao T, Rosenheim BE, Joye S, Bosman S, Brunner C, Yeager KM, Diercks AR, Hollander D (2015) Using Natural Abundance Radiocarbon To Trace the Flux of Petrocarbon to the Seafloor Following the Deepwater Horizon Oil Spill. Environmental Science & Technology 49:847-854

Clark MR, Koslow JA (2008) Impacts of fisheries on seamounts. In: Pitcher TJ, Morato T, Hart PJB, Clark MR, Haggan N, Santos RS (eds) Seamounts: Ecology, Fisheries & Conservation. John Wiley & Sons, Oxford

Clark MR, Rowden AA, Schlacher T, Williams A, Consalvey M, Stocks KI, Rogers AD, O'Hara TD, White M, Shank TM, Hall-Spencer JM (2010) The Ecology of Seamounts: Structure, Function, and Human Impacts. Annual Review of Marine Science 2:253-278

Coma R, Ribes M, Zabala M, Gili JM (1995) Reproduction and cycle of gonadal development in the Mediterranean gorgonian *Paramuricea clavata*. Marine ecology Progress series (Halstenbek) 117:173-183

Cordes EE, Jones DOB, Schlacher TA, Amon DJ, Bernardino AF, Brooke S, Carney R, DeLeo DM, Dunlop KM, Escobar-Briones EG, Gates AR, Génio L, Gobin J, Henry L-A, Herrera S, Hoyt S, Joye M, Kark S, Mestre NC, Metaxas A, Pfeifer S, Sink K, Sweetman AK, Witte U (2016) Environmental Impacts of the Deep-Water Oil and Gas Industry: A Review to Guide Management Strategies. Frontiers in Environmental Science 4

Cordes EE, Nybakken JW, VanDykhuizen G (2001) Reproduction and growth of *Anthomastus ritteri* (Octocorallia: Alcyonacea) from Monterey Bay, California, USA. Marine Biology 138:491-501

DeLeo DM, Ruiz-Ramos DV, Baums IB, Cordes EE (2015) Response of deep-water corals to oil and chemical dispersant exposure. Deep Sea Research Part II: Topical Studies in Oceanography 129:137-147

Doughty CL, Quattrini AM, Cordes EE (2014) Insights into the population dynamics of the deep-sea coral genus *Paramuricea* in the Gulf of Mexico. Deep Sea Research Part II: Topical Studies in Oceanography 99:71-82

Du Preez C, Tunnicliffe V (2011) Shortspine thornyhead and rockfish (Scorpaenidae) distribution in response to substratum, biogenic structures and trawling. Marine Ecology Progress Series 425:217-231

Etnoyer P, Warrenchuk J (2007) A catshark nursery in a deep gorgonian field in the Mississippi Canyon, Gulf of Mexico. Bulletin of Marine Science 81:553-559

Etnoyer PJ, Cairns SD (2016) Deep-Sea Coral Taxa in the US Gulf of Mexico: Depth and Geographical Distribution. The State of Deep-Sea Coral and Sponge Ecosystems of the United States. NOAA, NOAA Technical Memorandum X

Etnoyer PJ, Wickes LN, Silva M, Dubick JD, Balthis L, Salgado E, MacDonald IR (2015) Decline in condition of gorgonian octocorals on mesophotic reefs in the northern Gulf of Mexico: before and after the Deepwater Horizon oil spill. Coral Reefs:1-14

Fisher C, Roberts H, Cordes E, Bernard B (2007) Cold Seeps and Associated Communities of the Gulf of Mexico. Oceanography 20:118-129

Fisher CR, Demopoulos aWJ, Cordes EE, Baums IB, White HK, Bourque JR (2014a) Coral Communities as Indicators of Ecosystem-Level Impacts of the Deepwater Horizon Spill. BioScience 64:796-807

Fisher CR, Hsing P-Y, Kaiser CL, Yoerger DR, Roberts HH, Shedd WW, Cordes EE, Shank TM, Berlet SP, Saunders MG, Larcom EA, Brooks JM (2014b) Footprint of Deepwater Horizon blowout impact to deep-water coral communities. Proceedings of the National Academy of Sciences 111:11744-11749

Fosså JH, Mortensen PB, Furevik DM (2002) The deep-water coral *Lophelia pertusa* in Norwegian waters: distribution and fishery impacts. Hydrobiologia 471:1-12

Frometa J, DeLorenzo ME, Pisarski EC, Etnoyer PJ (2017) Toxicity of oil and dispersant on the deep water gorgonian octocoral *Swiftia exserta*, with implications for the effects of the Deepwater Horizon oil spill. Marine Pollution Bulletin 122:91-99

Girard F, Fu B, Fisher CR (2016) Mutualistic symbiosis with ophiuroids limited the impact of the Deepwater Horizon oil spill on deep-sea octocorals. Marine Ecology Progress Series 549:89-98

Guzmán HM, Jackson JBC, Weil E (1991) Short-term ecological consequences of a major oil spill on Panamanian subtidal reef corals. Coral Reefs 10:1-12

Hall-Spencer J, Allain V, Fosså JH (2002) Trawling damage to Northeast Atlantic ancient coral reefs. Proceedings of The Royal Society B 269:507-511

Henry L-A, Hart M (2005) Regeneration from Injury and Resource Allocation in Sponges and Corals – a Review. International Review of Hydrobiology 90:125-158

Hsing P-Y, Fu B, Larcom Ea, Berlet SP, Shank TM, Govindarajan AF, Lukasiewicz AJ, Dixon PM, Fisher CR (2013) Evidence of lasting impact of the Deepwater Horizon oil spill on a deep Gulf of Mexico coral community. Elementa: Science of the Anthropocene 1:000012

Jensen A, Frederiksen R (1992) The fauna associated with the bank-forming deepwater coral *Lophelia pertusa* (Scleractinaria) on the Faroe shelf. Sarsia 77:53-69

Koslow JA, Gowlett-Holmes K, Lowry JK, O'Hara T, Poore GCB, Williams A (2001) Seamount benthic macrofauna off southern Tasmania: Community structure and impacts of trawling. Marine Ecology Progress Series 213:111-125

Krieger KJ, Wing BL (2002) Megafauna associations with deepwater corals (*Primnoa* spp.) in the Gulf of Alaska. Hydrobiologia 471:83-90

Linares C, Coma R, Diaz D, Zabala M, Hereu B, Dantart L (2005) Immediate and delayed effects of a mass mortality event on gorgonian population dynamics and benthic community structure in the NW Mediterranean Sea. Marine Ecology Progress Series 305:127-137

Linares C, Coma R, Zabala M (2007) Effects of a mass mortality event on gorgonian reproduction. Coral Reefs 27:27-34

Lirman D (2000) Lesion regeneration in the branching coral *Acropora palmata*: effects of colonization, colony size, lesion size, and lesion shape. Marine Ecology Progress Series 197:209-215

McNutt M, Camilli R, Guthrie G, Hsieh P, Labson V, Lehr B, Maclay D, Ratzel A, Sogge MK (2011) Assessment of Flow Rate Estimates for the Deepwater Horizon / Macondo Well Oil Spill. Washington DC, United States

Meesters EH, Pauchli W, Bak RPM (1997) Predicting regeneration of physical damage on a reef-building coral by regeneration capacity and lesion shape. Marine Ecology Progress Series 146:91-99

Middelburg JJ, Mueller CE, Veuger B, Larsson AI, Form A, Oevelen Dv (2015) Discovery of symbiotic nitrogen fixation and chemoautotrophy in cold-water corals. Scientific Reports 5:17962

Oevelen Dv, Duineveld G, Lavaleye M, Mienis F, Soetaert K, Heip CHR (2009) The cold-water coral community as hotspot of carbon cycling on continental margins: A food-web analysis from Rockall Bank (northeast Atlantic). Limnology and Oceanography 54:1829-1844

Page CA, Lasker HR (2012) Effects of tissue loss, age and size on fecundity in the octocoral *Pseudopterogorgia elisabethae*. Journal of Experimental Marine Biology and Ecology 434:47-52

Passow U (2014) Formation of rapidly-sinking, oil-associated marine snow. Deep Sea Research Part II: Topical Studies in Oceanography 129:232-240

Passow U, Sweet J, Quigg A (2017) How the dispersant Corexit impacts the formation of sinking marine oil snow. Marine Pollution Bulletin

Passow U, Ziervogel K, Asper V, Diercks a (2012) Marine snow formation in the aftermath of the Deepwater Horizon oil spill in the Gulf of Mexico. Environmental Research Letters 7:035301-035301

Prouty NG, Fisher CR, Demopoulos AWJ, Druffel ERM (2014) Growth rates and ages of deep-sea corals impacted by the Deepwater Horizon oil spill. Deep Sea Research Part II: Topical Studies in Oceanography 129:196-212

R Core Team (2014) A Language and Environment for Statistical Computing. R Foundation for Statistical Computing, Vienna, Austria

Risk MJ, Heikoop JM, Snow MG, Beukens R (2002) Lifespans and growth patterns of two deep-sea corals: *Primnoa resedaeformis* and *Desmophyllum cristagalli*. Hydrobiologia 471:125-131

Roark EB, Guilderson TP, Dunbar RB, Fallon SJ, Mucciarone Da (2009) Extreme longevity in proteinaceous deep-sea corals. Proceedings of the National Academy of Sciences 106:5204-5208

Sánchez JA, Lasker HR (2003) Patterns of morphological integration in marine modular organisms: supra-module organization in branching octocoral colonies. Proceedings of The Royal Society B 270:2039-2044

Silva M, Etnoyer PJ, MacDonald IR (2015) Coral injuries observed at Mesophotic Reefs after the Deepwater Horizon oil discharge. Deep Sea Research Part II: Topical Studies in Oceanography

Suess E (1980) Particulate organic carbon flux in the oceans - surface productivity and oxygen utilization. Nature 288:260-263

Valentine DL, Fisher GB, Bagby SC, Nelson RK, Reddy CM, Sylva SP, Woo MA (2014) Fallout plume of submerged oil from Deepwater Horizon. Proceedings of the National Academy of Sciences 111:15906-15911

Van Dover CL (2007) The biological environment of polymetallic sulphides deposits, the potential impact of exploration and mining on this environment, and data required to establish environmental baselines in exploration areas Proceedings of the International Seabed Authority's Workshop

Watling L, France SC, Pante E, Simpson A (2011) Biology of deep-water octocorals. In: Lesser M (ed) Advances in Marine Biology, Book 60

White HK, Hsing PY, Cho W, Shank TM, Cordes EE, Quattrini AM, Nelson RK, Camilli R, Demopoulos AW, German CR, Brooks JM, Roberts HH, Shedd W, Reddy CM, Fisher CR (2012a) Impact of the Deepwater Horizon oil spill on a deep-water coral community in the Gulf of Mexico. Proceedings of the National Academy of Sciences 109:20303-20308

White HK, Lyons SL, Harrison SJ, Findley DM, Liu Y, Kujawinski EB (2014) Long-Term Persistence of Dispersants following the Deepwater Horizon Oil Spill. Environmental Science & Technology Letters 1:295-299

Yoshioka PM, Yoshioka BB (1991) A comparison of the survivorship and growth of shallow-water gorgonian species of Puerto Rico. Marine Ecology Progress Series 69:253-260

Chapter 3

Mutualistic symbiosis with ophiuroids limited the impact of the Deepwater Horizon oil spill on deep-sea octocorals

Fanny Girard, Bo Fu, Charles R. Fisher

Department of Biology, The Pennsylvania State University, 208 Mueller Laboratory, University Park, Pennsylvania 16802, USA

Published in Marine Ecology Progress Series (2016), 549: 89-98

Abstract

Deep-water corals form structurally complex biological habitats in the deep-sea that are generally associated with a diverse fauna. Yet, little is known about the effect of symbionts on coral resilience to natural or anthropogenic impact. This study focused on the influence of the ophiuroid symbiont *Asteroschema clavigerum* on the resilience of its host *Paramuricea biscaya* after the Deepwater Horizon oil spill in the Gulf of Mexico. Corals were imaged between 2011 and 2014 at four sites, three of which were impacted by the spill. Each colony was digitized to quantify the impact on corals. We developed a method to define an area under the influence of ophiuroids for each coral colony. The level of total visible impact, as well as recovery, were then compared within and outside this area. For the majority of colonies, recovery from visible impact and hydroid colonization was negatively correlated with distance from the ophiuroid. Total visible impact was lower within the area influenced by ophiuroids and branches within this area were more likely to recover. These results indicate that *P. biscaya* benefits from its association with *A. clavigerum*, likely through the physical action of ophiuroids removing material depositing on polyps, and perhaps inhibiting the settlement of hydroids. Although the beneficial role of the ophiuroids was demonstrated on corals impacted from an oil spill, we suggest that these benefits would also extend to corals in environments exposed to natural sedimentation events, perhaps allowing the corals to live in environments where sedimentation would otherwise limit their survival.

Introduction

Deep-water corals form structurally complex habitats utilized by numerous associated organisms (Buhl-Mortensen & Mortensen 2005, Roberts et al. 2006, Henry & Roberts 2007). Many species use deep-sea corals as a nursery, a source of food or as a substrate (Buhl-Mortensen & Mortensen 2005, Etnoyer & Warrenchuk 2007, Buhl-Mortensen et al. 2010, Mah et al. 2010, Baillon et al. 2012). Despite their importance, the interaction between deep-water corals, gorgonians in particular, and their associated fauna remains poorly understood.

Commensalism (in which one organism benefits from the association without affecting its host) is the most common type of relationship hypothesized between invertebrates and octocorals (Buhl-Mortensen 2004). Several species of actinaria (Bronsdon et al. 1993), polychaetes, crustaceans (Buhl-Mortensen & Mortensen 2004) and ophiuroids (Mosher & Watling 2009) have been reported as obligate symbionts of deep-water octocorals. However, the nature of the relationship between octocorals and their closely associated invertebrates is often not apparent and its consequences for the coral host are especially unclear.

The Euryalida, one of the two ophiuroid orders, includes four families: the Gorgonocephalidae (basket stars with branching arms), Asteronychidae, Euryalidae and Asteroschematidae (snake stars with non-branching arms). Euryalid ophiuroids have been little studied and knowledge on their feeding behavior, in particular, is sparse. However, several studies based on image and diet analyses imply that euryalids are predatory suspension feeders (Dearborn et al. 1986, Emson & Woodley 1987, Fujita & Ohta 1988, Grange 1991). Ophiuroids extend their arms to find zooplankton and can capture large live prey in an arm-loop (Warner 1982, Dearborn et al. 1986). Smaller prey and particles can be captured via several mechanisms: trapped by mucus-coated spines, trapped in mucus nets between spines or directly captured by the tube feet and transferred to the mouth (Pentreath 1970, Warner 1982).

The majority of studies, from depths ranging from 5 m to 1700 m, suggest that euryalids associated with corals use their host primarily to get better access to zooplankton and particles suspended in the water column, hence benefiting from the association. Submersible and laboratory observations show that the euryalid brittle star *Asteroschema tenue*, extends its arms in the water column at night while still clinging to the sea-whip gorgonian *Ellisella barbadensis* (Emson & Woodley 1987). Similar observations were made for *Asteronyx loveni* (Fujita & Ohta

1988). These studies imply that the association between ophiuroids and their coral host has parasitic aspects (ophiuroids benefit from the association at the expense of their host) but is mainly a commensal association. Some authors have suggested that this association could be mutualistic (both partners benefit from the association). It has been demonstrated that the ophiuroid *Astrobrachion constrictum*, in addition to suspension feeding, used its arms to remove particles deposited on coral branches, thus preventing smothering (Grange 1991, Stewart 1998). Grange (1991) also observed that corals associated with ophiuroids recovered faster from catastrophic events, such as landslides, than colonies that carried no ophiuroids.

In 2010, the Deepwater Horizon (DWH) blowout resulted in the release of approximately 4.9 million barrels of crude oil at a depth of 1500 m (McNutt et al. 2011). The first discovery of an impacted gorgonian community occurred 3.5 months after the well was capped. At this site most colonies were at least partially covered in a brown flocculent material that contained traces of oil from the Macondo well (White et al. 2012a, Hsing et al. 2013). Subsequent work on material removed from the corals showed that it also contained dioctyl sodium sulfosuccinate (DOSS), a compound diagnostic of the dispersant deployed during the spill (White et al. 2014). In 2011, two additional impacted communities were discovered (Fisher et al. 2014). These communities were also dominated by the octocoral *Paramuricea biscaya* (Grasshoff, 1977), commonly associated with the euryalid ophiuroid *Asteroschema clavigerum* (Verrill, 1884). Little is known about these two species and the nature of their association. Interestingly, *A. clavigerum* was always observed on healthy parts of visibly impacted coral colonies, suggesting that ophiuroids were either avoiding impacted branches or protecting portions of the coral colony.

The goals of this study were to assess the impact of the DWH oil spill on ophiuroid associates, characterize the nature of the association between *A. clavigerum* and *P. biscaya* and to determine whether ophiuroids affected coral recovery, using image analysis. We hypothesize that ophiuroids protected their hosts from some adverse effects of the spill, and had a positive effect on coral recovery from impact.

Materials and methods

Study sites and image acquisition

We imaged corals at four sites in the northern Gulf of Mexico. The first impacted site discovered, in BOEM (Bureau of Ocean Energy Management) lease block Mississippi Canyon (MC) 294, was located 13 km from the well. The two additional impacted communities discovered in 2011, MC 297 and MC 344, were 6 and 22 km from the well respectively. The last site, Atwater Valley (AT) 357, was located much farther away from the source of the oil spill (183 km) and coral colonies showed no evidence of recent impact.

The data reported here come from seven research cruises between 2010 and 2014 using Remotely Operated Vehicles (ROVs) to obtain high-resolution images of the coral colonies. MC 294 was the only site visited in 2010. During each visit as many coral colonies as possible were imaged, and if the corals had been imaged before, every effort was made to obtain images from the same heading and camera-subject distance to allow a detailed analysis of changes in the corals and their symbionts between visits.

Table 3-1. Total number of corals and number of corals hosting one or more ophiuroids at the three impacted sites and the reference site in 2011.

Sites	Total number of corals	Number of corals with one ophiuroid	Number of corals with more than one ophiuroid
MC 294	49	25	8
MC 297	69	44	4
MC 344	25	12	0
AT 357	82	32	25

Coral communities at the three impacted sites were dominated by *Paramuricea biscaya* and more than half of the corals at these sites hosted one or more ophiuroids from the species *Asteroschema clavigerum* (Table 3-1). Corals present at AT 357 were identified as *Paramuricea* sp. B3, and hosted at least one species of *Ophiocreas* in addition to *Asteroschema clavigerum*. Corals and their associates were identified in previous studies based on morphology and molecular barcoding (White et al. 2012a, Doughty et al. 2013). Experts were consulted for the identification of the ophiuroid species at AT 357.

Ophiuroid fidelity

The number of ophiuroids on each coral colony was recorded during each visit. Loss of ophiuroids and the percentage of ophiuroids that stayed on the same coral between each visit (fidelity) were determined for all four sites. We used the presence of scars (regenerating arms) to identify individual ophiuroids when possible. When no identifying marks were present, we assumed that ophiuroids that were at the same location on the colony from one year to another were the same individuals. Differences in fidelity among sites and years were tested with Fisher's exact test.

Relation between the presence of ophiuroids and level of impact

Coral colonies were digitized using Inkscape 0.48.5 and branches coded as visibly impacted (vi - excess of mucus, bare skeleton, absence of polyps), colonized by hydroids (hy) or not visibly impacted (nv), based on the method described in Hsing et al. (2013). The level of total visible impact was calculated based on the proportion of branches either colonized by hydroids or otherwise visibly impacted in images from 2011. The mean level of total visible impact in corals that did not host any ophiuroids and in colonies that had at least one ophiuroid associate were compared for each site and significant differences tested with the non-parametric Mann-Whitney Wilcoxon test.

Effect of impact on ophiuroids position on the colony

Ophiuroids were normally located at the center of their host colony. To determine whether the position occupied by the ophiuroids on corals was altered by impact to the coral, a polygon was defined around each colony that supported one brittle star, and the position of its centroid determined using ImageJ 1.48. For each coral colony, the distance between the centroid and the center of the ophiuroid oral disc was determined. This distance was then compared between corals that had a level of total visible impact over 20% of the colony and healthier corals (total visible impact lower than 20%) using the Mann-Whitney Wilcoxon test.

Determination of an area clearly under the influence of ophiuroids

In order to further investigate the role of ophiuroids in providing some resilience to impact from the spill we compared impact to a colony in areas clearly under the influence of the ophiuroid associate to the rest of the colony. To account for differences in arm length of different sized ophiuroids, we used the diameter of the ophiuroid's oral disc as our unit of measurement in these analyses. We first determined the maximum reach of the ophiuroids by measuring the

length of the arms of 18 individuals for which that was possible using ImageJ 1.48. In most cases all arms were too tightly coiled for this measurement, but among the 18 individuals that were measurable the arm lengths ranged from 19 to 34 times the diameter of the oral disc with an average of 24.5 times the disc diameter. This suggests that, at least theoretically, ophiuroids could have an influence on an area with a diameter about 50 times the diameter of the oral disc on average. In a separate analysis we determined a diameter of influence empirically for 7 coral colonies from MC 294 by plotting the level of total visible impact as a function of distance from the oral disc. Again our unit of measurement was the diameter of the oral disc of the ophiuroid on the coral being analyzed. Circles of increasing diameters were defined around each brittle star, and the cumulative level of total visible impact within each circle was calculated and plotted as a function of circle diameter (Fig. 3-1A&B). For all colonies, the curves had a sigmoidal shape, the level of impact started at zero and increased with distance from the oral disc until it reached an asymptote. Initially, a logistic regression model was fitted to each curve and the diameter of influence was defined where 99% of the value of the asymptote was reached (Fig. 3-1B). The average diameter of influence calculated using this method was equivalent to 36 times the diameter of the oral disc. In several cases, the perimeter of the circle approached the edge of the colony and the comparison between impact inside and outside the area of influence was limited. In order to increase the robustness of this comparison, we used the diameter corresponding to half the value of the asymptote (19 times the oral disc diameter) to delineate areas under the influence of ophiuroids (Fig. 3-1C). We then compared impact to portions of coral colonies inside and outside of areas of ophiuroid influence as of October 2011, using both diameters, and corals from MC 294 and MC 297 using the Mann-Whitney Wilcoxon test. Coral colonies present at AT 357 and MC 344 were not analyzed because all corals were healthy at AT 357, and not enough colonies could be used at MC 344 (only three impacted colonies carrying ophiuroids were big enough to be analyzed).

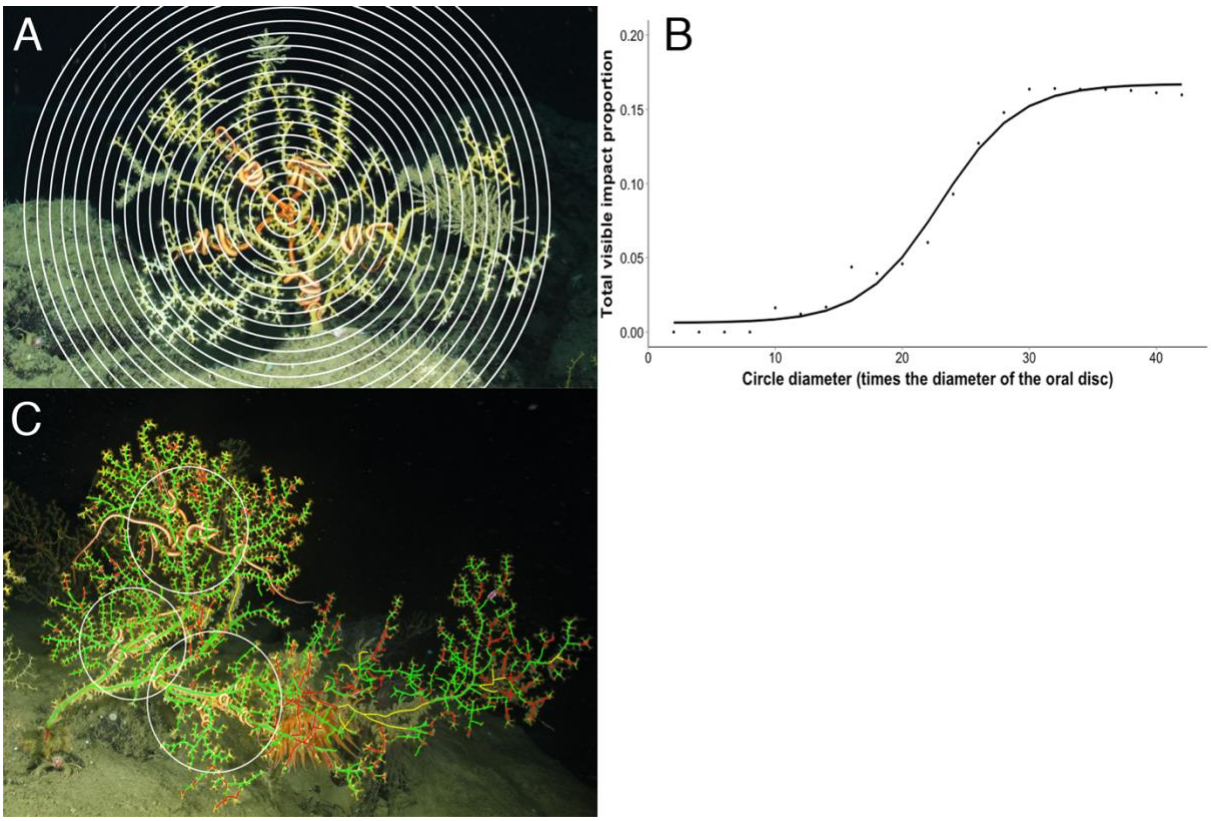

Figure 3-1. (A) Determination of the area influenced by ophiuroids: example of a coral colony from MC 294. The first circle has a diameter equivalent to twice the diameter of the ophiuroid oral disc, the second four times etc. until the entire colony is included. (B) Level of total visible impact and fitted logistic regression model as a function of the diameter of each circle. (C) Digitized image of a colony from MC 297. Each circle has a diameter equivalent to 19 times the diameter of the ophiuroid oral disc.

Ongoing effects of ophiuroids on coral colonies

To track changes in state of portions of the colony between 2011 and 2014, the branch state in 2014 was digitized on the 2011 images allowing a direct measurement of changing state. Changes in state of individual branches within and outside of the area of ophiuroid influence between 2011 and 2014 were compared using the Mann-Whitney Wilcoxon test. Ophiuroid positions on coral colonies from one year to another were very consistent, thus the position of the oral disc in 2011 was used for this analysis.

In a separate analysis, the correlation between visible impact or hydroid recovery and distance from the ophiuroid's oral disc (circles of increasing diameter) was measured for each colony using Spearman's rank correlation.

Non-parametric tests were used for all analyses because the data was not normally distributed, and none of the transformations we applied to the data sets resulted in normal distributions.

Analyses were performed in Minitab® 17.2.1 and the R programming environment version 3.1.0 (R Core Team 2014).

Results

About 70% of the corals at MC 294, MC 297 and AT 357, and 50% at MC 344 hosted at least one ophiuroid (Table 3-1). The proportion of corals hosting more than one brittle star varied from one site to another with the highest proportion at AT 357 (around 30%) and the lowest at MC 344 (0%). Larger colonies tended to host bigger brittle stars (Simple linear regression model: n = 95, intercept = 0.7524, slope = 0.0003, R^2adj = 0.2049, p-value < 0.0001) and the diameter of the ophiuroid's oral disc ranged from 0.3 to 1.5 cm with an average of 0.89 cm. Ophiuroids were always observed on healthy branches, with the exception of ophiuroids on corals that were impacted near 100% of the colony (Fig. 3-2A). Most of the time they were in the central area of coral colonies, and were rarely observed near the base of the colony or on distal branches. The position of the arms often appeared to have changed from one year to another, while the oral disc was normally in the same area (the average movement of the oral disc between 2011 and 2014 was equivalent to 3.5 ± 4.1 times the diameter of the oral disc).

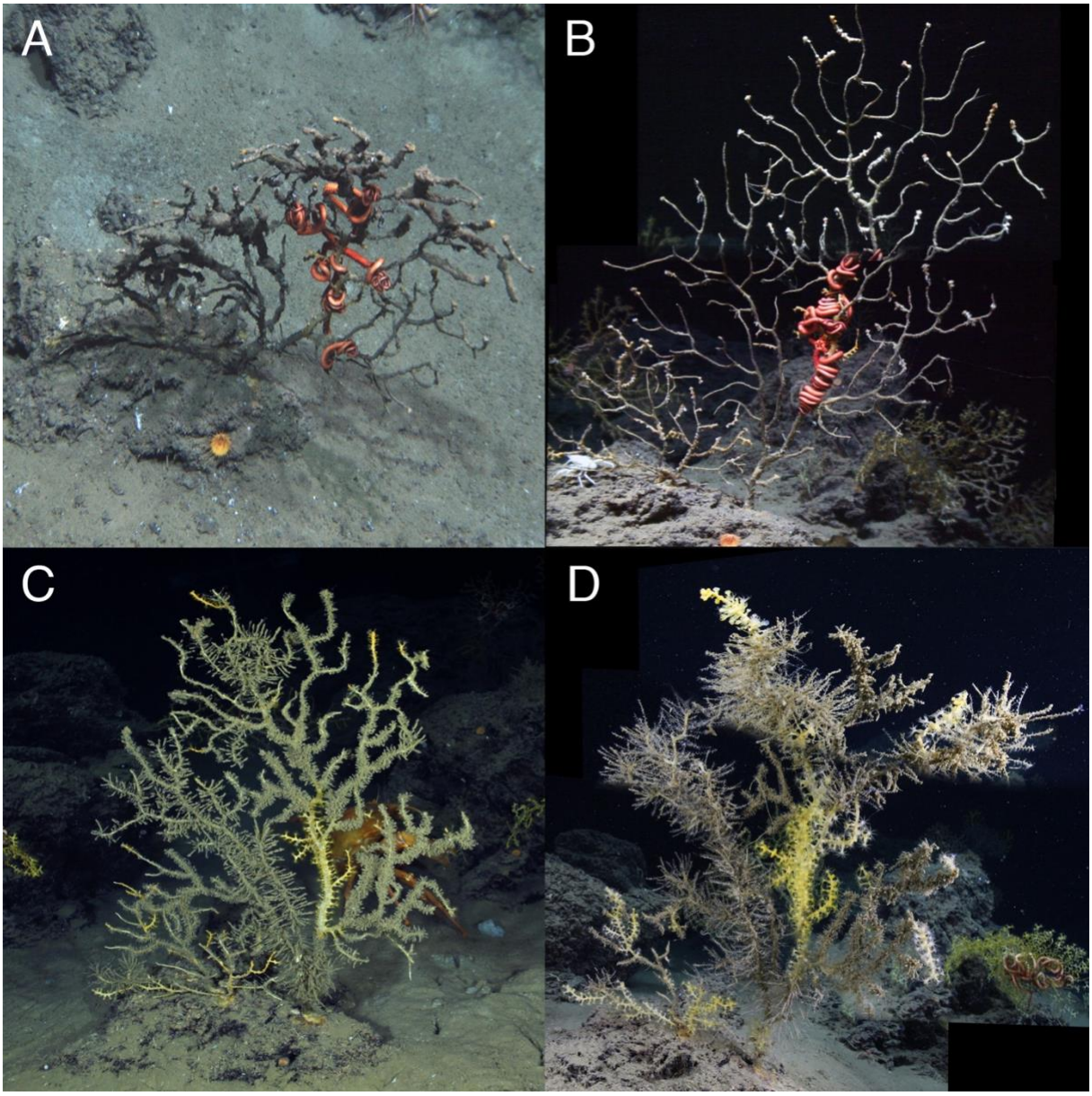

Figure 3-2. Impacted coral colony from MC 294 imaged in (A) November 2010, (B) December 2010, (C) October 2011 and (D) June 2014. Note that the only healthy portion of the colony corresponds to the position of its ophiuroid associate in 2010 (before it left the colony).

Ophiuroids did not seem to avoid contact with the polyps. There were at least two species of ophiuroids present on *Paramuricea* sp. B3 at AT 357, *Asteroschema clavigerum* and at least one species of *Ophiocreas*, while at the other sites, *Paramuricea biscaya* was only associated with *Asteroschema clavigerum*.

Between 2011 and 2014, the percentage of ophiuroids that stayed on the same coral

varied between 91 and 100% at both the impacted sites and the reference site, where none of the corals were visibly impacted by the spill (Fig. 3-3). At MC 294, the first impacted site discovered, fidelity was significantly lower between 2010 and 2011 (Fisher's exact test, p-value = 0.007). Only 67% of the brittle stars imaged in the late 2010 visits, when this site was discovered 3.5 months after the well was capped on 15 July 2010, were still clinging to their host in 2011.

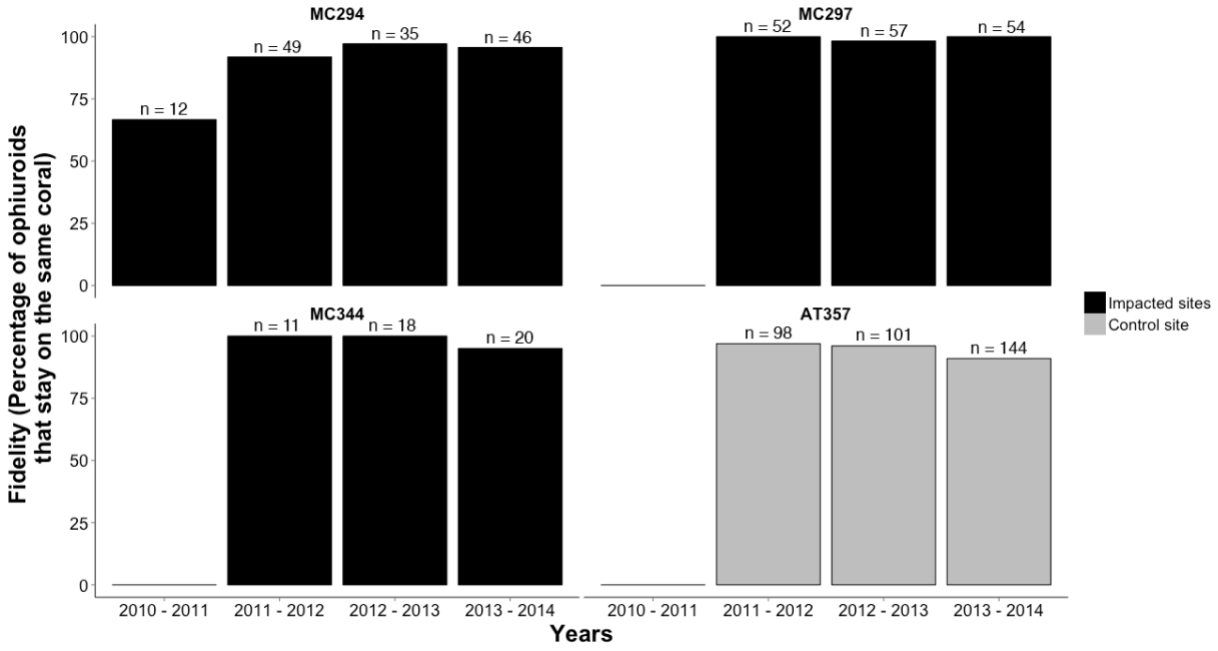

Figure 3-3. Percentage of ophiuroids that stayed on the same coral from one year to another (fidelity) between 2010 and 2014 and between 2011 and 2014 at the three impacted sites and the control site.

At all three impacted sites, the mean level of total visible impact of coral colonies that were associated with a brittle star was significantly lower compared to coral colonies without clinging ophiuroids (Mann-Whitney Wilcoxon, MC 294: p-value = 0.0003; MC 297: p-value = 0.0096; MC 344: p-value = 0.0015) (Fig. 3-4). There was no significant difference between corals with and without ophiuroids at the reference site (Mann-Whitney Wilcoxon, AT 357: p-value = 0.3072), where the average level of total visible impact for both groups was about 1%.

The average distance between ophiuroid oral discs and the center of their host colonies estimated by polygon centroids, was not significantly different between healthy and impacted

colonies (3.22 ± 2.3 cm and 5.09 ± 4 cm away respectively, Mann-Whitney Wilcoxon, p-value = 0.327).

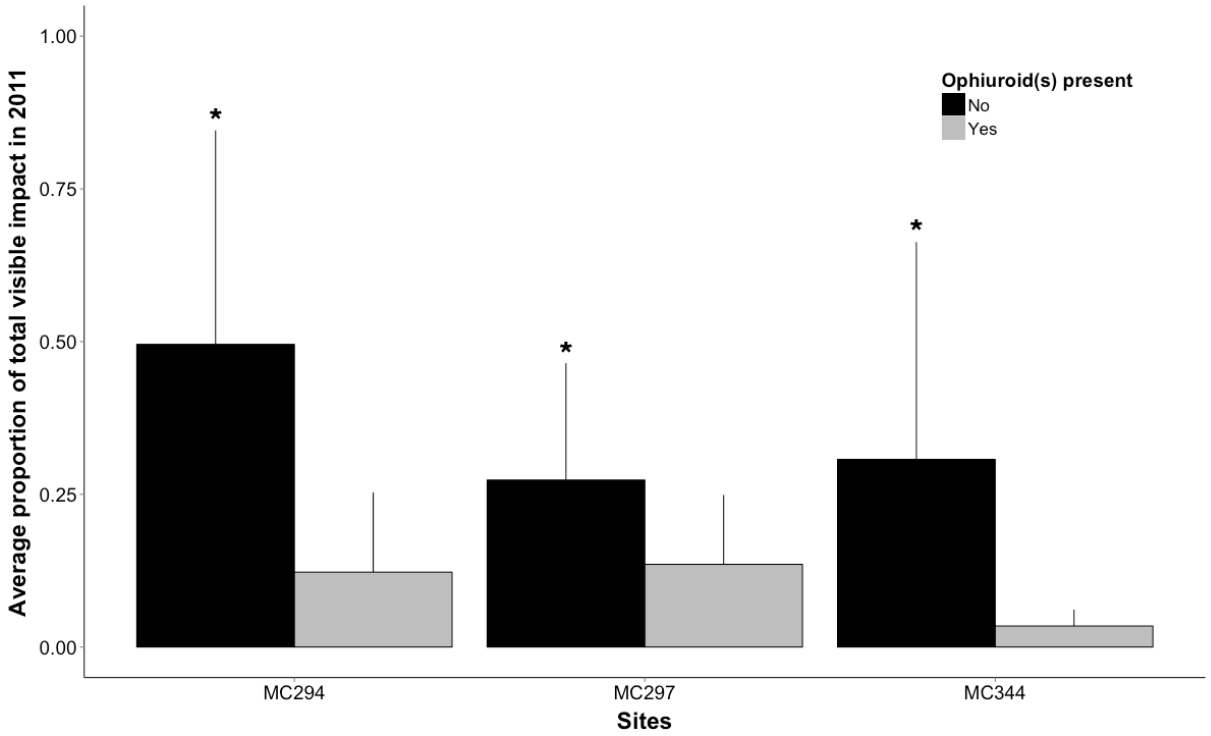

Figure 3-4. Mean level of total visible impact of coral colonies associated or not with ophiuroids. The error bars represent the standard deviation. Differences were tested with the Mann-Whitney Wilcoxon test and results were considered significant for a p-value < 0.05 (*).

The total level of visible impact was, on average, higher outside than inside the area influenced by ophiuroids, and this result was significant for MC 297. We observed similar patterns at both sites of a higher proportion of changes to a more favorable state in areas influenced by ophiuroids than in areas outside that influence, although the differences were only significant in some cases (Fig. 3-5). The proportion of branches that changed from impacted to healthy was significantly higher inside than outside the area influenced by brittle stars for both sites (Mann-Whitney Wilcoxon, p-value < 0.01). The same trends were observed when a larger diameter of influence was used for the analyses (Fig. H).

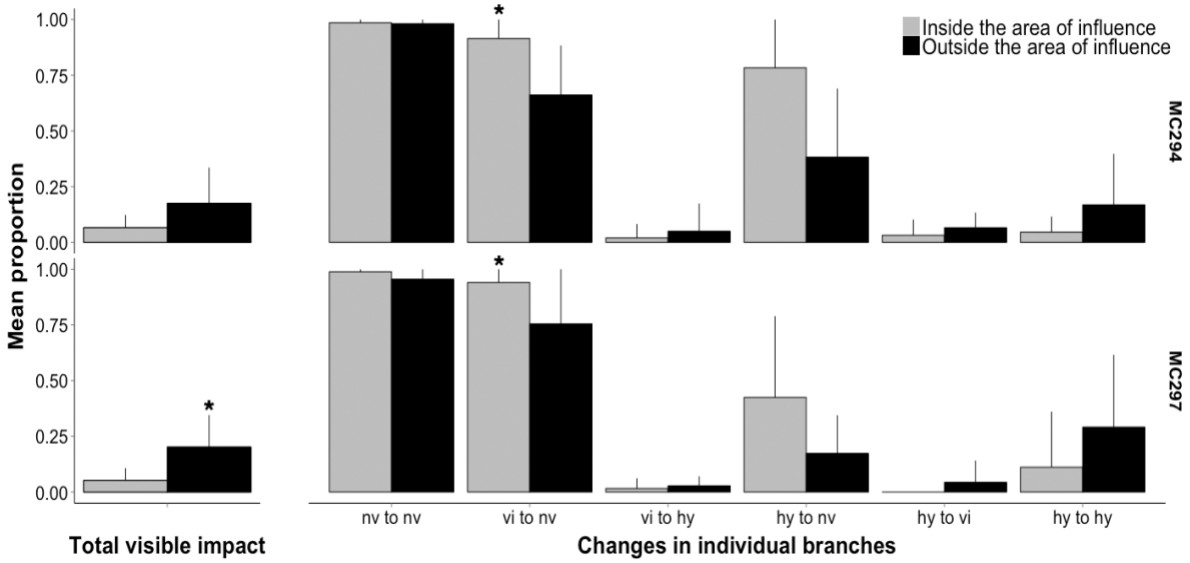

Figure 3-5. Average level of total visible impact (MC 294: n = 12; MC 297: n = 25) and proportion of branches that changed from one category to another between 2011 and 2014 (nv: no visible impact, vi: visibly impacted, hy: hydroid colonization) inside and outside the area influenced by ophiuroids (19 times the diameter of the oral disc) at both impacted sites. The error bars represent the standard deviation. Differences were tested with the Mann-Whitney Wilcoxon test and results were considered significant for a p-value < 0.05 (*).

For 7 of 8 colonies at MC 294 and 9 of 12 colonies at MC 297, recovery from visible impact was significantly negatively correlated with distance from the ophiuroids oral disc (Table 3-2). For 2 of these corals, there was a significant positive relation. There was no significant relation between recovery from visible impact and distance from the ophiuroids oral disc for the other 2 corals. There was no clear pattern for the relationship between branch recovery from hydroid colonization and distance from the ophiuroids oral disc (Table 3-2).

Table 3-2. Spearman's rho correlation coefficients between visible impact or hydroid recovery and distance from the ophiuroids oral disc (expressed as circle diameter). Results were considered significant for a p-value < 0.05 (*).

Coral colony	Site	Visible impact recovery	Hydroid recovery
A6	MC 294		-0.949
B6	MC 294		0.798 *
B9	MC 294	-0.949 *	-0.756 *
C5	MC 294	-0.9 *	
C8	MC 294	-0.913 *	
D1	MC 294	-0.873 *	
D5	MC 294	-0.79 *	
F2	MC 294	-0.895 *	-1 *
F3	MC 294	0.615 *	
F5	MC 294	-0.842 *	
M3-6	MC 297	0.642 *	-0.4
M3-8	MC 297	-0.841 *	
M3-11	MC 297	-0.767 *	0.095
M3-13	MC 297	-0.889 *	
M3-17	MC 297		-0.974 *
M3-18	MC 297	-0.876 *	
M6-9	MC 297	-0.969 *	
MM1-1	MC 297	-0.366	
MM1-9	MC 297	-0.431 *	
MM1-17	MC 297	-0.684 *	
MM1-18	MC 297	-0.087	
MM1-32	MC 297	-0.431 *	-0.667
MM1-40	MC 297	-0.952 *	-0.975 *

Discussion

The majority of coral colonies at each site were associated with at least one ophiuroid. Coral colonies at AT 357 sometimes carried several ophiuroids of different species indicating a more general association between ophiuroids and *Paramuricea* sp. B3 at this site. Conversely, *Paramuricea biscaya* was only associated with one species, *Asteroschema clavigerum*, at the other sites. Ophiuroids generally had their arms tightly coiled around coral branches and in some instances were clearly touching extended polyps. This type of interaction was observed with other species and suggests that the presence of the brittle star does not adversely affect the coral host and vice versa (Emson & Woodley 1987, Fujita & Ohta 1988, Grange 1991). Analysis of the stomach contents of obligate ophiuroid species have shown that ophiuroids do not feed on

polyps, and no damages due to ophiuroids have been found on corals (Emson & Woodley 1987, Grange 1991).

At all sites, ophiuroid fidelity after 2011 was close to 100%. High fidelity between an ophiuroid and a coral has been previously documented (Mosher & Watling 2009). The asteroschematid ophiuroid *Ophiocreas oedipus* spends its entire life attached to the octocoral *Metallogorgia melanotrichos*. Very small *O. oedipus* were found clinging to juvenile *M. melanotrichos* suggesting that the ophiuroids may directly settle on the corals (Mosher & Watling 2009). The fact that four very small *A. clavigerum* were observed on 3 different corals suggests that this species may also settle directly on *P. biscaya*. New adult individuals were observed between 2011 and 2014 on some colonies indicating occasional movement of brittle stars between colonies. The largest number of new adult ophiuroids was observed at AT 357 (15 new ophiuroids) where coral density is high with many corals directly adjacent to one another. Ophiuroid migrations were also documented at MC 294 with 7 newly established brittle stars documented over four years. In one instance a brittle star moving from one colony to another was observed. Considering the scarcity of coral communities, and the fact that the number of ophiuroids that appeared between 2011 and 2014 was always smaller than the number of ophiuroids that were lost, it is likely that the newly established ophiuroids came from other colonies within the same site. Between 2010 and 2011, 4 ophiuroids left their host at MC 294. Three of the four ophiuroids that were lost between 2010 and 2011 were initially on heavily impacted corals (see Fig. 3-2 for example). When MC 294 was discovered a few months after the Macondo well was capped, White et al. (2012a) observed that only 47% of the *A. clavigerum* associated with *P. biscaya* had a normal color (tan to red); the rest had distinctly white arms or were completely bleached. They also noted that several ophiuroids had their arms loosely coiled around coral branches, an abnormal behavior for this species. This suggests that *A. clavigerum* was likely directly impacted like the corals (White et al. 2012a) either through surface exposure to oil and/or dispersant or by ingesting contaminated particles or zooplankton (Mitra et al. 2012); this raises the possibility that some individuals died or left their host during the following year.

On average, *A. clavigerum* had a beneficial effect on its *P. biscaya* host over an area equivalent to at least 19 times the diameter of its oral disc. At MC 297, the total visible level of impact was significantly lower in the area influenced by ophiuroids than in the rest of the colony. Ophiuroid presence was correlated with a general trend of enhanced recovery from impact and

from hydroid colonization over a three-year period, although these trends were not always significant for hydroids. Moreover, corals that carried one or more ophiuroids were on average less visibly impacted than corals that did not host any. These results, coupled with the fact that the position of ophiuroids within colonies was not affected by the presence of impact, suggest that *A. clavigerum* did not avoid impacted branches. In other words, the correlation between ophiuroid position and healthy coral tissue was not a result of the ophiuroid moving into that area. Rather, the ophiuroids had a positive influence on the ability of *P. biscaya* to avoid visible damage from the effects of the DWH spill over areas of the colony under their influence, and also aided in recovery from this impact. Previous studies have concluded that the ophiuroid-coral association primarily benefits the ophiuroids by providing them with structure above the sea floor with enhanced access to food in the epibenthic water (Emson & Woodley 1987, Fujita & Ohta 1988). Our observations support those of Grange (1991) who observed that corals supporting ophiuroids were more likely to recover after catastrophic events such as landslides due to a positive influence of ophiuroids on their coral hosts. Our study also suggests that ophiuroids, in addition to protecting their coral host from sedimentation events, can enhance coral recovery after anthropogenic damage. Hsing et al. (2013) documented the onset of hydroid colonization on impacted portions of coral colonies one year after the Deepwater Horizon oil spill. Subsequently, overall hydroid colonization tended to increase over time. We demonstrated that the presence of ophiuroids had a positive effect on coral recovery from hydroid colonization, perhaps by removing hydroid colonies and preventing further settlement.

Understanding the interaction between all members of deep-sea communities is important to better assess recovery potential after anthropogenic impacts. As developing technology facilitates anthropogenic activities at ever greater ocean depths, the potential for impact to virtually all deep-sea ecosystems is increasing (Ramirez-Llodra et al. 2011). Deep-water corals are particularly vulnerable to bottom trawling (Koslow et al. 2001, Fosså et al. 2002, Hall-Spencer et al. 2002), other fishing activities, (Clark & Koslow 2008, Fisher et al. 2014), and increasing oil extraction and mining activities (Clark et al. 2010, White et al. 2012a, Hsing et al. 2013, Fisher et al. 2014). Because of their slow growth rates (Andrews et al. 2002, Roark et al. 2009), recovery and re-growth of deep-sea corals damaged or killed by anthropogenic activities will take decades to centuries. Moreover, our study highlights the consequences of the destruction of deep-water coral assemblages on biodiversity. *Asteroschema clavigerum*, as well

as other organisms, depend entirely on corals for their survival and would not persist in the absence of their host.

Conclusions

In addition to impact on corals, there was a loss of commensal ophiuroids associated with the DWH oil spill. It seems that ophiuroids did not preferentially move to healthy portions of the colony after impact, but instead, protected the branches to which they were attached (see Fig. 2A,B&C for example). These branches remained healthy throughout the study period, even long after some ophiuroids left their hosts, indicating a lasting effect of these associates (see Fig. 2D for example). Ophiuroids not only help protect their hosts from sedimentation or deposition of deleterious material on their surface, but also have a positive effect on coral recovery after impact. *Asteroschema clavigerum* uses *Paramuricea biscaya* to rise above the sea floor and get better access to food while its host reaps the benefits of the "cleaning" behavior of the ophiuroid. Coral colonies associated with ophiuroids were less impacted by the Deepwater Horizon oil spill and impacted branches were more likely to recover in the years following the spill. This association is a clear example of mutualism and demonstrates how symbiosis can significantly increase the partners' resilience to anthropogenic impact.

Acknowledgements

We thank the crews of the ships and deep submergence vehicles used for this study. We also would like to thank I. MacDonald for providing the digital still camera in 2011 and T. Shank and W. Cho for their help with species identification. Additional thanks to S. Vohsen, R. Dannenberg, J. Mentch, M. Kurmann, D. McKean and S. Berlet for their support at sea and in the lab, and to K. Shea, T. LaJeunesse and I. Baums for valuable inputs to the analysis. This research was made possible by a grant from the Gulf of Mexico Research Initiative. Data are publicly available through the Gulf of Mexico Research Initiative Information and Data Cooperative (GRIIDC) at https://data.gulfresearchinitiative.org (doi: <10.7266/N7NG4NJP>, <10.7266/N7HQ3WVD>, <10.7266/N7D21VJQ>, <10.7266/N78913TC>,

<10.7266/N74J0C2M>). This is contribution no. 373 from the Ecosystem Impacts of Oil and Gas Inputs to the Gulf (ECOGIG) consortium.

References

Andrews AH, Cordes EE, Mahoney MM, Munk K, Coale KH, Cailliet GM, Heifetz J (2002) Age, growth and radiometric age validation of a deep-sea, habitat-forming gorgonian (*Primnoa resedaeformis*) from the Gulf of Alaska. Hydrobiologia 471:101-110

Baillon S, Hamel J-F, Wareham VE, Mercier A (2012) Deep cold-water corals as nurseries for fish larvae. Frontiers in Ecology and the Environment 10:351-356

Bronsdon SK, Tyler Pa, Rice aL, Gage JD (1993) Reproductive biology of two epizoic anemones from the deep north eastern Atlantic Ocean. Journal of the Marine Biological Association of the United Kingdom 73:531-542

Buhl-Mortensen L (2004) Symbiosis in Deep-Water Corals. Symbiosis 37:33-61

Buhl-Mortensen L, Mortensen PB (2004) Crustaceans associated with the deep-water gorgonian corals *Paragorgia arborea* (L., 1758) and *Primnoa resedaeformis* (Gunn., 1763). Journal of Natural History 38:1233-1247

Buhl-Mortensen L, Mortensen PB (2005) Distribution and diversity of species associated with deep-sea gorgonian corals off Atlantic Canada. In: Freiwald A, Roberts JM (eds) Cold-Water Corals and Ecosystems, Berlin

Buhl-Mortensen L, Vanreusel A, Gooday AJ, Levin La, Priede IG, Buhl-Mortensen P, Gheerardyn H, King NJ, Raes M (2010) Biological structures as a source of habitat heterogeneity and biodiversity on the deep ocean margins. Marine Ecology 31:21-50

Clark MR, Koslow JA (2008) Impacts of fisheries on seamounts. In: Pitcher TJ, Morato T, Hart PJB, Clark MR, Haggan N, Santos RS (eds) Seamounts: Ecology, Fisheries & Conservation. John Wiley & Sons, Oxford

Clark MR, Rowden AA, Schlacher T, Williams A, Consalvey M, Stocks KI, Rogers AD, O'Hara TD, White M, Shank TM, Hall-Spencer JM (2010) The Ecology of Seamounts: Structure, Function, and Human Impacts. Annual Review of Marine Science 2:253-278

Dearborn JH, Ferrari FD, Edwards KC (1986) Can pelagic aggregation cause benthic statiation? Feeding biology of the Antarctic brittle star *Astrotoma agassizii* (Echinodermata: Ophiuroidea). Antarctic Reasearch Series 44:1-28

Doughty CL, Quattrini AM, Cordes EE (2013) Insights into the population dynamics of the deep-sea coral genus *Paramuricea* in the Gulf of Mexico. Deep Sea Research Part II: Topical Studies in Oceanography 99:71-82

Emson RH, Woodley JD (1987) Submersible and laboratory observations on *Asteroschema tenus*, a long-armed euryaline brittle star epizoic on gorgonians. Marine Biology 96:31-45

Etnoyer P, Warrenchuk J (2007) A catshark nursery in a deep gorgonian field in the Mississippi Canyon, Gulf of Mexico. Bulletin of Marine Science 81:553-559

Fisher CR, Hsing P-Y, Kaiser CL, Yoerger DR, Roberts HH, Shedd WW, Cordes EE, Shank TM, Berlet SP, Saunders MG, Larcom EA, Brooks JM (2014) Footprint of Deepwater Horizon blowout impact to deep-water coral communities. Proceedings of the National Academy of Sciences 111:11744-11749

Fosså JH, Mortensen PB, Furevik DM (2002) The deep-water coral *Lophelia pertusa* in Norwegian waters: distribution and fishery impacts. Hydrobiologia 471:1-12

Fujita T, Ohta S (1988) Photographic observations of the life style of a deep-sea ophiuroid *Asteronyx loveni* (Echinodermata). Deep Sea Research Part A Oceanographic Research Papers 35:2029-2043

Grange KR (1991) Mutualism between the antipatharian *Antipathes fiordensis* and the ophiuroid *Astrobrachion constrictum* in New Zealand fjords. Hydrobiologia 216/217:297-303

Hall-Spencer J, Allain V, Fosså JH (2002) Trawling damage to Northeast Atlantic ancient coral reefs. Proceedings of The Royal Society B 269:507-511

Henry L-A, Roberts JM (2007) Biodiversity and ecological composition of macrobenthos on cold-water coral mounds and adjacent off-mound habitat in the bathyal Porcupine Seabight, NE Atlantic. Deep Sea Research Part I: Oceanographic Research Papers 54:654-672

Hsing P-Y, Fu B, Larcom Ea, Berlet SP, Shank TM, Govindarajan AF, Lukasiewicz AJ, Dixon PM, Fisher CR (2013) Evidence of lasting impact of the Deepwater Horizon oil spill on a deep Gulf of Mexico coral community. Elementa: Science of the Anthropocene 1:000012

Koslow JA, Gowlett-Holmes K, Lowry JK, O'Hara T, Poore GCB, Williams A (2001) Seamount benthic macrofauna off southern Tasmania: Community structure and impacts of trawling. Marine Ecology Progress Series 213:111-125

Mah C, Nizinski M, Lundsten L (2010) Phylogenetic revision of the Hippasterinae (Goniasteridae; Asteroidea): systematics of deep sea corallivores, including one new genus and three new species. Zoological Journal of the Linnean Society 160:266-301

McNutt M, Camilli R, Guthrie G, Hsieh P, Labson V, Lehr B, Maclay D, Ratzel A, Sogge MK (2011) Assessment of Flow Rate Estimates for the Deepwater Horizon / Macondo Well Oil Spill. Washington DC, United States

Mitra S, Kimmel DG, Snyder J, Scalise K, McGlaughon BD, Roman MR, Jahn GL, Pierson JJ, Brandt SB, Montoya JP, Rosenbauer RJ, Lorenson TD, Wong FL, Campbell PL (2012) Macondo-1 well oil-derived polycyclic aromatic hydrocarbons in mesozooplankton from the northern Gulf of Mexico. Geophysical Research Letters 39:1-7

Mosher CV, Watling L (2009) Partners for life: a brittle star and its octocoral host. Marine Ecology Progress Series 397:81-88

Pentreath RJ (1970) Feeding mechanisms and the functional morphology of podia and spines in some New Zealand ophiuroids (Echinodermata). Journal of Zoology 161:395-429

R Core Team (2014) A Language and Environment for Statistical Computing. R Foundation for Statistical Computing, Vienna, Austria

Ramirez-Llodra E, Tyler PA, Baker MC, Bergstad OA, Clark MR, Escobar E, Levin LA, Menot L, Rowden AA, Smith CR, van Dover CL (2011) Man and the last great wilderness: Human impact on the deep sea. PLoS ONE 6:e22588

Roark EB, Guilderson TP, Dunbar RB, Fallon SJ, Mucciarone Da (2009) Extreme longevity in proteinaceous deep-sea corals. Proceedings of the National Academy of Sciences 106:5204-5208

Roberts JM, Wheeler AJ, Freiwald A (2006) Reefs of the deep: the biology and geology of cold-water coral ecosystems. Science 312:543-547

Stewart B (1998) Can a snake star earn its keep? Feeding and cleaning behaviour in *Astrobrachion constrictum* (Farquhar) (Echinodermata: Ophiuroidea), a euryalid brittle-star living in association with the black coral, *Antipathes fjordensis* (Grange, 1990). Journal of Experimental Marine Biology and Ecology 221:173-189

Warner G (1982) Food and feeding mechanisms: Ophiuroidea. In: Jangoux M, Lawrence JM (eds) Echinoderm nutrition. A.A. Balkema, Rotterdam

White HK, Hsing PY, Cho W, Shank TM, Cordes EE, Quattrini AM, Nelson RK, Camilli R, Demopoulos AW, German CR, Brooks JM, Roberts HH, Shedd W, Reddy CM, Fisher CR (2012a) Impact of the Deepwater Horizon oil spill on a deep-water coral community in the Gulf of Mexico. Proceedings of the National Academy of Sciences 109:20303-20308

White HK, Lyons SL, Harrison SJ, Findley DM, Liu Y, Kujawinski EB (2014) Long-Term Persistence of Dispersants following the Deepwater Horizon Oil Spill. Environmental Science & Technology Letters 1:295-299

Chapter 4

Projecting the recovery of a long-lived deep-sea coral species after the Deepwater Horizon oil spill using state-structured models

Fanny Girard, Katriona Shea, Charles R. Fisher

Department of Biology, The Pennsylvania State University, 208 Mueller Laboratory, University Park, Pennsylvania 16802, USA

In press: Journal of Applied Ecology

Abstract

Deep-water coral communities are hotspots of diversity and biomass in the deep sea. Most deep-sea coral species are long-lived and slow-growing, and are thus expected to recover slowly after disturbance. A better understanding of the recovery potential of these organisms is necessary to make appropriate management decisions. We used data from high resolution monitoring of individual coral colonies that were impacted by the Deepwater Horizon oil spill (April 2010) to parameterise and validate an annual, impact-dependent, state-structured matrix model to estimate the time to recovery for each coral colony. We projected the dynamics of three branch states: visibly healthy, unhealthy and hydroid-colonized. Although we implicitly included branch loss in the model, we focused on the short-term return of extant, damaged, branches to a visibly healthy state and did not consider the far longer-term re-growth of lost branches. Our model estimates that, depending on the initial level of impact, corals impacted by the spill will take up to three decades to recover to a state where all remaining branches appear healthy, though the majority of corals are projected to reach that state within a decade. By that time, some of these colonies will have lost a significant number of branches, leading to approximately 10% reduction in total biomass at all impacted sites. Overall, our model overestimates recovery, but branch loss estimates were reliable. Thus, the available growth rate data suggest that hundreds of years may be necessary for impacted communities to grow back to their initial biomass. Our study quantifies the very slow recovery rate of deep-sea corals and demonstrates the imperative of prioritizing a precautionary approach for these deep-sea ecosystems over restoration after the fact. As anthropogenic pressure on the deep sea is likely to increase, we suggest the establishment of coral-monitoring sites implemented as part of Marine Protected Areas to limit and detect impact to deep-sea corals. Furthermore, estimates from our model may be used to plan

shorter- and longer-term monitoring programmes after impact and to provide a timeline for policy.

Introduction

The blowout of the Deepwater Horizon drilling platform on 20 April 2010 in the northern Gulf of Mexico led to the largest accidental oil spill in history. Approximately 4.9 million barrels (780 million litres) of crude oil were released over an 87-day period, before the well was capped in July 2010. In response to the spill, seven million litres of dispersant were applied, with three million litres applied at depth, directly at the wellhead (McNutt et al. 2011). The Deepwater Horizon oil spill was unprecedented, not only because of its volume and duration, but also because the oil was released directly into the deep sea, at a depth of 1520 m (Peterson et al. 2012). The deep-water plume, that persisted for several months at a depth of about 1100 m (Camilli et al. 2010), as well as a large marine snow formation event in oil-contaminated surface water (Passow et al. 2012), had the potential to impact numerous, poorly known, deep-sea communities.

In November 2010, a few months after the well was capped, an impacted deep-sea octocoral community was discovered (White et al. 2012a). This community was located in Mississippi Canyon (MC) 294 (all site names are based on the US Bureau of Ocean Energy Management lease block designation for 3 by 3 nautical mile square areas of the sea floor leased for oil and gas activities), 13 km away from the well at a depth of 1370 m. The majority of the corals at this site exhibited signs of impact; they were covered in a brown flocculent material (floc) which contained traces of oil from the Macondo well, as well as dioctyl sodium sulfosuccinate (DOSS), a surfactant used in the dispersant Corexit applied in the aftermath of the spill (White et al. 2012a; White et al. 2014). In 2011, two more impacted coral communities were discovered at MC 297 and MC 344 located 6 and 22 km away from the well at 1560 and 1850 m depth respectively (Fisher et al. 2014). Coral colonies were not covered in floc but displayed the very characteristic pattern of spatially patchy impact and hydroid colonization across the colony observed on corals from MC 294 at the same time, after the floc had disappeared.

Deep-water corals are found at all latitudes in the deep sea (Watling et al. 2011) and are used by numerous species as habitat, feeding grounds, or nurseries (Buhl-Mortensen 2004; Etnoyer & Warrenchuk 2007; Du Preez & Tunnicliffe 2011; Baillon et al. 2012). In addition to enhancing biodiversity, cold-water corals have been shown to play a role in carbon cycling (Oevelen et al. 2009; Cathalot et al. 2015). Corals from the octocorallia subclass, although not reef-forming, can occur in very dense assemblages, and provide structurally complex habitats that can also support a high diversity of organisms (Buhl-Mortensen & Mortensen 2004; Buhl-Mortensen & Mortensen 2005; Roberts, Wheeler & Freiwald 2006; Buhl-Mortensen et al. 2010)

Given their important role in structuring deep-sea communities, a fuller understanding of how these corals will recover from acute damage in general, and the Deepwater Horizon spill in particular, is essential. Recovery comprises two main processes in this coral system: the observable recovery of extant, but damaged, biomass to a healthy state and the replacement of lost biomass (specifically, regrowth of lost branches). Recovery processes are complex and dependent on numerous factors (Henry & Hart 2005). Regeneration from injuries can depend on the size, age, genotype or morphology of the corals, as well as external factors such as the environment, the presence of predators, competition, etc. (Lasker 1990; Meesters, Noordeloos & Bak 1994; Meesters, Wesseling & Bak 1996; Henry & Hart 2005; Linares et al. 2005).

Many deep-water coral species have very low metabolic and growth rates and are extremely long lived (Andrews et al. 2002; Roark et al. 2009). In the northern Gulf of Mexico, some *Paramuricea biscaya* (Grasshoff 1977) colonies, the octocoral species that was most affected by the spill, have been estimated to be over 600 years old (Prouty et al. 2014). The low metabolic and growth rates of these corals suggest that it could take many years before even moderately impacted colonies completely recover (in terms of both return to health of extant branches, and regrowth of lost branches) from the impacts of the spill.

A slow and complex recovery of corals impacted by the Deepwater Horizon oil spill has already been suggested by several studies. Two years after the Deepwater Horizon oil spill, even though the median level of visible impact at MC 294 had decreased, most impacted *Paramuricea biscaya* still showed signs of injury, and hydroid overgrowth, which started in 2011, was still expanding on some colonies (Hsing et al. 2013). Hydroids colonized damaged portions of the colonies, impeding tissue regeneration and weakening the coral's skeleton due to the added epibiont mass (Bavestrello et al. 1997). Branch loss was observed on some colonies, and the

recovery of individual damaged branches, and branches colonized by hydroids was negatively correlated with the initial level of impact to the colony. The recovery patterns of impacted coral colonies also varied with the presence or absence of the brittle star (ophiuroid) *Asteroschema clavigerum* (Verrill 1894) on the corals. *A. clavigerum* ophiuroids both provided protection from impact and facilitated the recovery of damaged coral branches (Girard, Fu & Fisher 2016).

Long-term monitoring of impacted coral colonies is the best way to study the recovery of these long-lived, slow-growing organisms. However, collecting data in the deep sea is challenging and expensive, and expectations are that it will take decades to centuries for full regrowth and recovery of these coral communities. Thus, we here specifically focused on how long it will take for observable recovery to health of extant coral biomass. Estimates of time to visible recovery will allow for the appropriate planning of both the overall duration of a recovery monitoring plan, and also of the frequency of visits necessary for recovery assessment. After extant coral recovery, less frequent monitoring may subsequently document the slower regrowth process, which was not addressed in the present study. For our study, we used a structured matrix model (Caswell 2001) to estimate how long it will take for the impacted corals to visibly recover from damage and hydroid colonization, and thus for how long monitoring will be informative about the health of remaining coral biomass.

Materials and methods

Study sites and data acquisition

The data used for this model were collected as part of a long-term monitoring study at three sites that were impacted by the Deepwater Horizon oil spill. These sites, in BOEM lease blocks MC 294, MC 297 and MC 344, were located 13, 6 and 22 km away from the Macondo well respectively, and the dominant coral species at these sites was *Paramuricea biscaya*. Corals from this species have a planar morphology, all branches are in the same plane and are thus visible in the same photograph, making them well suited for image analysis (Fig. 4-1).

We monitored 49, 56 and 61 individual coral colonies between 2011 and 2017 at MC 294, MC 297 and MC 344, respectively. High definition images of the same colonies were taken every year using digital still cameras and Remotely Operated Vehicles (ROVs). A particular effort was made to use the same headings (compass bearings), and camera-object distance each

time to facilitate comparisons. We chose to use images collected in October 2011 as the baseline for this study because this was the first complete, high quality, dataset collected from all three sites, and the oil containing floc had fallen off the corals by this time, revealing the presence or absence of visible damage. We digitized images from the 2011 cruise using Inkscape 0.48.5, and coded coral branches as visibly healthy, unhealthy (obvious tissue damage, bare skeleton, or excess mucous production) or colonized by hydroids (Fig. 4-1). We coded branches conservatively; whenever it was not clear whether a branch was unhealthy we coded it as healthy, and when the presence of hydroids was not obvious we coded the branch as unhealthy.

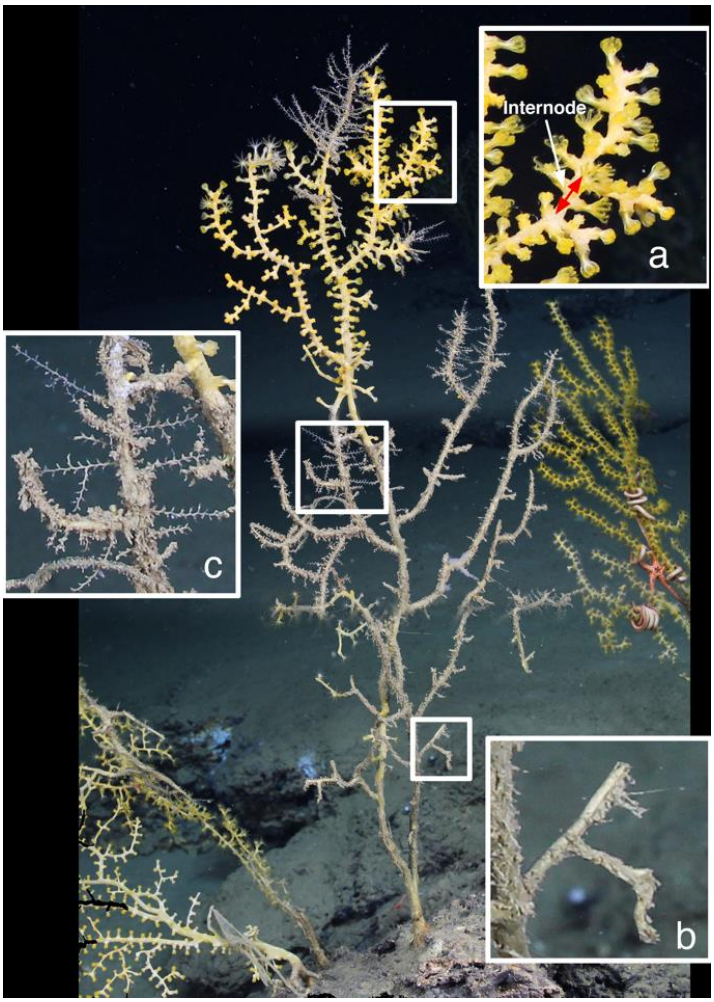

Figure 4-1. Impacted coral colony from MC 294. The three branch/internode states are visible: a few branches are visibly healthy (a), but the majority are either unhealthy (b) or colonized by hydroids (c).

To determine the condition of coral colonies after 2011, we used the 2011 image as a template, and re-coded branches every year based on their new state. After 2011, we added a new category for branch loss. We followed changes from one state category to another on individual branches between consecutive years using the digitized high-definition images. We counted the total number of branches on each coral colony using the cell counter tool in ImageJ 1.4, and measured the proportion of branches that were in each state for every year. We then tracked changes in individual branches and measured the proportion of branches that changed from one state to another, or not, between consecutive years.

In addition to quantifying impact for each coral colony, we estimated total branch length for each coral. To estimate the size of each colony, a perforated

resilient plastic ball ("wiffle ball"), with a diameter of 8.9 cm, mounted on a pole was held next to each coral colony and imaged with the colony to provide scale. For these measurements, the mounted ball was held in the manipulator of the ROV, in contact with the colony, and imaged in the same plane. We then used these images to calculate the total branch length of each coral (cumulative length of all branches). We used total branch length as a measure of coral size and a proxy for biomass.

Model

We projected the level of total visible impact for each coral colony using an annual impact-dependent state-structured matrix model (Caswell 2001) where three states were considered: branches could either be healthy, unhealthy or colonized by hydroids (Fig. 4-1). In this model, internodes (distance between the base of two branches – Fig. 4-1a), used here as a proxy for branches, constituted individuals. The number of branches in each category at time t + 1 was given by the linear equation:

$$\mathbf{n}(t + 1) = \mathbf{U}\mathbf{n}(t)$$

Where $\mathbf{n}(t)$ is a vector representing the number of branches in each state, and $\mathbf{U}$ is the projection matrix, containing the transition probabilities between each of the three states (see Table I for the full model structure).

The transition probabilities were dependent on the level of total visible impact of the colony (sum of the proportion of unhealthy and hydroid-colonized branches) each year, thus the projection matrix changed at every model time step, making the model impact-dependent. In this model, the sum of the transition probabilities for each state was less than or equal to one; probabilities less than one denote branch loss. Regrowth of new, healthy, branches was explicitly excluded from this model as we focused on the recovery to health of extant coral biomass, and growth rates for this coral species are extremely slow (Prouty et al. 2014).

We assumed that all coral colonies responded the same way to impact and that the transition probabilities only depended on the current state of the system, as is common in matrix modelling (Caswell 2001). The number of branches in each state in 2011 were used as initial conditions as, in 2010, fewer corals were imaged at MC 294, and none were imaged at MC 297 or MC 344.

Parameter estimation

We estimated the transition probabilities for the projection matrix with Generalized Linear Mixed Models (GLMM). We used the total visible impact proportion (IMP), and total branch length in 2011 (SIZE) - both continuous variables - for each coral as fixed effects in the statistical model. Since we imaged the same coral colonies every year, we treated year (YEAR) as a random effect. We also included coral colony (CORAL) as a random effect to avoid overdispersion (when the variability in the data is larger than the variability expected under the assumed distribution (binomial in the case of proportion data), leading to poor model fitting). For each branch state (healthy, unhealthy or hydroid-colonized), we used the same 3-step sequence of nested binomial GLMMs using a logit link function to estimate the effect of impact proportion and size on the proportion of branches that changed from one state to another:

1. We first modelled the proportion of branches that broke. The response variable for this model consisted of two columns: one for the number of branches that broke and the other for the number of branches that did not break (which sum to the total number of branches in the focal state).
2. We then modelled the proportion of branches that stayed in the same state between consecutive years, considering only branches that did not break.
3. Finally, we tested the effect of impact and size on the proportion of branches that transitioned to either of the remaining two states, considering only branches that did not break and did not remain in the same state.

Each step was thus performed on nested subsets of the data, starting with the relevant subset (for instance, only healthy branches were used when modelling the transition from healthy to any other state). For each transition probability, we started with the same full model:

Transition probability ~ IMP + SIZE + IMP*SIZE + (1|YEAR) + (1|CORAL)

and selected the minimum adequate model (Table 4-1).

The marginal estimates from the minimum adequate model were then used to predict the transition probabilities used in the matrix model for all coral colonies. When impact proportion or size did not have a significant effect on a particular transition, the weighted mean for this proportion was used to estimate the transition probability.

Table 4-1. Parameters selected for each transition probability and associated model coefficients based on the Generalized Linear Mixed Models (GLMMs).

		Intercept		IMP		SIZE	
Transition	Model	Estimate	Std. error	Estimate	Std. error	Estimate	Std. error
H → B	0.0067						
H → H	~ IMP	5.45	0.194	-4.10	0.523		
H → I	0.811						
I → B	0.0989						
I → I	~ IMP	-1.23	0.384	1.79	0.444		
I → H	~ IMP	2.42	0.431	-4.90	0.708		
Hy → B	0.122						
Hy → Hy	~ IMP	-0.671	0.389	1.82	0.699		
Hy → H	~ IMP + Size	0.425	0.570	-3.81	0.517	0.145	0.0591

IMP: Total visible impact (unhealthy and hydroid-colonized branches); SIZE: Total branch length; H: Healthy branches, I: Unhealthy branches; Hy: Branches colonized by hydroids; B: Branches that broke
Random factors: Imaging year and individual colony number

We tested models parameterised using all possible combination of years (the effect of different years on model outcomes was inconsistent and rarely significant – see Appendix J). We then used the data from 2011 to 2015 at MC 294 for model parameterisation because corals at this site displayed the largest range of impact levels, and impact at this site was directly linked to the Deepwater Horizon oil spill (traces of oil and dispersant were detected in the deposit that covered coral branches). Although the impact distribution indicates that corals at MC 297 and MC 344 were also impacted by the oil spill, the extent of impact in 2010 is unknown for these corals as they were only discovered in 2011. Corals at MC 294, as well as MC 297 and MC 344, were then used to validate model projections, in order to determine whether the estimates based on the MC 294 corals could be generalized to other sites.

Model validation

For each coral colony at MC 294, MC 297 and MC 344, we projected the proportion of branches in each state in 2016 and 2017 and plotted it against the observed proportions for the same years. We then fitted linear regression models to assess the adequacy of model projections. For this analysis, we only included 91 corals (33, 41 and 17 at MC 294, MC 297 and MC 344 respectively) that were imaged every year between 2011 and 2017.

Recovery estimation

We estimated the time to visible recovery (95% of the remaining, extant colony is visibly healthy) for every impacted coral colony at MC 294, MC 297 and MC 344 (38, 49 and 38 corals at MC 294, MC 297 and MC 344 respectively). Our model never projected 100% visible

recovery, instead a steady state was reached between healthy, unhealthy and hydroid-colonized branches, with the proportion of healthy branches always being approximately 0.95. Since corals lost branches over time, we also estimated how much of the initial colony still existed after visible recovery (proportion of surviving branches). To evaluate the effect of the initial level of impact on the time to visible recovery and proportion of surviving branches, we ran deterministic simulations over a 50-year period using all possible combinations of proportion of unhealthy and hydroid-colonized branches as initial conditions (we used a step size of 0.01 to discretize these variables). We used the average number of branches (170 (SD:150.5)) and total branch length (3.11 m) measured in 2011 at MC 294, MC 297 and MC 344 for all simulations.

Elasticity analysis

We conducted an elasticity analysis by looking at the effect of a 0.1% decrease in each transition probability (separately) on the time to visible recovery, and comparing the difference between the respective estimated time to visible recovery projected for all possible values of damage and hydroid colonization proportions (step size of 0.01) using deterministic simulations over a 50-year period.

All analyses were performed in R (R Core Team 2014). GLMMs were fitted with the lme4 (version 1.1-12) R package (Bates et al. 2015), while the model was coded using the popbio (version 2.4.3) package (Stubben & Milligan 2007).

Results

The level of total visible impact significantly affected all transition probabilities except for the transitions from a healthy to an unhealthy state (Table 4-1). Coral size only had a significant effect on the transition from hydroid colonization to healthy. Neither impact nor size had a significant effect on the proportion of branches of any state that broke between consecutive years.

The time to visible recovery and proportion of surviving branches after visible recovery were estimated for 38, 49 and 38 coral colonies at MC 294, MC 297 and MC 344 respectively. These corals covered the full possible range of total visible impact, with the majority of colonies being lightly impacted (less than 20% impacted) and a few colonies having a level of impact close to 100%. The model projected that, although it will take up to 27 years for the most impacted coral colonies to visibly recover, the majority of coral colonies will have recovered

within 10 years (Fig. 4-2). The average and median times to recovery were both equal to 5 years (SD: 4 years). The most heavily impacted coral colonies were found at MC 294 and corals here were projected to take 7 years (SD: 6 year; median: 4 years) on average to recover. An average of 5 years (SD: 3 years) will be necessary for corals to visibly recover at both MC 297 and MC 344, with some colonies needing up to 12 years (median: 5 years) at MC 297, and 11 years (median: 7 years) at MC 344 to visibly recover.

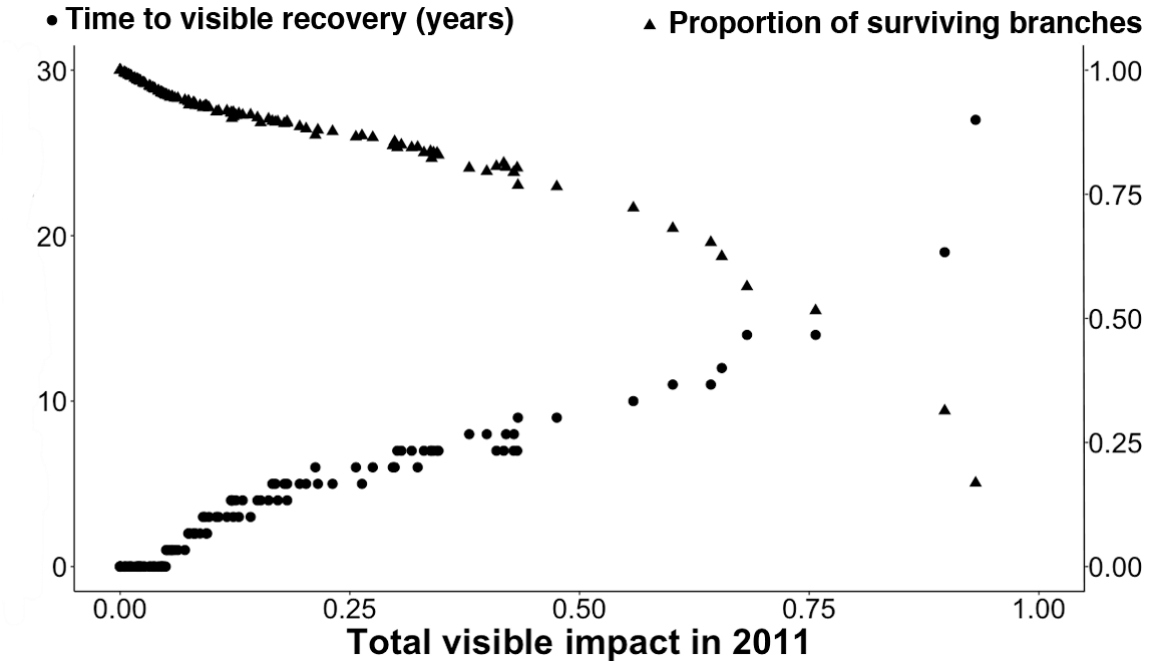

Figure 4-2. Estimated time to visible recovery and proportion of surviving branches for all corals at MC 294, MC 297 and MC 344 as a function of total visible impact (unhealthy and hydroid-colonized branches) in 2011.

The most impacted colonies were projected to lose more branches, and as a consequence, to have a lower proportion of surviving branches (Fig.4-2). For example, the most impacted coral colony included in this study was observed at MC 294 and over 90% of the colony was impacted in 2011. The model projected that this particular colony will look healthy by 2038, but, by that time, only 17% of the initial colony will remain. On average, 81% (SD: 20%; median: 89%), 88% (SD: 7%; median: 89%) and 86% (SD: 8%; median: 84%) of branches at MC 294, MC 297 and MC 344 were projected to remain after visible recovery.

Based on model simulations, we estimated that it could take up to 28 years for an impacted coral colony to recover to the point that approximately 95% of the colony is visibly

healthy, depending on its initial level of impact (Fig. 4-3a). The higher the initial proportion of unhealthy or hydroid-colonized branches, the longer it will take for a colony to recover. Moreover, for the same proportion of unhealthy and hydroid-colonized branches, the time to visible recovery was slightly longer when branches were colonized by hydroids (Fig. 4-3a).

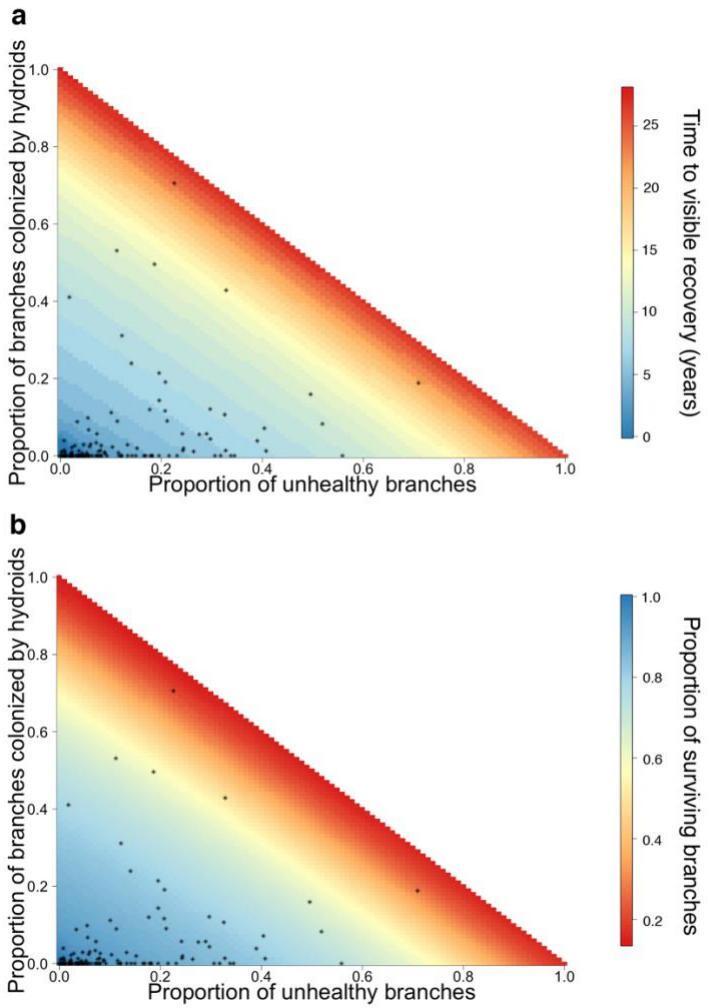

Figure 4-3. Time to visible recovery (a) and proportion of surviving branches (b) estimated by the model for different proportions of unhealthy and hydroid-colonized branches. Projections were based on simulations run for a period of 50 years. Only the proportion of branches in each of the three states varied; all other parameters were fixed as described in the Methods. The black stars represent the initial proportion values of the corals observed at all three impacted sites (MC 294, MC 297 and MC 344).

The proportion of surviving branches after a colony visibly recovered was also dependent on the initial level of total visible impact (Fig. 4-3b). It varied between 0.99 for colonies that were initially lightly impacted and 0.14 for heavily impacted colonies. This effect was also slightly more pronounced for hydroid-colonized compared to unhealthy branches.

The time to visible recovery was the most sensitive to a decrease in the probability of a healthy branch remaining healthy, with a 0.1% decrease in this probability delaying visible recovery by one year (Figure K). Similar decreases in all the other transition probabilities had no detectable effect on the time to visible recovery (the few instances where an effect appears are due to the results not being

completely smooth as they were based on numerical simulations).

After summing the total branch length of all impacted coral colonies at both sites we found a total length of 141 m at MC 294, 136 m at MC 297, and 59 m at MC 344 in 2011. By the time all coral colonies at these sites were projected to have visibly recovered (after 27 years at MC 294, 12 years at MC 297 and 11 years at MC 344), the projected total branch lengths were 121 m, 124 m and 57 m, indicating an expected 14%, 9% and 3% reduction in total biomass at MC 294, MC 297 and MC 344, respectively.

Overall, the model tended to overestimate recovery. The projected proportions of healthy branches were higher than the proportions observed in 2016 and 2017 for most corals at all impacted sites (Fig. 4-4). Conversely, the projected proportions of unhealthy and hydroid-colonized branches were significantly lower than the observed proportions in both 2016 and 2017. Branch loss projections were more reliable but still underestimated (Fig. 4-4). The same trends were observed in both 2016 and 2017, and projection accuracy was the same for MC 294 (used for parameterisation) as for MC 297 and MC 344, which were not included in model parameterisation.

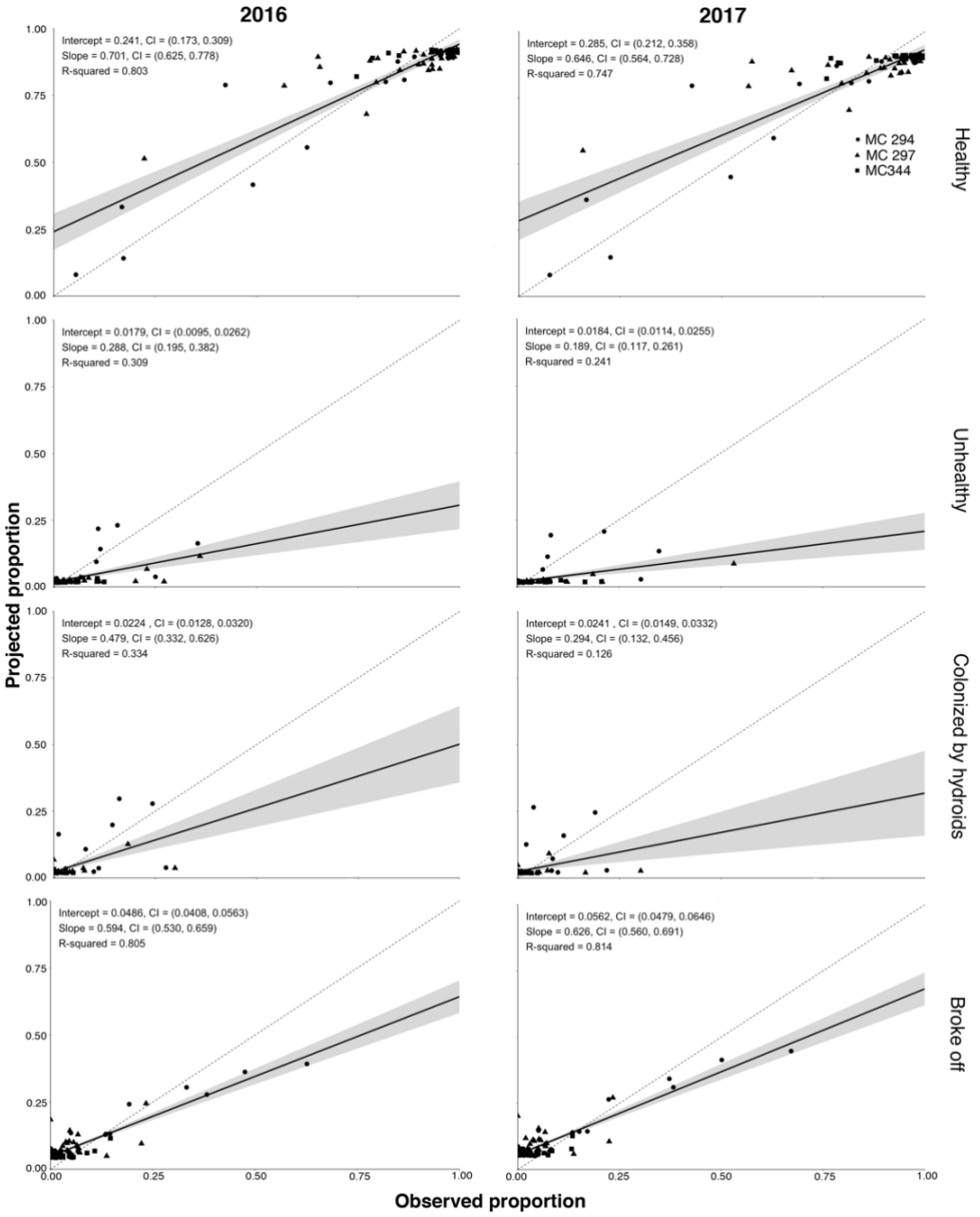

Figure 4-4. Comparison between the observed and projected proportion of branches in the three different states (healthy, unhealthy and hydroid-colonized) in 2016 and 2017 and of branches that broke between 2011 and 2016/2017. Linear regression models were fitted to the data. The slope, intercept, R-squared value and their corresponding 95% confidence intervals are indicated.

Discussion

At least 81 coral colonies were clearly impacted by the 2010 Deepwater Horizon oil spill at MC 294, MC 297 and MC 344, and our model projected that, even though most coral colonies will have visibly recovered within a decade, it will take up to ~27 years for some of these corals to visibly recover.

We estimated approximately a 3 to 14% reduction in total biomass at our field sites by the time all corals appear to have recovered. Similar trends were observed with *Paramuricea clavata* after a mass mortality event in the Mediterranean Sea where, in some places, 70% of the biomass was lost (Cerrano et al. 2005; Linares et al. 2005). Due to the slow growth rates observed for these deep-sea corals in the Gulf of Mexico (Prouty et al. 2014), it will likely take hundreds of years before these coral communities grow back to their original biomass. Moreover, in addition to growing slowly, these corals also have low recruitment rates (Linares et al. 2008; Doughty, Quattrini & Cordes 2014). As a result, the recovery of the impacted coral communities depends strongly on the ability of individual coral colonies to recover from damage. Importantly, recovery depends on the ability of coral colonies to remain healthy as suggested by the higher sensitivity of time to visible recovery to the probability of a healthy branch remaining healthy (likely due to the fact that the healthy to healthy transition probability was the largest).

Our results provide further evidence for the low resilience of deep-sea corals to disturbance, and the fragility of cold-water coral ecosystems. With new advances in technology and increase in human population, the number of threats to deep-sea ecosystems increases. A large body of literature show that fishing activities, and especially bottom trawling, are major threats to deep-water coral communities (Koslow et al. 2001; Hall-Spencer, Allain & Fosså 2002; Clark & Koslow 2008; Clark et al. 2010). Even though the impact of oil extraction and future mining activities is not as well characterized, there is a growing concern that the direct physical disturbance and sediment plumes produced by these activities may be as detrimental as trawling (Van Dover 2007; Clark et al. 2010; Cordes et al. 2016).

To limit the impacts of human activities on deep-sea coral communities, an increasing number of fisheries closures, Marine Protected Areas and Special Areas of Conservation have been designated. However, so far only a few studies have assessed the effectiveness of these

conservation measures. A follow-up study assessing recovery at the Darwin Mounds, after their closure from bottom trawling in 2003, found that protection was successful in maintaining live coral cover, but that areas that were heavily fished prior to closure showed no signs of recovery by 2011 (Huvenne et al. 2016). These results emphasize that prevention of anthropogenic impact is essential for the conservation of deep-sea ecosystems.

While branch loss estimations for both 2016 and 2017 were reliable, our model underestimated the proportion of impacted (unhealthy or hydroid-colonized) branches. It is possible that the factors we considered in this model were not sufficient to fully explain recovery. One factor that we did not include in our model, but that may have played an important role in recovery, is the size of individual lesions (damaged areas). Preliminary exploration of our dataset showed that lesion size was significantly negatively correlated with the recovery of both unhealthy and hydroid colonized branches. Moreover, the coral colonies for which the impact projections were the poorest were the corals that had the largest lesions. Similar effects of lesion size on regeneration have been observed for other coral species (Meesters, Pauchli & Bak 1997; Lirman 2000).

In this study, we parameterised our model based on visible impact, and did not take potential sub-acute effects into consideration. Crude oil has been shown to physiologically affect several fish species (Incardona et al. 2014), and toxicity experiments on different octocoral species indicated that mixtures of oil and dispersant were particularly toxic to corals (DeLeo et al. 2015; Frometa et al. 2017). In addition to direct contact with oil and/or dispersant, corals could have ingested contaminated marine snow or zooplankton, potentially affecting their viability in the longer term (Mitra et al. 2012; Passow 2014). It is thus possible that our model overestimated coral recovery because it did not include potential non-acute, long-term impact.

Finally, we modelled branch dynamics, and branches were treated as independent units. Matrix models assume that individuals are independent, and that the survival of a specific individual has no impact on the fates of other individuals (Caswell 2001). Corals are colonial, modular organisms, they are formed of replicated modules (polyps) that are capable of all physiological functions but are interconnected and genetically identical. Therefore, branches, which constitute individuals in our model, are not completely independent, and violating the assumption of independence may have affected the accuracy of our model projections. Cases where this assumption is violated generally require more complex models (Caswell 2001), but

we had insufficient data to develop such models. However, the non-independence of individuals likely had a limited effect on our model projections due to the fact that we modelled branch loss (the main source of non-independence since branch loss depended mostly on the location of breakage rather than the state of the branches that were lost) first when parameterizing the model, and thus branch loss did not directly influence the estimation of transition probabilities between the different states.

Another consequence of branches being interconnected is that a change in one part of a coral colony will be likely to affect the rest of the colony (Sánchez & Lasker 2003). For instance, the observed effect of the total initial impact to *Paramuricea biscaya* colonies on the recovery of individual branches after the Deepwater Horizon oil spill indicated that damage to one part of the colony influenced the recovery of other parts of the colony (Hsing et al. 2013). Other studies have shown that, although the presence of surrounding healthy tissue was important for the regeneration of small lesions, colony integration and energy re-allocation play an important role in recovery (Oren et al. 2001). We used an impact-dependent model to include the effect of total visible impact on the recovery of individual branches but, for a future study, this colony level integration could be better accounted for by using more sophisticated models.

Our model suggests that corals that were the most impacted by the Deepwater Horizon oil spill could take up to three decades before the remaining branches visibly recover, and that visible recovery of individual colonies is dependent on their initial level of impact. However, the bulk of the recovery is expected on timescales on the order of a decade. There was no difference in the accuracy of model projections between sites that were used (MC 294) or not (MC 297 and MC 344) to parameterise the model, suggesting that our results can be generalized to other coral communities dominated by *P. biscaya* in the northern Gulf of Mexico. We here studied corals impacted by an oil spill but our approach could be used to design monitoring projects following any type of anthropogenic impact on deep-sea octocorals. Specifically, our modelling approach can be used to evaluate the duration and frequency of a monitoring programme needed to document recovery based on different initial impact levels. In the case of the communities impacted by the Deepwater Horizon oil spill, annual monitoring for a decade following the spill, which would allow researchers to both document recovery and collect additional data to revise and improve the model, would be ideal. However, considering the high costs associated with doing research in the deep sea, we suggest continued monitoring every two years for a decade

instead; this is sufficiently frequent to characterize coral recovery (changes in coral health are slow), though it provides fewer data for the model. Subsequently, lower frequency monitoring for a further two decades would be necessary to assess non-acute effects and to follow the potential recovery of the most heavily impacted colonies.

The significant branch loss observed and estimated indicates that hundreds of years will be necessary for both individual corals and the communities to grow back to their original size, and hence for the associated deep-sea communities to fully recover. Further, the considerable loss in coral biomass at each of the impacted sites was estimated without including any of the colonies killed initially, or damaged coral colonies that were collected as part of the Natural Resource Damage Assessment Program. Overall, our results highlight the urgent need to better understand the biology of these organisms, and future modelling work could then include additional factors that might influence recovery. The low resilience of these deep-sea corals supports the need to limit impact to these extremely vulnerable ecosystems, rather than rely on restoration to bring communities back after impact. Marine Protected Areas implemented in association with photo-based monitoring would have the potential to both limit anthropogenic impact to deep-sea corals, and detect changes in the health of corals resulting from mechanical, chemical, or thermal insults.

Acknowledgments

We thank the crews of the ships and deep submergence facilities involved in this study as well as I. MacDonald for providing the digital still camera in 2011. We would also like to thank S. Vohsen, C. Du Preez, B. Fu, R. Dannenberg, J. Mentch, M. Kurmann, D. McKean, S. Berlet, S. Smith, A. Weinheimer and M. McGuigan for their assistance with data collection and analysis. Finally, we thank the members of the Shea lab, A. McKee in particular, as well as B. Teller and E. Jongejans for their input in the model analysis and help with the code. This research was made possible by a grant from the Gulf of Mexico Research Initiative. Data are publicly available through the Gulf of Mexico Research Initiative Information and Data Cooperative (GRIIDC) at https://data.gulfresearchinitiative.org (doi: <10.7266/N7NG4NJP>, <10.7266/N7HQ3WVD>, <10.7266/N7D21VJQ>, <10.7266/N78913TC>,

<10.7266/N74J0C2M> and R4.x268.186:0001). This is contribution no. 475 from the Ecosystem Impacts of Oil and Gas Inputs to the Gulf (ECOGIG) consortium.

References

Andrews, A.H., Cordes, E.E., Mahoney, M.M., Munk, K., Coale, K.H., Cailliet, G.M. & Heifetz, J. (2002) Age, growth and radiometric age validation of a deep-sea, habitat-forming gorgonian (*Primnoa resedaeformis*) from the Gulf of Alaska. Hydrobiologia, 471, 101-110.

Baillon, S., Hamel, J.-F., Wareham, V.E. & Mercier, A. (2012) Deep cold-water corals as nurseries for fish larvae. Frontiers in Ecology and the Environment, 10, 351-356.

Bates, D., Maechler, M., Bolker, B.M. & Walker, S. (2015) Fitting Linear Mixed-Effects Models Using lme4. Journal of Statistical Software, 67, 1-48.

Bavestrello, G., Cerrano, C., Zanzi, D. & Cattaneo-Vietti, R. (1997) Damage by fishing activities to the Gorgonian coral *Paramuricea clavata* in the Ligurian Sea. Aquatic Conservation: Marine and Freshwater Ecosystems, 7, 253-262.

Buhl-Mortensen, L. (2004) Symbiosis in Deep-Water Corals. *Symbiosis*, 37, 33-61.

Buhl-Mortensen, L. & Mortensen, P.B. (2004) Crustaceans associated with the deep-water gorgonian corals *Paragorgia arborea* (L., 1758) and *Primnoa resedaeformis* (Gunn., 1763). Journal of Natural History, 38, 1233-1247.

Buhl-Mortensen, L. & Mortensen, P.B. (2005) Distribution and diversity of species associated with deep-sea gorgonian corals off Atlantic Canada. Cold-Water Corals and Ecosystems (eds A. Freiwald & J.M. Roberts), pp. 849-879. Berlin.

Buhl-Mortensen, L., Vanreusel, A., Gooday, A.J., Levin, L.a., Priede, I.G., Buhl-Mortensen, P., Gheerardyn, H., King, N.J. & Raes, M. (2010) Biological structures as a source of habitat heterogeneity and biodiversity on the deep ocean margins. Marine Ecology, 31, 21-50.

Camilli, R., Reddy, C.M., Yoerger, D.R., Van Mooy, B.A.S., Jakuba, M.V., Kinsey, J.C., McIntyre, C.P., Sylva, S.P. & Maloney, J.V. (2010) Tracking Hydrocarbon Plume Transport and Biodegradation at Deepwater Horizon. *Science*, 330, 201-204.

Caswell, H. (2001) *Matrix population models: construction, analysis, and interpretation*. Sinauer Associates, Sunderland, Massachusetts.

Cathalot, C., Van Oevelen, D., Cox, T.J.S., Kutti, T., Lavaleye, M., Duineveld, G. & Meysman, F.J.R. (2015) Cold-water coral reefs and adjacent sponge grounds: Hotspots of benthic respiration and organic carbon cycling in the deep sea. Frontiers in Marine Science, 2, 37.

Cerrano, C., Arillo, a., Azzini, F., Calcinai, B., Castellano, L., Muti, C., Valisano, L., Zega, G. & Bavestrello, G. (2005) Gorgonian population recovery after a mass mortality event. Aquatic Conservation: Marine and Freshwater Ecosystems, 15, 147-157.

Clark, M.R. & Koslow, J.A. (2008) Impacts of fisheries on seamounts. Seamounts: Ecology, Fisheries & Conservation (eds T.J. Pitcher, T. Morato, P.J.B. Hart, M.R. Clark, N. Haggan & R.S. Santos), pp. 413-441. John Wiley & Sons, Oxford.

Clark, M.R., Rowden, A.A., Schlacher, T., Williams, A., Consalvey, M., Stocks, K.I., Rogers, A.D., O'Hara, T.D., White, M., Shank, T.M. & Hall-Spencer, J.M. (2010) The Ecology of Seamounts: Structure, Function, and Human Impacts. Annual review of marine science, 2, 253-278.

Cordes, E.E., Jones, D.O.B., Schlacher, T.A., Amon, D.J., Bernardino, A.F., Brooke, S., Carney, R., DeLeo, D.M., Dunlop, K.M., Escobar-Briones, E.G., Gates, A.R., Génio, L., Gobin, J., Henry, L.-A., Herrera, S., Hoyt, S., Joye, M., Kark, S., Mestre, N.C., Metaxas, A., Pfeifer, S., Sink, K., Sweetman, A.K. & Witte, U. (2016) Environmental Impacts of the Deep-Water Oil and Gas Industry: A Review to Guide Management Strategies. Frontiers in Environmental Science, 4.

DeLeo, D.M., Ruiz-Ramos, D.V., Baums, I.B. & Cordes, E.E. (2015) Response of deep-water corals to oil and chemical dispersant exposure. Deep Sea Research Part II: Topical Studies in Oceanography, 129, 137-147.

Doughty, C.L., Quattrini, A.M. & Cordes, E.E. (2014) Insights into the population dynamics of the deep-sea coral genus *Paramuricea* in the Gulf of Mexico. Deep Sea Research Part II: Topical Studies in Oceanography, 99, 71-82.

Du Preez, C. & Tunnicliffe, V. (2011) Shortspine thornyhead and rockfish (Scorpaenidae) distribution in response to substratum, biogenic structures and trawling. Marine Ecology Progress Series, 425, 217-231.

Etnoyer, P. & Warrenchuk, J. (2007) A catshark nursery in a deep gorgonian field in the Mississippi Canyon, Gulf of Mexico. Bulletin of Marine Science, 81, 553-559.

Fisher, C.R., Hsing, P.-Y., Kaiser, C.L., Yoerger, D.R., Roberts, H.H., Shedd, W.W., Cordes, E.E., Shank, T.M., Berlet, S.P., Saunders, M.G., Larcom, E.A. & Brooks, J.M. (2014) Footprint of *Deepwater Horizon* blowout impact to deep-water coral communities. Proceedings of the National Academy of Sciences, 111, 11744-11749.

Frometa, J., DeLorenzo, M.E., Pisarski, E.C. & Etnoyer, P.J. (2017) Toxicity of oil and dispersant on the deep water gorgonian octocoral *Swiftia exserta*, with implications for the effects of the Deepwater Horizon oil spill. Marine Pollution Bulletin, 122, 91-99.

Girard, F., Fu, B. & Fisher, C.R. (2016) Mutualistic symbiosis with ophiuroids limited the impact of the Deepwater Horizon oil spill on deep-sea octocorals. Marine Ecology Progress Series, 549, 89-98.

Hall-Spencer, J., Allain, V. & Fosså, J.H. (2002) Trawling damage to Northeast Atlantic ancient coral reefs. Proceedings of The Royal Society B, 269, 507-511.

Henry, L.-A. & Hart, M. (2005) Regeneration from Injury and Resource Allocation in Sponges and Corals – a Review. International Review of Hydrobiology, 90, 125-158.

Hsing, P.-Y., Fu, B., Larcom, E.a., Berlet, S.P., Shank, T.M., Govindarajan, A.F., Lukasiewicz, A.J., Dixon, P.M. & Fisher, C.R. (2013) Evidence of lasting impact of the Deepwater Horizon oil spill on a deep Gulf of Mexico coral community. Elementa: Science of the Anthropocene, 1, 000012.

Huvenne, V.A.I., Bett, B.J., Masson, D.G., Le Bas, T.P. & Wheeler, A.J. (2016) Effectiveness of a deep-sea cold-water coral Marine Protected Area, following eight years of fisheries closure. Biological Conservation, 200, 60-69.

Incardona, J.P., Gardner, L.D., Linbo, T.L., Brown, T.L., Esbaugh, A.J., Mager, E.M., Stieglitz, J.D., French, B.L., Labenia, J.S., Laetz, C.A., Tagal, M., Sloan, C.A., Elizur, A., Benetti, D.D., Grosell, M., Block, B.A. & Scholz, N.L. (2014) Deepwater Horizon crude oil impacts the developing hearts of large predatory pelagic fish. Proceedings of the National Academy of Sciences, 111, E1510-E1518.

Koslow, J.A., Gowlett-Holmes, K., Lowry, J.K., O'Hara, T., Poore, G.C.B. & Williams, A. (2001) Seamount benthic macrofauna off southern Tasmania: Community structure and impacts of trawling. Marine Ecology Progress Series, 213, 111-125.

Lasker, H.R. (1990) Clonal Propagation and Population Dynamics of a Gorgonian Coral. Ecology, 71, 1578-1589.

Linares, C., Coma, R., Diaz, D., Zabala, M., Hereu, B. & Dantart, L. (2005) Immediate and delayed effects of a mass mortality event on gorgonian population dynamics and benthic community structure in the NW Mediterranean Sea. Marine Ecology Progress Series, 305, 127-137.

Linares, C., Coma, R., Garrabou, J., Díaz, D. & Zabala, M. (2008) Size distribution, density and disturbance in two Mediterranean gorgonians: *Paramuricea clavata* and *Eunicella singularis*. Journal of Applied Ecology, 45, 688-699.

Lirman, D. (2000) Lesion regeneration in the branching coral Acropora palmata: effects of colonization, colony size, lesion size, and lesion shape. Marine Ecology Progress Series, 197, 209-215.

McNutt, M., Camilli, R., Guthrie, G., Hsieh, P., Labson, V., Lehr, B., Maclay, D., Ratzel, A. & Sogge, M.K. (2011) Assessment of Flow Rate Estimates for the Deepwater Horizon / Macondo Well Oil Spill. pp. 1-22. Washington DC, United States.

Meesters, E.H., Noordeloos, M. & Bak, R.P.M. (1994) Damage and regeneration links to coral growth in the reef-building coral *Montastrea annularis*. Marine Ecology Progress Series, 112, 119 - 128.

Meesters, E.H., Pauchli, W. & Bak, R.P.M. (1997) Predicting regeneration of physical damage on a reef-building coral by regeneration capacity and lesion shape. Marine Ecology Progress Series, 146, 91-99.

Meesters, E.H., Wesseling, I. & Bak, R.P.M. (1996) Partial Mortality in Three Species of Reef-Building Corals and the Relation with Colony Morphology. Bulletin of Marine Science, 58, 838-852.

Mitra, S., Kimmel, D.G., Snyder, J., Scalise, K., McGlaughon, B.D., Roman, M.R., Jahn, G.L., Pierson, J.J., Brandt, S.B., Montoya, J.P., Rosenbauer, R.J., Lorenson, T.D., Wong, F.L. & Campbell, P.L. (2012) Macondo-1 well oil-derived polycyclic aromatic hydrocarbons in mesozooplankton from the northern Gulf of Mexico. Geophysical Research Letters, 39, 1-7.

Oevelen, D.v., Duineveld, G., Lavaleye, M., Mienis, F., Soetaert, K. & Heip, C.H.R. (2009) The cold-water coral community as hotspot of carbon cycling on continental margins: A food-web analysis from Rockall Bank (northeast Atlantic). Limnology and Oceanography, 54, 1829-1844.

Oren, U., Benayahu, Y., Lubinevsky, H. & Loya, Y. (2001) Colony integration during regeneration in the stony coral *Favia favus* Ecology, 82, 802-813.

Passow, U. (2014) Formation of rapidly-sinking, oil-associated marine snow. Deep Sea Research Part II: Topical Studies in Oceanography, 129, 232-240.

Passow, U., Ziervogel, K., Asper, V. & Diercks, a. (2012) Marine snow formation in the aftermath of the Deepwater Horizon oil spill in the Gulf of Mexico. Environmental Research Letters, 7, 035301-035301.

Peterson, C.H., Anderson, S.S., Cherr, G.N., Ambrose, R.F., Anghera, S., Bay, S., Blum, M., Condon, R., Dean, T.A., Graham, M., Guzy, M., Hampton, S., Joye, S., Lambrinos, J., Mate, B., Meffert, D., Powers, S.P., Somasundaran, P., Spies, R.B., Taylor, C.M., Tjeerdema, R. & Adams, E.E. (2012) A Tale of Two Spills: Novel Science and Policy Implications of an Emerging New Oil Spill Model. BioScience, 62, 461-469.

Prouty, N.G., Fisher, C.R., Demopoulos, A.W.J. & Druffel, E.R.M. (2014) Growth rates and ages of deep-sea corals impacted by the Deepwater Horizon oil spill. Deep Sea Research Part II: Topical Studies in Oceanography, 129, 196-212.

R Core Team (2014) A Language and Environment for Statistical Computing. R Foundation for Statistical Computing, Vienna, Austria.

Roark, E.B., Guilderson, T.P., Dunbar, R.B., Fallon, S.J. & Mucciarone, D.a. (2009) Extreme longevity in proteinaceous deep-sea corals. Proceedings of the National Academy of Sciences, 106, 5204-5208.

Roberts, J.M., Wheeler, A.J. & Freiwald, A. (2006) Reefs of the deep: the biology and geology of cold-water coral ecosystems. Science, 312, 543-547.

Sánchez, J.A. & Lasker, H.R. (2003) Patterns of morphological integration in marine modular organisms: supra-module organization in branching octocoral colonies. Proceedings of The Royal Society B, 270, 2039-2044.

Stubben, C.J. & Milligan, B.G. (2007) Estimating and Analyzing Demographic Models Using the popbio Package in R. Journal of Statistical Software, 22, 1-23.

Van Dover, C.L. (2007) The biological environment of polymetallic sulphides deposits, the potential impact of exploration and mining on this environment, and data required to establish environmental baselines in exploration areas Proceedings of the International Seabed Authority's Workshop, pp. 169-183.

Watling, L., France, S.C., Pante, E. & Simpson, A. (2011) Biology of deep-water octocorals. Advances in Marine Biology (ed. M. Lesser), pp. 42-101.

White, H.K., Hsing, P.Y., Cho, W., Shank, T.M., Cordes, E.E., Quattrini, A.M., Nelson, R.K., Camilli, R., Demopoulos, A.W., German, C.R., Brooks, J.M., Roberts, H.H., Shedd, W., Reddy, C.M. & Fisher, C.R. (2012a) Impact of the *Deepwater Horizon* oil spill on a deep-water coral community in the Gulf of Mexico. Proceedings of the National Academy of Sciences, 109, 20303-20308.

White, H.K., Lyons, S.L., Harrison, S.J., Findley, D.M., Liu, Y. & Kujawinski, E.B. (2014) Long-Term Persistence of Dispersants following the Deepwater Horizon Oil Spill. Environmental Science & Technology Letters, 1, 295-299.

Chapter 5

Conclusion and future directions

Because long-term monitoring in the deep sea is challenging, temporal data on deep-sea ecosystems are scarce (Glover et al. 2010). Well studied ecosystems include sedimented environments such as the HAUSGARTEN observatory, west of Svalbard (Soltwedel et al. 2005), the Porcupine abyssal plain (Billett et al. 2010) and 'Station M' in the north-east Pacific (Kuhnz et al. 2014), as well as chemosynthetic ecosystems (Glover et al. 2010). Hydrothermal vents are particularly well studied as high resolution temporal data, often collected as part of underwater observatories, on individual vent edifices and sites are available (Sarrazin et al. 1997, Shank et al. 1998, Podowski 2010, Cuvelier et al. 2011, Sen et al. 2014). However, there are few temporal studies on deep-sea coral communities and they focus mostly on the scleractinian *Lophelia pertusa* (Lundälv et al. 2008, Huvenne et al. 2016). The long-term monitoring project initiated after the Deepwater Horizon oil spill provides the first repetitive high-resolution dataset on deep-water octocorals.

Based on high-definition photographs of individual coral colonies collected between 2011 and 2017, I demonstrated that the overall recovery of corals impacted by the Deepwater Horizon oil spill was slow and continues to depend on the initial level of impact to the colony. The recovery of individual branches between consecutive years depended of the initial level of total visible impact and this effect was still significant between 2016 and 2017. Visibly impacted branches were more likely to break than visibly healthy branches, and branch loss was still higher at two of the impacted sites than at the reference sites between 2016 and 2017. While the fate of the corals that were impacted by the Deepwater Horizon oil spill is still uncertain, the work described here indicates that hundreds of years may be necessary for the impacted coral communities to fully recover to their original biomass. The impact-dependent, state-structured matrix model I developed supports these conclusions. The model projects that, even though the majority of impacted coral colonies will have visibly recovered (95% of the colony is visibly healthy) within a decade, some colonies could take up to three decades to visibly recover depending on their initial level of impact. The model also projects that some of these impacted colonies will lose a large number of branches, leading to a 10% biomass loss at some of the

impacted sites by the time all colonies appear visibly healthy. All these estimates are conservative as the model tended to overestimate recovery. The uncertainties in model projection suggest that important factors influencing recovery were not taken into consideration. For example, I showed that the ophiuroid *Asteroschema clavigerum* facilitated the recovery of its coral host when present. On average, corals carrying at least one ophiuroid in 2011 were less impacted than corals that did not have any ophiuroid associates at that time. The level of impact to branches within the area influenced by ophiuroids was lower compared to that outside that area, and unhealthy or hydroid-colonized branches were more likely to recover when they were inside the area under the influence of ophiuroids. These results indicate that ophiuroids are not the only beneficiary of their association with corals, as was previously assumed. Both the host and its associate benefit; ophiuroids by using corals as a way to rise above the sea-floor to get better access to food in the water column, and corals by being "cleaned" by ophiuroids, which likely used their arms to remove particles depositing on coral branches and prevent the settlement of epibionts.

Marine organisms are important biological indicators of the presence of pollutants in the environment. In coastal environments, bivalves are generally used to detect exposure to oil or other contaminants. After the Deepwater Horizon oil spill, the need for bioindicators in the deep sea was obvious. Soft-sediment infaunal communities are sensitive to environmental changes and have been proposed as indicators of oil exposure in the deep sea. As observed near corals that were impacted by the Deepwater Horizon oil spill, a high abundance of polychaete families known to be oil tolerant and a low abundance in crustaceans such as amphipods are both characteristic of exposure to oil (Montagna et al. 2013, Fisher et al. 2014, Demopoulos et al. 2016). However, a good prior knowledge of non-impacted background infaunal communities is required. The red crab *Chaceon quinquedens* has also been proposed as sentinel to detect oil contamination (Douglas et al. 2018). Red crabs filter the surface sediment to feed, and thus are potentially exposed to newly deposited oil. They accumulate PAHs in their tissue that can be detectable for years due to the crab's slow metabolism (Douglas et al. 2018). However, crabs are mobile, making spatial correlations to the source of contamination difficult to identify, and acute (deadly) exposure is very hard to detect as carcasses do not last long in the deep sea (Jones et al. 1998). Because of their morphology and life history, octocorals, such as *Paramuricea biscaya*, are very well adapted for visual monitoring programs and impact detection. They are sessile,

filter-feeding organisms that constantly exchange metabolic gases, or potential dissolved toxicant, with the surrounding water. They are long-lived (Prouty et al. 2014), have a slow metabolism, and even when damaged or killed, the colonies remain in place for years, providing a record of impact. Healthy colonies are almost completely covered in live tissues, and small changes in their health can be easily detected with image-based monitoring (Hsing et al. 2013, Fisher et al. 2014, Chapter 2).

Transect-based visual surveys are commonly used to monitor the health of deep-water coral communities (Vad et al. 2017) or assess their recovery after impact (Huvenne et al. 2016). However, the monitoring method employed to assess the long-term impact of the Deepwater Horizon oil spill could detect changes in the health of individual coral colonies that would not have been visible with monitoring based on transects. The establishment of image-based monitoring sites throughout the northern Gulf of Mexico would not only allow the detection of future impact to the deep sea by using corals as sentinels, but would also provide baseline data on the biology of deep-sea corals. Information on the biology of most deep-sea octocoral species is still lacking. Here I demonstrate that, using time-series of high-resolution photographs of individual coral colonies, it is possible to learn more about the interaction between corals and their associates, and to parameterize models to project the recovery of impacted corals and optimize monitoring programs following impact. It is also possible to estimate growth rates with image-based monitoring by measuring the increase in branch length between years (Girard et al. in prep.). Growth rates and ages of octocorals are generally estimated with isotopic methods (Robinson et al. 2014), which have the disadvantage of requiring the collection of entire coral colonies, and are therefore much better suited to demonstrating potential longevity for a species than examining growth rates under different conditions. Although non-destructive methods have been developed for shallow-water octocorals (Brazeau & Lasker 1992, Coma et al. 1998, Lasker et al. 2003, Matsumoto 2004, Stone et al. 2017), so far only one study attempted to use a non-invasive method to measure the growth of deep-sea octocorals (Bennecke et al. 2016). The analysis of high-resolution images of individual coral colonies showed that both healthy and impacted corals grew between 2011 and 2017 (Girard et al. in prep.). Growth rates were slow (on average 2.5 cm a year for *Paramuricea* sp. B3 and between 1.2 and 0.14 cm/year for *Paramuricea biscaya*) and extremely variable both within sites (some colonies never grew) and within colonies (only a few branches, generally at the top of the colony, grew). The level of total

visible impact to coral colonies had a significant effect on coral growth. Until 2014, impacted coral colonies grew slower than visibly healthy colonies. After 2014, the growth of impacted corals was comparable to healthy corals and, in some cases, higher (Girard et al. in prep.). Based on growth rates estimated from the images, most *Paramuricea biscaya* colonies appear to be between 500 and 700 years old, which is similar to estimates based on radiocarbon decay for coral colonies collected at the same sites (Prouty et al. 2014). Some colonies could be over 2000 years old (Girard et al. in prep.).

The slow growth rates, combined with the slow recovery and high branch loss observed between 2011 and 2017, and projected by the model, highlight the need to prevent impact to deep-sea corals instead of relying on restoration after the fact. This goal can be achieved through fishery closures, Marine Protected Areas (MPA), and generally stronger environmental protection laws. However, except for a study that showed that protection from fisheries at the Darwin Mounds was successful (Huvenne et al. 2016), little evidence exists about the effectiveness of deep-sea MPAs. Implementing image-based monitoring as part of MPAs would provide a tool to evaluate the effectiveness of conservation measures. This would be particularly relevant in the northern Gulf of Mexico where corals are exposed to many environmental stressors linked to energy extraction and fishing activities. A certain number of sites in the northern Gulf of Mexico, including the two reference sites (GC 852 and AT 357) described in Chapter 2, are currently under consideration for designation as Habitat Area of Particular Concern (HAPC) with fishing regulations (NOAA 2017). These two reference sites were added to the list in part due to the monitoring work initiated after the Deepwater Horizon oil spill, demonstrating that better knowledge of the biology and life history of deep-sea corals is essential to affect policy.

Following the Deepwater Horizon oil spill, significant funding had been allocated to assess impacts from the spill throughout the Gulf of Mexico region. As knowledge on the recovery ability of different ecosystems increased, attention has been shifting toward restoration. Of the $20.8 billion B.P. settlement, $270 million has been allocated for deep-sea and coral habitat restoration. Restoration techniques have been developed for damaged coral reefs in shallow water, and are usually based on transplantation of nursery-grown corals (Rinkevich 1995, Montoya Maya et al. 2016) or of fragments (Guzmán 1991, Linares et al. 2008). However, restoration in the deep sea has never been attempted. Even though the deep-sea corals monitored

between 2011 and 2017 displayed some growth, the slow growth rates estimated suggest that coral transplantation may not be very effective at these depths and would be more appropriate in intermediate depth waters (for instance to restore mesophotic coral communities that were impacted by the spill (Silva et al. 2015)). Instead, impact prevention and monitoring of deep-sea coral communities should be prioritized.

This dissertation focused on *Paramuricea* spp. corals and aimed at assessing the long-term impact of the Deepwater Horizon oil spill on coral communities. Several coral colonies from different species have been monitored using the same method at other sites in the northern Gulf of Mexico. Individual *Callogorgia delta* colonies have been imaged annually since 2015 in BOEM lease blocks GC 234, MC 751 and MC 885, and since 2017 in GC 249. *C. delta* is the only coral species that has been observed growing in close proximity to natural hydrocarbon seeps, and its isotopic signature suggests that, at least, part of *C. delta*'s food source derives from seeps (Quattrini et al. 2013, Becker et al. in prep.). Like *P. biscaya*, *C. delta* has a planar morphology and, thus, is a good candidate for image analysis. Colonies of *C. delta* growing near to or far away from hydrocarbon seeps have been monitored annually to determine whether natural hydrocarbon seepage affects the overall health and growth of coral colonies. The analyses of images collected as part of this monitoring project will considerably increase our knowledge on the biology of this species and its potential ability to tolerate hydrocarbons.

Another monitoring project, also initiated in 2015, aimed at testing the impact of sampling on different deep-sea octocoral species. As sampling of deep-sea coral branches for research purposes (physiology, phylogenetics, and population genetics) increases, it is critical that its effects on the colonies studied are characterized. To assess the effect of sampling on coral health, every *Paramuricea* spp. and *Callogorgia delta* colonies sampled as part of various projects that our group has been involved with were imaged with a high resolution still camera before and after sampling. These colonies were then monitored annually using the methods described in this dissertation. Preliminary results indicate that the majority of colonies had healed within the first year following sampling and the colonies analyzed so far (*C. delta* especially) had started to re-grow. The complete analysis of this dataset will provide an estimate of how well coral recover after being sampled, and perhaps, of the number of branches that can be safely collected without causing irreversible damage to the colony.

In summary, it is possible to answer a wide array of scientific questions about the biology and ecology of deep-sea octocorals using image-based monitoring, a non-destructive method. Based on high-resolution images I assessed the long-term impact of the Deepwater Horizon oil spill on *Paramuricea biscaya*, developed a model to project the time to recovery, which suggests that monitoring for an additional 20 years (even if at lower frequency) may be necessary to determine the ultimate fate of impacted corals, and answered fundamental question about the biology of this octocoral species; I characterized the nature of the interaction between corals and their ophiuroid associate, and estimated growth rates. With continuing improvements in underwater imaging technologies and advances in machine learning and automated analyses, image analysis will become an even more powerful tool to study the biology of deep-sea ecosystems.

References

Becker EL, Cordes EE, Macko SA, Hovey KJ, Fisher CR (in prep.) Evidence for a nutritional tie between a deepwater coral and hydrocarbon seeps in the Gulf of Mexico.

Bennecke S, Kwasnitschka T, Metaxas A, Dullo W-C (2016) In situ growth rates of deep-water octocorals determined from 3D photogrammetric reconstructions. Coral Reefs:1-13

Billett DSM, Bett BJ, Reid WDK, Boorman B, Priede IG (2010) Long-term change in the abyssal NE Atlantic: The 'Amperima Event' revisited. Deep Sea Research Part II: Topical Studies in Oceanography 57:1406-1417

Brazeau DA, Lasker HR (1992) Growth Rates and Growth Strategy in a Clonal Marine Invertebrate, the Caribbean Octocoral Briareum asbestinum. The Biological Bulletin 183:269-277

Coma R, Ribes M, Zabala M, Gili JM (1998) Growth in a Modular Colonial Marine Invertebrate. Estuarine, Coastal and Shelf Science 47:459-470

Cuvelier D, Sarrazin J, Colaço A, Copley JT, Glover AG, Tyler PA, Santos RS, Desbruyères D (2011) Community dynamics over 14 years at the Eiffel Tower hydrothermal edifice on the Mid-Atlantic Ridge. Limnology and Oceanography 56:1624-1640

Demopoulos AWJ, Bourque JR, Cordes E, Stamler KM (2016) Impacts of the Deepwater Horizon oil spill on deep-sea coral-associated sediment communities. Marine Ecology Progress Series 561:51-68

Douglas GS, Liu B, Wong W, Litman E, Hardenstine J (2018) Red Crabs as Sentinel Organisms in Exposure of Deep-Sea Benthos to Macondo Oil Following the Deepwater Horizon Oil Spill A2 - Stout, Scott A. In: Wang Z (ed) Oil Spill Environmental Forensics Case Studies. Butterworth-Heinemann

Fisher CR, Demopoulos aWJ, Cordes EE, Baums IB, White HK, Bourque JR (2014) Coral Communities as Indicators of Ecosystem-Level Impacts of the Deepwater Horizon Spill. BioScience 64:796-807

Glover AG, Gooday AJ, Bailey DM, Billett DSM, Chevaldonné P, Colaço A, Copley J, Cuvelier D, Desbruyères D, Kalogeropoulou V, Klages M, Lampadariou N, Lejeusne C, Mestre NC, Paterson GLJ, Perez T, Ruhl H, Sarrazin J, Soltwedel T, Soto EH, Thatje S, Tselepides A, Van Gaever S, Vanreusel A (2010) Chapter One - Temporal Change in Deep-Sea Benthic Ecosystems: A Review of the Evidence From Recent Time-Series Studies. In: Lesser M (ed) Advances in Marine Biology, Book 58. Academic Press

Guzmán HM (1991) Restoration of Coral Reefs in Pacific Costa Rica. Conservation Biology 5:189-194

Hsing P-Y, Fu B, Larcom Ea, Berlet SP, Shank TM, Govindarajan AF, Lukasiewicz AJ, Dixon PM, Fisher CR (2013) Evidence of lasting impact of the Deepwater Horizon oil spill on a deep Gulf of Mexico coral community. Elementa: Science of the Anthropocene 1:000012

Huvenne VAI, Bett BJ, Masson DG, Le Bas TP, Wheeler AJ (2016) Effectiveness of a deep-sea cold-water coral Marine Protected Area, following eight years of fisheries closure. Biological Conservation 200:60-69

Jones EG, Collins MA, Bagley PM, Addison S, Priede IG (1998) The fate of cetacean carcasses in the deep sea: observations on consumption rates and succession of scavenging species in the abyssal north-east Atlantic Ocean. Proceedings of the Royal Society of London Series B: Biological Sciences 265:1119-1127

Kuhnz LA, Ruhl HA, Huffard CL, Smith KL (2014) Rapid changes and long-term cycles in the benthic megafaunal community observed over 24 years in the abyssal northeast Pacific. Progress in Oceanography 124:1-11

Lasker HR, Boller ML, Castanaro J, Sánchez JA (2003) Determinate growth and modularity in a gorgonian octocoral. The Biological bulletin 205:319-330

Linares C, Coma R, Zabala M (2008) Restoration of threatened red gorgonian populations: An experimental and modelling approach. Biological Conservation 141:427-437

Lundälv T, Fosså JH, Buhl Mortensen P, Jonsson LG, White M, Guihen D, Unnithan V (2008) Development in a trawl-damaged coral habitat (Tisler reef, NE Skagerrak) during four years of trawl protection. 4th International Symposium on Deep-Sea Corals, Wellington, New Zealand, December 2008

Matsumoto AK (2004) Heterogeneous and compensatory growth in *Melithaea flabellifera* (Octocorallia: Melithaeidae) in Japan. Hydrobiologia 530:389-397

Montagna PA, Baguley JG, Cooksey C, Hartwell I, Hyde LJ, Hyland JL, Kalke RD, Kracker LM, Reuscher M, Rhodes ACE (2013) Deep-Sea Benthic Footprint of the Deepwater Horizon Blowout. PLOS ONE 8:e70540

Montoya Maya PH, Smit KP, Burt AJ, Frias-Torres S (2016) Large-scale coral reef restoration could assist natural recovery in Seychelles, Indian Ocean. Nature Conservation 16

NOAA (2017) Draft Options for Amendment 9 to the Fishery Management Plan for the Coral and Coral Reefs of the Gulf of Mexico, U.S. Waters. Coral Habitat Areas Considered for Management in the Gulf of Mexico

Podowski EL (2010) Biotic and abiotic factors affecting distributions of megafauna in diffuse flow on andesite and basalt along the Eastern Lau Spreading Center, Tonga. Marine ecology Progress series (Halstenbek) 418:25-45

Prouty NG, Fisher CR, Demopoulos AWJ, Druffel ERM (2014) Growth rates and ages of deep-sea corals impacted by the Deepwater Horizon oil spill. Deep Sea Research Part II: Topical Studies in Oceanography 129:196-212

Quattrini AM, Georgian SE, Byrnes L, Stevens A, Falco R, Cordes EE (2013) Niche divergence by deep-sea octocorals in the genus *Callogorgia* across the continental slope of the Gulf of Mexico. Molecular Ecology 22:4123-4140

Rinkevich B (1995) Restoration Strategies for Coral Reefs Damaged by Recreational Activities: The Use of Sexual and Asexual Recruits. Restoration Ecology 3:241-251

Robinson LF, Adkins JF, Frank N, Gagnon AC, Prouty NG, Brendan Roark E, de Flierdt Tv (2014) The geochemistry of deep-sea coral skeletons: A review of vital effects and

applications for palaeoceanography. Deep Sea Research Part II: Topical Studies in Oceanography 99:184-198

Sarrazin J, Robigou V, Juniper SK, Delaney JR (1997) Biological and geological dynamics over four years on a high-temperature sulfide structure at the Juan de Fuca Ridge hydrothermal observatory. Marine Ecology Progress Series 153:5-24

Sen A, Podowski EL, Becker EL, Shearer EA, Gartman A, Yücel M, Hourdez S, Luther GW, III, Fisher CR (2014) Community succession in hydrothermal vent habitats of the Eastern Lau Spreading Center and Valu Fa Ridge, Tonga. Limnology and Oceanography 59:1510-1528

Shank TM, Fornari DJ, Von Damm KL, Lilley MD, Haymon RM, Lutz RA (1998) Temporal and spatial patterns of biological community development at nascent deep-sea hydrothermal vents (9°50′N, East Pacific Rise). Deep Sea Research Part II: Topical Studies in Oceanography 45:465-515

Silva M, Etnoyer PJ, MacDonald IR (2015) Coral injuries observed at Mesophotic Reefs after the Deepwater Horizon oil discharge. Deep Sea Research Part II: Topical Studies in Oceanography

Soltwedel T, Bauerfeind E, Bergmann M, Budaeva N, Hoste E, Jaeckisch N, von Juterzenka K, Matthiessen J, Mokievsky V, Nöthig E-M, Quéric N-V, Sablotny B, Sauter E, Schewe I, Urban-Malinga B, Wegner J, Wlodarska-Kowalczuk M, Klages M (2005) HAUSGARTEN: Multidisciplinary investigations at a deep-sea, long-term observatory in the Arctic Ocean. Oceanography 18:46-61

Stone RP, Malecha PW, Masuda MM (2017) A Five-Year, In Situ Growth Study on Shallow-Water Populations of the Gorgonian Octocoral *Calcigorgia spiculifera* in the Gulf of Alaska. PLOS ONE 12:e0169470

Vad J, Orejas C, Moreno-Navas J, Findlay HS, Roberts JM (2017) Assessing the living and dead proportions of cold-water coral colonies: implications for deep-water Marine Protected Area monitoring in a changing ocean. PeerJ 5:e3705

Appendix A

Coefficients from the GLM models testing the effect of Site on the total visible impact proportion calculated including branch loss

Table A. Coefficients from the GLM models testing the effect of Site on the total visible impact proportion calculated including branch loss (sum of unhealthy, hydroid-colonized branches and lost branches). The reference sites (AT 357 between 2011 and 2016 and GC 852 between 2016 and 2017) were used as a reference for the comparisons. The difference between the estimated mean for the reference and each of the impacted site was tested with a t test (quasibinomial distribution).

		Intercept	MC 294	MC 297	MC 344
2011	Estimate	-3.69	2.42	1.91	1.40
	Std.Error	0.437	0.510	0.514	0.955
	t-value	-8.44	4.75	3.71	1.46
	Pr(>|t|)	1.87e-14***	4.45e-06***	0.0003***	0.146
2012	Estimate	-4.39	2.67	1.88	1.82
	Std.Error	0.418	0.468	0.460	0.588
	t-value	-10.5	5.71	4.10	3.10
	Pr(>|t|)	<2e-16***	5.21e-08***	6.62e-05***	0.0023**
2013	Estimate	-4.29	2.52	1.69	1.69
	Std.Error	0.446	0.495	0.500	0.620
	t-value	-9.63	5.09	3.38	2.72
	Pr(>|t|)	<2e-16***	1.05e-06***	0.0009***	0.0072**
2014	Estimate	-4.12	2.26	1.47	1.52
	Std.Error	0.376	0.428	0.447	0.540
	t-value	-10.9	5.27	3.29	2.81
	Pr(>|t|)	<2e-16***	3.89e-07***	0.0012**	0.0055**
2015	Estimate	-3.32	1.63	0.671	1.07
	Std.Error	0.302	0.361	0.394	0.438
	t-value	-11.0	4.52	1.71	2.45
	Pr(>|t|)	<2e-16***	1.17e-05***	0.0902.	0.0153*
2016	Estimate	-2.61	0.919	0.0808	0.439
	Std.Error	0.339	0.400	0.424	0.469
	t-value	-7.70	2.30	0.191	0.937
	Pr(>|t|)	1.56e-12***	0.0230*	0.849	0.350
2017	Estimate	-4.14	2.41	1.68	2.04
	Std.Error	0.485	0.522	0.537	0.564
	t-value	-8.54	4.62	3.12	3.62

Pr(>|t|)	3.97e-15***	6.92e-06***	0.002087**	0.0004***

*p-value<0.01; **p-value<0.01; *** p-value<0.001

Appendix B

Coefficients from the GLM models testing the effect of Site on the total visible impact proportion calculated without including branch loss

Table B. Coefficients from the GLM models testing the effect of Site on the total visible impact proportion calculated without including branch loss (sum of unhealthy and hydroid-colonized branches). The reference sites (AT 357 between 2011 and 2016 and GC 852 between 2016 and 2017) were used as a reference for the comparisons. The difference between the estimated mean for the reference and each of the impacted site was tested with a t test (quasibinomial distribution).

		Intercept	MC 294	MC 297	MC 344
2011	Estimate	-3.69	2.42	1.91	1.40
	Std.Error	0.437	0.509	0.514	0.955
	t-value	-8.44	4.75	3.712	1.46
	Pr(>|t|)	1.87e-14***	4.45e-06***	0.0003***	0.146
2012	Estimate	-4.77	2.90	2.18	2.18
	Std.Error	0.498	0.545	0.536	0.648
	t-value	-9.57	5.32	4.06	3.36
	Pr(>|t|)	<2e-16***	3.33e-07***	7.55e-05***	0.0010***
2013	Estimate	-4.90	2.76	2.11	2.23
	Std.Error	0.553	0.598	0.597	0.688
	t-value	-8.85	4.62	3.54	3.24
	Pr(>|t|)	1.87e-15***	8.00e-06***	0.0005***	0.0015**
2014	Estimate	-5.06	2.72	2.16	2.28
	Std.Error	0.518	0.561	0.569	0.633
	t-value	-9.77	4.85	3.80	3.60
	Pr(>|t|)	<2e-16***	2.63e-06***	0.0002***	0.0004***
2015	Estimate	-4.78	2.54	1.78	2.37
	Std.Error	0.556	0.599	0.617	0.635
	t-value	-8.60	4.24	2.88	3.74
	Pr(>|t|)	6.04e-15***	3.77e-05***	0.0045**	0.0003***
2016	Estimate	-3.69	1.19	0.664	1.22
	Std.Error	0.496	0.560	0.570	0.594
	t-value	-7.45	2.12	1.17	2.05
	Pr(>|t|)	6.3e-12***	0.0359*	0.246	0.0418*
2017	Estimate	-4.30	1.66	1.25	1.81
	Std.Error	0.482	0.547	0.556	0.575
	t-value	-8.91	3.03	2.25	3.14

Pr(>|t|)	3.77e-16***	0.0028**	0.0256*	0.0019**

*p-value<0.01; **p-value<0.01; *** p-value<0.001

Appendix C

GLM coefficients and significance level of the effect of the initial (2011) total visible impact proportion on the proportion of branches that transitioned to a healthy state

Table C. GLM coefficients and significance level of the effect of the initial (2011) total visible impact proportion on the proportion of branches that transitioned from healthy to healthy, unhealthy to healthy and hydroid-colonized to healthy at all three impacted sites. A quasibinomial instead of a binomial error distribution was used in the GLM model when over dispersion was detected.

MC 294

		Healthy to Healthy				Unhealthy to Healthy				Hydroid-colonized to Healthy			
		Estimate	Std.Error	t-value	p-value	Estimate	Std.Error	t-value	p-value	Estimate	Std.Error	t-value	p-value
2011-2012	(Intercept)	5.02	0.454	11.0	1.92e-10***	1.57	0.282	5.58	1.96e-06***	0.575	0.746	0.771	0.455
	Impact	-4.11	0.883	-4.65	0.000124***	-3.95	0.542	-7.30	8.30e-09***	-4.03	1.19	-3.37	0.00555**
2012-2013	(Intercept)	5.02	0.443	11.3	2.11e-10***	1.26	0.504	2.50	0.024671*	0.194	0.414	0.469	0.647145
	Impact	-4.91	0.875	-5.61	1.44e-05***	-4.26	0.962	-4.43	0.000484***	-4.50	0.838	-5.37	0.000127***
2013-2014	(Intercept)	4.97	0.338	14.7	1.65e-13***	0.666	0.447	1.49	0.152804	0.139	0.608	0.228	0.824
	Impact	-2.64	0.847	-3.11	0.00477**	-3.56	0.801	-4.44	0.000279***	-2.91	0.986	-2.96	0.0131*
2014-2015	(Intercept)	5.57	0.425	13.1	3.60e-14***	1.18	0.373	3.16	0.0042**	0.0593	0.489	0.121	0.90483
	Impact	-4.58	0.864	-5.30	9.12e-06***	-3.61	0.707	-5.11	3.13e-05***	-3.10	0.873	-3.55	0.00227**
2015-2016	(Intercept)	4.79	0.173	27.7	< 2e-16***	0.663	0.545	1.22	0.237	-1.27	0.576	-2.21	0.042*
	Impact	-3.84	0.348	-11.0	< 2e-16***	-3.34	0.934	-3.58	0.00178**	-1.21	0.945	-1.28	0.220
2016-2017	(Intercept)	4.32	0.397	10.9	9.34e-12***	0.987	0.586	1.68	0.10631	-0.497	0.555	-0.896	0.384
	Impact	-0.917	1.466	-0.625	0.537	-4.11	1.06	-3.86	0.00084***	-2.44	0.984	-2.48	0.0245*

MC 297

	Healthy to Healthy	Unhealthy to Healthy	Hydroid-colonized to Healthy

		Estimate	Std.Error	t-value	p-value	Estimate	Std.Error	t-value	p-value	Estimate	Std.Error	t-value	p-value
2011-2012	(Intercept)	4.31	0.288	15.0	< 2e-16***	1.85	0.253	7.28	2.7e-09***	-0.486	0.427	-1.14	0.264
	Impact	-3.72	1.29	-2.89	0.0057**	-3.52	0.880	-4.00	0.000221**	-3.10	1.42	-2.18	0.037*
2012-2013	(Intercept)	4.65	0.261	17.8	< 2e-16***	0.425	0.248	1.71	0.0942.	-0.0503	0.516	-0.098	0.923
	Impact	-5.96	0.910	-6.55	6.47e-08***	-1.86	0.876	-2.12	0.0396*	-4.58	1.66	-2.76	0.0101*
2013-2014	(Intercept)	4.57	0.346	13.2	8.7e-16***	0.169	0.346	0.489	0.628	0.261	1.28	0.204	0.841
	Impact	-4.68	1.45	-3.23	0.00255**	-0.708	1.33	-0.532	0.598	-6.31	4.07	-1.55	0.141
2014-2015	(Intercept)	4.75	0.286	16.6	<2e-16***	0.777	0.284	2.74	0.006161**	1.02	0.669	1.53	0.141
	Impact	-4.18	1.23	-3.40	0.00172**	-3.64	1.09	-3.32	0.000887***	-9.04	2.40	-3.76	0.00123**
2015-2016	(Intercept)	4.42	0.439	10.1	7.08e-12***	0.338	0.416	0.812	0.423	0.172	0.827	0.208	0.838
	Impact	-3.98	1.93	-2.06	0.047*	-2.76	1.52	-1.82	0.0783.	-6.18	2.69	-2.30	0.0356*
2016-2017	(Intercept)	4.19	0.387	10.8	1.06e-12***	-1.10	0.545	-2.03	0.0526.	0.440	0.857	0.514	0.613
	Impact	-1.47	1.97	-0.746	0.461	-0.136	1.94	-0.0700	0.945	-7.82	2.84	-2.76	0.013*

MC 344

		Healthy to Healthy				Unhealthy to Healthy				Hydroid-colonized to Healthy			
		Estimate	Std.Error	t-value	p-value	Estimate	Std.Error	t-value	p-value	Estimate	Std.Error	t-value	p-value
2011-2012	(Intercept)	6.14	0.847	7.24	7.13e-07***	1.0074	0.499	2.02	0.0570.	-2.55	3.18	-0.802	0.481
	Impact	-9.62	3.16	-3.05	0.0066**	-9.81	2.63	-3.73	0.00132**	-0.247	6.36	-0.039	0.971
2012-2013	(Intercept)	5.62	0.327	17.2	< 2e-16***	-0.825	0.386	-2.14	0.0397*	-1.56	0.690	-2.27	0.0367*
	Impact	-9.07	1.09	-8.34	< 2e-16***	-1.98	1.20	-1.65	0.107	-2.48	2.38	-1.04	0.312
2013-2014	(Intercept)	2.89	0.613	4.72	3.2e-05***	-0.985	0.384	-2.57	0.015*	-1.32	0.620	-2.13	0.0528.
	Impact	-1.14	5.89	-0.193	0.848	-0.137	1.18	-0.116	0.908	-2.57	2.76	-0.933	0.368
2014-2015	(Intercept)	6.05	0.510	11.9	< 2e-16***	0.649	0.308	2.11	0.048004*	-1.29	0.708	-1.83	0.0977.
	Impact	-6.89	2.45	-2.82	0.00488**	-5.28	1.36	-3.89	0.000903***	-1.63	3.03	-0.537	0.603
2015-2016	(Intercept)	4.09	0.298	13.7	2.04e-13***	0.717	0.518	1.39	0.181	-1.03	0.846	-1.22	0.257
	Impact	-5.17	2.03	-2.55	0.0171*	-8.57	2.17	-3.95	0.000733***	-0.581	5.23	-0.111	0.914
2016-2017	(Intercept)	4.55	0.264	17.3	< 2e-16***	0.461	0.387	1.19	0.246	-2.75	1.38	-1.99	0.0676.
	Impact	-3.70	1.56	-2.36	0.0181*	-6.20	1.56	-3.98	0.000593***	2.16	4.75	0.455	0.657

Appendix D

Coefficients from the GLM models testing the effect of Site on total branch loss

Table D Coefficients from the GLM models testing the effect of Site on the ratio between the total number of breaking event and total cumulative number of branches. The reference sites (AT 357 between 2011 and 2016 and GC 852 between 2016 and 2017) were used as a reference for the comparisons. The difference between the estimated mean for the reference and each of the impacted site was tested with Wald's z test (binomial distribution) or t test (quasibinomial distribution).

		Intercept	MC 294	MC 297	MC 344
2011-2012	Estimate	-5.85	2.52	0.850	0.672
	Std.Error	0.504	0.554	0.649	1.26
	t-value	-11.6	4.55	1.31	0.533
	Pr(>|t|)	< 2e-16***	1.16e-05***	0.192	0.595
2012-2013	Estimate	-7.60	4.03	2.15	1.85
	Std.Error	1.44	1.46	1.52	1.83
	t-value	-5.29	2.75	1.42	1.01
	Pr(>|t|)	4.32e-07***	0.0067**	0.159	0.315
2013-2014	Estimate	-6.44	1.27	0.990	1.05
	Std.Error	0.314	0.411	0.392	0.536
	t-value	-20.6	3.09	2.53	1.96
	Pr(>|t|)	< 2e-16***	0.0023**	0.0124*	0.0517.
2014-2015	Estimate	-6.36	1.72	0.561	1.10
	Std.Error	0.481	0.561	0.649	0.738
	t-value	-13.2	3.06	0.865	1.49
	Pr(>|t|)	< 2e-16***	0.0026**	0.388	0.137
2015-2016	Estimate	-5.11	1.19	-0.0446	0.978
	Std.Error	0.396	0.445	0.507	0.488
	t-value	-12.9	2.67	-0.0880	2.00
	Pr(>|t|)	< 2e-16***	0.0085**	0.930	0.0467*
2016-2017	Estimate	-5.79	0.923	-0.134	0.979
	Std.Error	0.338	0.424	0.512	0.462
	t-value	-17.2	2.18	-0.261	2.12
	Pr(>|t|)	< 2e-16***	0.0308*	0.794	0.0352*

*p-value<0.01; **p-value<0.01; *** p-value<0.001

Appendix E

Results from the pairwise Wilcoxon Signed Rank tests for changes in total branch loss over time at all three impacted sites

Table E. Results from the pairwise Wilcoxon Signed Rank tests for changes in total branch loss (ratio of the total number of breakpoints per month and total number of branches) over time at all three impacted sites. The p-values and their significance are indicated with the number of coral colonies used for the analyses in brackets. Results were considered significant for a p-value < 0.003 after Bonferroni correction of $\alpha = 0.05$ (*).

MC 294	*2012-2013*	*2013-2014*	*2014-2015*	*2015-2016*	*2016-2017*
2011-2012	0.387 (24)	0.002* (26)	0.006 (27)	0.059 (27)	0.007 (23)
2012-2013		0.003* (24)	0.108 (22)	0.177 (21)	0.025 (18)
2013-2014			0.057 (26)	0.098(25)	0.059 (22)
2014-2015				0.098 (34)	0.938 (31)
2015-2016					0.220 (31)
MC 297	2012-2013	2013-2014	2014-2015	2015-2016	2016-2017
2011-2012	0.335 (48)	0.202 (49)	0.008 (46)	0.075 (44)	0.018 (37)
2012-2013		0.788 (58)	0.537 (56)	0.7282 (54)	0.478 (45)
2013-2014			0.417 (57)	0.502 (56)	0.687 (46)
2014-2015				0.622 (56)	0.984 (46)
2015-2016					0.828 (46)
MC 344	2012-2013	2013-2014	2014-2015	2015-2016	2016-2017
2011-2012	0.361 (23)	0.726 (23)	0.673 (21)	0.162 (21)	0.787 (28)
2012-2013		0.625 (46)	0.209 (37)	0.151 (39)	0.760 (29)
2013-2014			0.209 (38)	0.006 (37)	0.308 (29)
2014-2015				1 (50)	0.379 (42)
2015-2016					0.379 (56)

Appendix F

Coefficients from the GLM models testing the effect of Site on healthy branch loss

Table F. Coefficients from the GLM models testing the effect of Site on the ratio between the total number of breaking event in healthy parts of the colony and total cumulative number of healthy branches. The reference sites (AT 357 between 2011 and 2016 and GC 852 between 2016 and 2017) were used as a reference for the comparisons. The difference between the estimated mean for the reference and each of the impacted site was tested with Wald's z test (binomial distribution) or t test (quasibinomial distribution).

		Intercept	MC294	MC297	MC344
2011-2012	Estimate	-6.16	1.00	-0.145	-0.322
	Std.Error	0.486	0.725	0.824	1.88
	t-value	-12.7	1.38	-0.176	-0.171
	Pr(>|t|)	< 2e-16***	0.169	0.861	0.865
2012-2013	Estimate	-8.39	3.17	1.76	0.628
	Std.Error	0.707	0.742	0.764	1.22
	z-value	-11.9	4.27	2.31	0.513
	Pr(>|z|)	< 2e-16***	1.97e-05***	0.0211*	0.608
2013-2014	Estimate	-6.26	0.243	0.0527	0.445
	Std.Error	0.218	0.385	0.327	0.437
	z-value	-28.7	0.632	0.161	1.02
	Pr(>|z|)	< 2e-16***	0.527	0.872	0.308
2014-2015	Estimate	-6.59	0.561	-0.0215	0.929
	Std.Error	0.528	0.760	0.795	0.818
	t-value	-12.5	0.738	-0.0270	1.14
	Pr(>|t|)	< 2e-16***	0.462	0.978	0.258
2015-2016	Estimate	-5.09	-1.10	-1.81	-0.609
	Std.Error	0.385	0.768	0.882	0.742
	t-value	-13.2	-1.44	-2.05	-0.821
	Pr(>|t|)	< 2e-16***	0.153	0.0425*	0.413
2016-2017	Estimate	-6.46	0.267	-0.434	0.763
	Std.Error	0.278	0.421	0.469	0.410
	z-value	-23.3	0.635	-0.926	1.86
	Pr(>|z|)	< 2e-16***	0.526	0.355	0.0629.

*p-value<0.01; **p-value<0.01; *** p-value<0.001

Appendix G

Results from the pairwise Wilcoxon Signed Rank tests for changes in healthy branch loss over time at all three impacted sites

Table G. Results from the pairwise Wilcoxon Signed Rank tests for changes in healthy branch loss (ratio of the total number of breakpoints per month in visibly healthy areas and total number of visibly healthy branches) over time at all three impacted sites. The p-values and their significance are indicated with the number of coral colonies used for the analyses in brackets. Results were considered significant for a p-value < 0.003 after Bonferroni correction of $\alpha = 0.05$ (*).

MC 294	*2012-2013*	*2013-2014*	*2014-2015*	*2015-2016*	*2016-2017*
2011-2012	0.351 (22)	0.965 (25)	0.666 (26)	0.23 (24)	0.529 (23)
2012-2013		0.266 (22)	0.343 (20)	0.255 (18)	0.044 (17)
2013-2014			0.266 (25)	0.625 (23)	0.813 (22)
2014-2015				0.776 (33)	0.142 (30)
2015-2016					0.364 (31)
MC 297	2012-2013	2013-2014	2014-2015	2015-2016	2016-2017
2011-2012	0.587 (46)	1 (44)	1 (45)	0.296 (40)	0.529 (35)
2012-2013		0.636 (54)	0.887 (51)	0.338 (48)	1 (43)
2013-2014			1 (53)	0.451 (50)	0.556 (44)
2014-2015				0.284 (50)	0.556 (44)
2015-2016					0.402 (44)
MC 344	2012-2013	2013-2014	2014-2015	2015-2016	2016-2017
2011-2012	1 (23)	0.855 (22)	0.584 (18)	0.045 (21)	1 (18)
2012-2013		0.402 (43)	0.205 (31)	0.017 (30)	0.590 (29)
2013-2014			0.221 (31)	0.0084 (31)	0.554 (28)
2014-2015				0.3604 (42)	0.476 (39)
2015-2016					0.920 (54)

Appendix H

Impact and recovery of individual branches inside and outside the area influenced by ophiuroids (36 times the oral disc diameter)

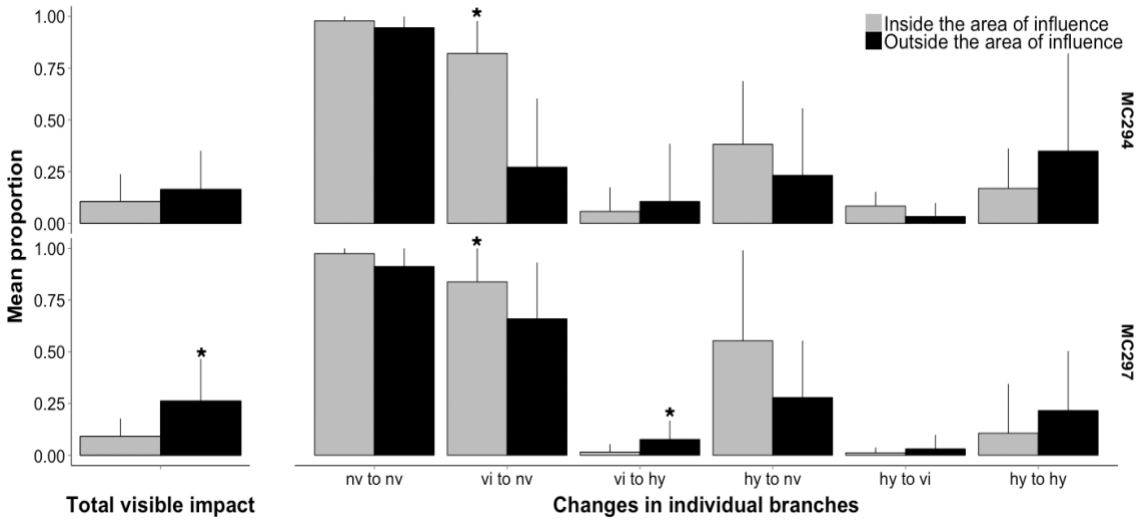

Figure H. Average level of total visible impact (MC 294: n = 9; MC 297: n = 18) and proportion of branches that changed from one category to another between 2011 and 2014 (nv: no visible impact, vi: visibly impacted, hy: hydroid colonization) inside and outside the area influenced by ophiuroids (36 times the diameter of the oral disc) at both impacted sites. The error bars represent the standard deviation. Differences were tested with the Mann-Whitney Wilcoxon test and results were considered significant for a p-value < 0.05 (*).

Appendix I

Transition probabilities and projection matrix

Table I. Transition probabilities and projection matrix U used in the model. Each column of the projection matrix sums to (1 – the probability of breaking).

Transition	Probability	Projection matrix **U**
H → B	0.0067	
H → H	0.993*P(HH)	
H → I	0.993*(1-P(HH))*0.811	
H → Hy	0.993*(1-P(HH))*0.189	
I → B	0.0989	
I → I	0.901*P(II)	
I → H	0.901*(1-P(II))*P(IH)	
I → Hy	0.901*(1-P(II))*(1-P(IH))	
Hy → B	0.122	
Hy → Hy	0.878*P(HyHy)	
Hy → H	0.878*(1-P(HyHy))*P(HyH)	
Hy → I	0.878*(1-P(HyHy))*(1-P(HyH))	

$$\begin{pmatrix} H \to H & I \to H & Hy \to H \\ H \to I & I \to I & Hy \to I \\ H \to Hy & I \to Hy & Hy \to Hy \end{pmatrix}$$

IMP: Total visible impact (unhealthy and hydroid-colonized branches); SIZE: Total branch length; H: Healthy branches, I: Unhealthy branches; Hy: Branches colonized by hydroids; B: Branches that broke

Appendix J

Comparison of the 2016 projections for models parameterised using data from different years

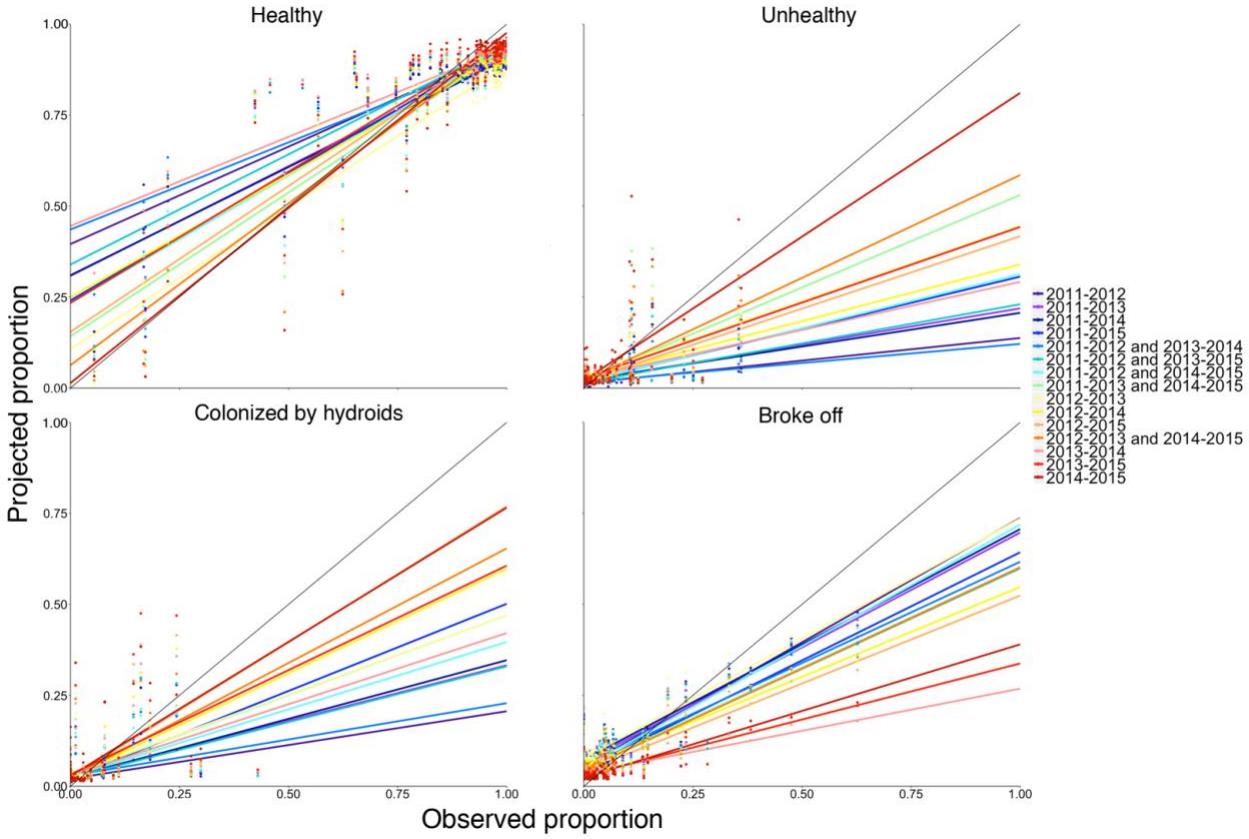

Figure J. Comparison between the observed and projected proportion of branches in the 3 different states (healthy, unhealthy and hydroid-colonized) in 2016 and of branches that broke between 2011 and 2016 for models parameterised using data from different years. Linear regression models were fitted to the data.

We tested the difference between the linear regression models corresponding to models parameterised with data from different years using analyses of covariance (ANCOVA). For each state, we tested the difference between 105 pairs of models, and defined the significance level for these tests at $\alpha = 0.05/105 = 0.0005$ after Bonferroni correction.

Healthy branches: The intercept of the linear regression models estimated from the 2012-2013 dataset was significantly different from the intercepts estimated from the 2011-2012, 2011-2014, 2011-2015, 2011-2012/2013-2014, 2011-2012/2013-2015 and 2011-2012/2014-2015 datasets. We also observed a significant difference between the 2013-2014 intercept and 2011-2013, 2011-2013/2014-2015, 2012-2013 and 2012-2014 intercepts, as well as between the 2014-2015 and 2012-2013 intercepts.

We observed significant differences between the slopes of the linear regressions estimated from the projections based on the 2011-2012/2013-2014 dataset and 2012-2013, 2011-2012/2014-2015, 2011-2013/2014-2015, 2012-2015, 2013-2015 and 2014-2015 datasets. The slope of the linear regression models estimated from the 2013-2014 dataset was significantly different from the slopes estimated from the 2014-2015, 2011-2015, 2011-2012/2014-2015, 2011-2013/2014-2015, 2012-2013, 2012-2014, 2012-2015 and 2011-2012/2014-2015 datasets. Finally, there was also a significant difference between the slopes estimated from the 2012-2013/2014-2015 dataset and 2011-2012, 2011-2013, 2011-2014 and 2011-2012/2013-2014 datasets as well as between the 2011-2012 dataset and 2012-2015 and 2014-2015 datasets.

Unhealthy branches: We only observed a significant difference between the 2011-2012 intercept and 2012-2013, 2012-2014, 2013-2014 and 2013-2015 intercepts, as well as between the 2011-2012/2013-2014, 2012-2013, 2013-2014 and 2013/2015 intercepts.

The slope estimated based on the 2011-2012 dataset was significantly different from the slopes estimated from the 2012-2015, 2012-2013/2014-2015, 2013-2015 and 2014-2015 datasets. We also detected a significance differences between the 2011-2012/2013-2015 slope and 2012-2015, 2012-2013/2014-2015, 2013-2015 and 2014-2015 slopes.

Branches colonized by hydroids: No significant differences were observed between any of the intercepts.

We observed a significant difference between the slope estimated based on the 2011-2012 dataset and the slopes estimated from the 2013-2015 and 2014-2015 dataset. There was also a significant difference between the 2011-2012/2013-2014 slope and the 2012-2015, 2013-2015 and 2014-2015 slopes.

Broken branches: The intercepts estimated based on the 2013-2014, 2013-2015 and 2014-2015 datasets were not significantly different from each other, but significantly different from the intercepts estimated from all the other models except for 2012-2015 for 2013-2015. We observed a significant difference between the 2012-2013 intercept and 2011-2015, 2011-2012/2013-2014, 2011-2012/2013-2015, 2011-2012/2014-2015 and 2011-2013/2014-2015 intercepts. There was also a significant difference between the 2011-2012 intercept and 2011-2012/2013-2015 and 2012-2015 intercepts, the 2011-2013 intercept and 2011-2015, 2011-2012/2013-2015, 2011-2013/2014-2015, 2012-2014, 2012-2015 and 2012-2013/2014-2015 intercepts, the 2011-2014 intercept and 2011-2015, 2011-2013/2014-2015, 2012-2014 and 2012-2015 intercepts and the 2012-2013 intercept and 2012-2014, 2012-2015, 2012-2013/2014-2015 intercepts.

There was a significant difference between the slopes estimated based on the 2013-2014, 2013-2015 and 2014-2015 datasets and the slopes estimated from all the other models except for 2012-2015 for 2013-2015, 2011-2012/2013-2015, 2012-2015 and 2012-2013/2014-2015 for 2014-2015.

Appendix K

Elasticity analysis

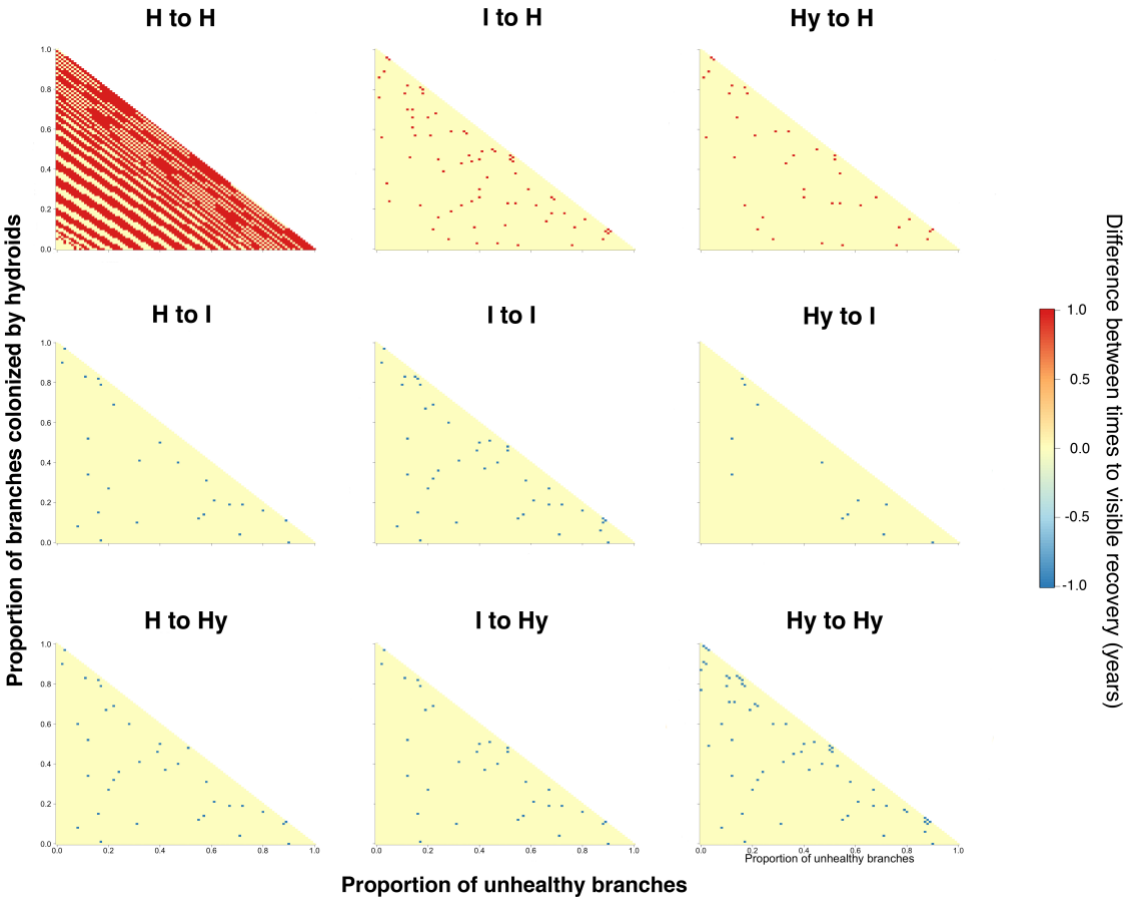

Figure K. Elasticity of time to visible recovery (years) to a 0.1% decrease in each of the transition probabilities (time to recovery value calculated when there is no change in transition probabilities subtracted from the value obtained after a 0.1% decrease). Elasticity calculations for different combinations of unhealthy and hydroid-colonized branch proportions were based on simulations run for a period of 50 years. As these results are based on numerical simulations they are not completely smooth, but in general elasticity is very low except for the H-H transition.

Appendix L

Model code

```
# Packages
library(lme4) # GLMM
library(popbio) # Used for model projection
library(fields) # Necessary for the image plots

##############################################################################

                                ##Parameterisation##

# Define the GLMM (Generalized Linear Mixed Model) function for each transition probability
# The level of total visible impact and size (total branch length) in 2011 were used as fixed
variables while the year of imaging and coral identity were added as random effects.
# nv, nh and hy are the files containing all transition and variable values between 2011 and 2015

nv <- read.table("nv_counts_size_novn_MC294_11-15.csv", header=T, sep=",")
attach(nv)

# Proportion of healthy branches that broke
# Constant 0.006682734

# If did not break
# Probability that a healthy branch remains healthy
yhh <- cbind(nv_to_nv, nv_to_nh + nv_to_hy)
modelhh<-glmer(yhh ~ Impact + (1 | Year) + (1 | Coral), family = binomial)

# If does not remain healthy
# Probability that a healthy branch becomes unhealthy vs colonized by hydroids
# Constant 0.8114035

detach(nv)

nh <- read.table("nh_counts_size_novn_MC294_11-15.csv", header=T, sep=",")
attach(nh)

# Proportion of unhealthy branches that broke
# Constant 0.09889503

# If did not break
```

```
# Probability that an unhealthy branch remains unhealthy
yii <- cbind(nh_to_nh, nh_to_nv + nh_to_hy)
modelii<-glmer(yii ~ Impact + (1 | Year) + (1 | Coral), family = binomial)

# If does not remain unhealthy
# Probability that an unhealthy branch becomes healthy vs colonized by hydroids
yih <- cbind(nh_to_nv, nh_to_hy)
modelih<-glmer(yih ~ Impact + (1 | Year) + (1 | Coral), family = binomial)

detach(nh)

hy <- read.table("hy_counts_size_novn_MC294_11-15.csv", header=T, sep=",")
attach(hy)

# Proportion of branches colonized by hydroids that broke
# constant 0.1215116

# If did not break
# Probability that a branch colonized by hydroids remains colonized by hydroids
yhyhy <- cbind(hy_to_hy, hy_to_nv + hy_to_nh)
modelhyhy<-glmer(yhyhy ~ Impact + (1 | Year) + (1 | Coral), family = binomial)

# If does not remain colonized by hydroids
# Pobability that a branch colonized by hydroids becomes healthy vs unhealthy
yhyh <- cbind(hy_to_nv, hy_to_nh)
modelhyh<-glmer(yhyh ~ Impact +Size + (1 | Year) + (1 | Coral), family = binomial)

detach(hy)

################################################################################

                                ### Simulations ###

# Create a table containing all the possible combinations of initial proportion of unhealthy and
hydroid-colonized branches
# 100 possible unhealthy and hydroid-colonized branch proportion values were considered

# Create an empty matrix to store the initial proportions data
sim<-matrix(,nrow=3, ncol=5151)

# Fix the number of branches used for all simulations
# We chose 170 branches which was the average number of branches at MC294 and MC297 and
MC 344
b<-170

#initialize
```

```
start<-0
end<-0

# Fill the matrix
for (i in 0:100){
  start<-start
  imp<-seq(0*b, (1-0.01*i)*b, length = 101-i) # Create a vector containing the number of impacted branches calculated from all possible proportion values
  hy<-rep((0.01*i)*b, 101-i) # Create a vector containing the number of colonized by hydroids branches calculated from the same proportion
  h<-b-(imp+hy) # Calculate the number of healthy branches based on the number of impacted and colonized by hydroids branches
  end<-end+length(imp)
  # Insert all three vectors in the initial conditions table
  sim[1,start:end]<-h
  sim[2,start:end]<-imp
  sim[3,start:end]<-hy
  start<-end+1
}

# Create a data frame
sim_table<-data.frame(sim)

# Make prediction for a period of 50 years
# Define the initial conditions

ini<-sim_table # Initial number of branches in each state
siz<-read.table("initial_size_simulations_100_170br.csv", header=T, sep=",") # Average total branch length in 2011 at both impacted sites

# Create empty tables that will contain the projected number of branches in each state
final_tableH <- data.frame(matrix(ncol = 5151, nrow = 51))
colnames(final_tableH) <- colnames(sim_table)
row.names(final_tableH) <-seq(0,50, by=1)

final_tableI <- data.frame(matrix(ncol = 5151, nrow = 51))
colnames(final_tableI) <- colnames(sim_table)
row.names(final_tableI) <-seq(0,50, by=1)

final_tableHy <- data.frame(matrix(ncol = 5151, nrow = 51))
colnames(final_tableHy) <- colnames(sim_table)
row.names(final_tableHy) <-seq(0,50, by=1)

# Make projections for all possible initial conditions
for (j in 1:5151){ # all possible combinations of unhealthy or colonized by hydroids branch proportions
```

```
# Set initial conditions
n <- c(ini[1:3, j])
N<-(n[2]+n[3])/(n[1]+n[2]+n[3]) # Calculate the proportion of total visible impact

# Predict the transition probabilities based on the values of the fixed factors
pred <- data.frame(Coral = colnames(ini)[j], Impact = N, Size = siz[j-1,1])

pred$prophh <- predict(modelhh,newdata=pred,type="response",re.form=NA)
pred$propii <- predict(modelii,newdata=pred,type="response",re.form=NA)
pred$propih <- predict(modelih,newdata=pred,type="response",re.form=NA)
pred$prophyhy <- predict(modelhyhy,newdata=pred,type="response",re.form=NA)
pred$prophyh <- predict(modelhyh,newdata=pred,type="response",re.form=NA)
# Probabilities of breaking
HB <- 0.006682734
IB <- 0.09889503
HyB <- 0.1215116

# Calculate all transition probabilities
HH<- (1-HB)*pred$prophh
II<- (1-IB)*pred$propii
HyHy<- (1 - HyB)*pred$prophyhy
HI<- (1-HB)*(1-HH)*0.8114035
IH<- (1-IB)*(1-II)*pred$propih
HyH<-(1-HyB)*(1-HyHy)*pred$prophyh
HHy<- (1-HB)*(1-HH)*(1-HI)
IHy<- (1-IB)*(1-II)*(1-IH)
HyI<- (1-HyB)*(1-HyHy)*(1-HyH)

# Make sure that the sum of all transition probabilities is equal to (1 - probability of breaking)
HH2 <- HH/(HH + HI + HHy + HB)
HI2 <- HI/(HH + HI + HHy + HB)
HHy2 <- HHy/(HH + HI + HHy + HB)
HH <- HH2
HI <- HI2
HHy <- HHy2

IH2 <- IH/(IH + II + IHy + IB)
II2<- II/(IH + II + IHy + IB)
IHy2 <- IHy/(IH + II + IHy + IB)
IH <- IH2
II <- II2
IHy <- IHy2

HyH2 <- HyH/(HyH + HyI + HyHy + HyB)
HyI2 <- HyI/(HyH + HyI + HyHy + HyB)
HyHy2 <- HyHy/(HyH + HyI + HyHy + HyB)
```

```
HyH <- HyH2
HyI <- HyI2
HyHy <- HyHy2

# Create the projection matrix
M<-matrix(c(HH, HI, HHy, IH, II, IHy, HyH, HyI, HyHy), nrow = 3, ncol = 3)

# Create an empty table to store the values projected at each step of the model
proj <- data.frame(matrix(ncol = 51, nrow = 3))
colnames(proj) <- seq(0,50, by=1)
row.names(proj) <-c("H","I","Hy")

# Project the number of branches in all 3 states
for (i in 1:51){ # Projections for a 50 year period
  proj[1:3,i] <- n # Add the initial counts to the projection table
  p <- pop.projection(M,n,iterations=2) # Project for the following year
  n = p$stage.vectors[1:3,2] # Extract the new count values
  N<-(n[2]+n[3])/(n[1]+n[2]+n[3]) # Calculate the new proportion of total visible impact
  # Predict the transition probabilities based on the new total visible impact proportion
  pred <- data.frame(Coral = colnames(ini)[j], Impact = N, Size = siz[j-1,1])
  pred$prophh <- predict(modelhh,newdata=pred,type="response",re.form=NA)
  pred$propii <- predict(modelii,newdata=pred,type="response",re.form=NA)
  pred$propih <- predict(modelih,newdata=pred,type="response",re.form=NA)
  pred$prophyhy <- predict(modelhyhy,newdata=pred,type="response",re.form=NA)
  pred$prophyh <- predict(modelhyh,newdata=pred,type="response",re.form=NA)
  HB <- 0.006682734
  IB <- 0.09889503
  HyB <- 0.1215116
  # Create a new projection matrix
  HH<- (1-HB)*pred$prophh
  II<- (1-IB)*pred$propii
  HyHy<- (1 - HyB)*pred$prophyhy
  HI<- (1-HB)*(1-HH)*0.8114035
  IH<- (1-IB)*(1-II)*pred$propih
  HyH<-(1-HyB)*(1-HyHy)*pred$prophyh
  HHy<- (1-HB)*(1-HH)*(1-HI)
  IHy<- (1-IB)*(1-II)*(1-IH)
  HyI<- (1-HyB)*(1-HyHy)*(1-HyH)
  # Make sure that the sum of all transition probabilities is equal to (1 - probability of breaking)
  HH2 <- HH/(HH + HI + HHy + HB)
  HI2 <- HI/(HH + HI + HHy + HB)
  HHy2 <- HHy/(HH + HI + HHy + HB)
  HH <- HH2
  HI <- HI2
  HHy <- HHy2
  IH2 <- IH/(IH + II + IHy + IB)
```

```
    II2<- II/(IH + II + IHy + IB)
    IHy2 <- IHy/(IH + II + IHy + IB)
    IH <- IH2
    II <- II2
    IHy <- IHy2
    HyH2 <- HyH/(HyH + HyI + HyHy + HyB)
    HyI2 <- HyI/(HyH + HyI + HyHy + HyB)
    HyHy2 <- HyHy/(HyH + HyI + HyHy + HyB)
    HyH <- HyH2
    HyI <- HyI2
    HyHy <- HyHy2
    # Create the projection matrix
    M<-matrix(c(HH, HI, HHy, IH, II, IHy, HyH, HyI, HyHy), nrow = 3, ncol = 3)
  }
  # Store all predicted number of branches in each state
  final_tableH[1:51,j]<-t(proj)[1:51, 1]
  final_tableI[1:51,j]<-t(proj)[1:51, 2]
  final_tableHy[1:51,j]<-t(proj)[1:51, 3]
print(j)
  }

# Time to visible recovery and proportion of surviving branches calculations
# Create an empty table that will contain the projected proportion of healthy branches
# These proportions will be calculated without taking branch loss into consideration
propH <- data.frame(matrix(ncol = 5151, nrow = 51))
colnames(propH) <- colnames(sim_table)
row.names(propH) <-seq(0,50, by=1)

# Re-name the projection tables
numbH<-final_tableH
numbI<-final_tableI
numbHy<-final_tableHy

# Calculate all proportions and include them in the table
for (i in 1:5151){
  propH[,i]<-
(as.numeric(numbH[,i])/(as.numeric(numbH[,i])+as.numeric(numbI[,i])+as.numeric(numbHy[,i]
)))
}

# Create an empty table that will contain the projected proportion of healthy branches
# This time branch loss will be included in the proportion calculations
propHvn <- data.frame(matrix(ncol = 5151, nrow = 51))
colnames(propHvn) <- colnames(sim_table)
row.names(propHvn) <-seq(0,50, by=1)
```

```
# Calculate all proportions and include them in the table
for (i in 1:5151){
  propHvn[,i]<-
(as.numeric(numbH[,i])/(as.numeric(numbH[1,i])+as.numeric(numbI[1,i])+as.numeric(numbHy[
1,i])))
}

# Calculate the time to visible recovery and proportion of surviving branches
# Create an empty table that will store all these values
sens_table <- data.frame(matrix(ncol = 5151, nrow = 2))
colnames(sens_table) <- colnames(sim_table)

# Fill the table
Hsimvn <- propHvn
for (i in 1:5151){
  Hsim <- propH
  tmax<-max(Hsimvn[,i]) # Calculate the proportion of surviving branches
  Hsim<-droplevels(Hsim[Hsim[,i]<=0.95,])
  teq<-dim(Hsim)[1] # Calculate the time to visible recovery
  # Add these values to the table
  sens_table[1,i]<-teq
  sens_table[2,i]<-tmax
  print(i)
}

sens_table_nochange<-sens_table

# Finally create two matrices
# One containing the time to visible recovery values estimated for all combinations of unhealthy
and hydroid colonized branch proportions
# The second one containing the proportion of surviving branches

# Time to visible recovery
# Create an empty matrix
Meq<-matrix(,nrow=101, ncol=101)

# Initialize
start <- 1

# Fill the matrix
sens_m<-as.matrix(sens_table_nochange)
for (i in 1:101){
  start = start
  end = start + (101-i)
  Meq[1:(102-i),i]<-as.numeric(sens_m[1,start:end])
  start = end + 1
```

```
print(i)
}

# Proportion of surviving branches
# Create an empty matrix
Mb<-matrix(,nrow=101, ncol=101)

# Initialize
start <- 1

# Fill the matrix
sens_m<-as.matrix(sens_table_nochange)
for (i in 1:101){
  start = start
  end = start + (101-i)
  Mb[1:(102-i),i]<-as.numeric(sens_m[3,start:end])
  start = end + 1
}

# Plots both matrices
# Define the x and y axes
X<-seq(0, 1, 0.01)
Y<-seq(0, 1, 0.01)

# Define a color palette
r.palette= colorRampPalette(c("#2c7bb6","#abd9e9", "#ffffbf","#fdae61","#d7191c"))(100)
r.breaks<- seq(0, 1, length = 101)

# Time to visible recovery
par(mar=c(5.5,5.5,5.5,5.5))
image.plot(X, Y, Meq, xlab="Proportion of unhealthy branches", ylab="", col=r.palette, las=1,
cex.lab=3, cex.axis=2, main="Time to visible recovery", cex.main= 4)
title(ylab="Proportion of branches colonized by hydroids", line=3.5, cex.lab=3, cex.axis=2)
# Add the initial proportion values observed for corals at both impacted sites
values <- read.table("impact_values.csv", header=T, sep=",") # Import the data frame containing
all observed proportion values
points(values$I, values$Hy, col="black", pch=8) # Add the points to the graph

# Proportion of surviving branches
par(mar=c(5.5,5.5,5.5,5.5))
image.plot(X, Y, Mb, xlab="Proportion of unhealthy branches", ylab="", col=rev(r.palette),
las=1, cex.lab=3, cex.axis=2,main="Proportion of surviving branches", cex.main=4)
title(ylab="Proportion of branches colonized by hydroids", line=3.5, cex.lab=3, cex.axis=2)
# Add the initial proportion values observed for corals at both impacted sites
values <- read.table("impact_values.csv", header=T, sep=",") # Import the data frame containing
all observed proportion values
```

```
points(values$I, values$Hy, col="black", pch=8) # Add the points to the graph

##############################################################################

### Impact projections for corals at all three impacted sites ###

# Define the initial conditions
ini<-read.table("initial_impact_counts.csv", header=T, sep=",") # Initial number of branches in each state for corals observed at MC 294, MC 297 and MC 344
siz<-read.table("initial_size.csv", header=T, sep=",") # Total size of each coral colony in 2011

# Run the code described earlier making sure that the number of repeats in the for loop corresponds to the number of corals in the initial condition table (instead of the number of possible combinations of unhealthy and hydroid colonized branch proportions)

##############################################################################

### Elasticity analysis ###

# For this analysis, run the model based on simulations described previously, but each time decrease one of the transition probabilities by 0.1%

ini<-sim_table
siz<-read.table("initial_size_simulations_100_170br.csv", header=T, sep=",")

# Example of a 0.1% change in the healthy to healthy transition probability

final_tableH <- data.frame(matrix(ncol = 5151, nrow = 51))
colnames(final_tableH) <- colnames(sim_table)
row.names(final_tableH) <-seq(0,50, by=1)

final_tableI <- data.frame(matrix(ncol = 5151, nrow = 51))
colnames(final_tableI) <- colnames(sim_table)
row.names(final_tableI) <-seq(0,50, by=1)

final_tableHy <- data.frame(matrix(ncol = 5151, nrow = 51))
colnames(final_tableHy) <- colnames(sim_table)
row.names(final_tableHy) <-seq(0,50, by=1)

for (j in 1:5151){
  # Set initial conditions
  n <- c(ini[1:3, j])
  N<-(n[2]+n[3])/(n[1]+n[2]+n[3]) # Calculate the proportion of total visible impact

  pred <- data.frame(Coral = colnames(ini)[j], Impact = N, Size = siz[j-1,1])
```

```
pred$prophh <- predict(modelhh,newdata=pred,type="response",re.form=NA)
pred$propii <- predict(modelii,newdata=pred,type="response",re.form=NA)
pred$propih <- predict(modelih,newdata=pred,type="response",re.form=NA)
pred$prophyhy <- predict(modelhyhy,newdata=pred,type="response",re.form=NA)
pred$prophyh <- predict(modelhyh,newdata=pred,type="response",re.form=NA)
HB <- 0.006682734
IB <- 0.09889503
HyB <- 0.1215116

# Transition probabilities
HH<- (1-HB)*pred$prophh - (0.001*(1-HB)*pred$prophh) # 0.1% decrease in the healthy to healthy transition probability
II<- (1-IB)*pred$propii
HyHy<- (1 - HyB)*pred$prophyhy
HI<- (1-HB)*(1-HH)*0.8114035
IH<- (1-IB)*(1-II)*pred$propih
HyH<-(1-HyB)*(1-HyHy)*pred$prophyh
HHy<- (1-HB)*(1-HH)*(1-HI)
IHy<- (1-IB)*(1-II)*(1-IH)
HyI<- (1-HyB)*(1-HyHy)*(1-HyH)

HH2 <- HH/(HH + HI + HHy + HB)
HI2 <- HI/(HH + HI + HHy + HB)
HHy2 <- HHy/(HH + HI + HHy + HB)
HH <- HH2
HI <- HI2
HHy <- HHy2

IH2 <- IH/(IH + II + IHy + IB)
II2<- II/(IH + II + IHy + IB)
IHy2 <- IHy/(IH + II + IHy + IB)
IH <- IH2
II <- II2
IHy <- IHy2

HyH2 <- HyH/(HyH + HyI + HyHy + HyB)
HyI2 <- HyI/(HyH + HyI + HyHy + HyB)
HyHy2 <- HyHy/(HyH + HyI + HyHy + HyB)
HyH <- HyH2
HyI <- HyI2
HyHy <- HyHy2

# Projection matrix
M<-matrix(c(HH, HI, HHy, IH, II, IHy, HyH, HyI, HyHy), nrow = 3, ncol = 3)

# Projection
```

```
proj <- data.frame(matrix(ncol = 51, nrow = 3))
colnames(proj) <- seq(0,50, by=1)
row.names(proj) <-c("H","I","Hy")

for (i in 1:51){
  proj[1:3,i] <- n
  p <- pop.projection(M,n,iterations=2)
  n = p$stage.vectors[1:3,2]
  N<-(n[2]+n[3])/(n[1]+n[2]+n[3])
  pred <- data.frame(Coral = colnames(ini)[j], Impact = N, Size = siz[j-1,1])
  pred$prophh <- predict(modelhh,newdata=pred,type="response",re.form=NA)
  pred$propii <- predict(modelii,newdata=pred,type="response",re.form=NA)
  pred$propih <- predict(modelih,newdata=pred,type="response",re.form=NA)
  pred$prophyhy <- predict(modelhyhy,newdata=pred,type="response",re.form=NA)
  pred$prophyh <- predict(modelhyh,newdata=pred,type="response",re.form=NA)
  HB <- 0.006682734
  IB <- 0.09889503
  HyB <- 0.1215116
  HH<- (1-HB)*pred$prophh - (0.001*(1-HB)*pred$prophh) # 0.1% decrease in the healthy to
healthy transition probability
  II<- (1-IB)*pred$propii
  HyHy<- (1 - HyB)*pred$prophyhy
  HI<- (1-HB)*(1-HH)*0.8114035
  IH<- (1-IB)*(1-II)*pred$propih
  HyH<-(1-HyB)*(1-HyHy)*pred$prophyh
  HHy<- (1-HB)*(1-HH)*(1-HI)
  IHy<- (1-IB)*(1-II)*(1-IH)
  HyI<- (1-HyB)*(1-HyHy)*(1-HyH)
  HH2 <- HH/(HH + HI + HHy + HB)
  HI2 <- HI/(HH + HI + HHy + HB)
  HHy2 <- HHy/(HH + HI + HHy + HB)
  HH <- HH2
  HI <- HI2
  HHy <- HHy2
  IH2 <- IH/(IH + II + IHy + IB)
  II2<- II/(IH + II + IHy + IB)
  IHy2 <- IHy/(IH + II + IHy + IB)
  IH <- IH2
  II <- II2
  IHy <- IHy2
  HyH2 <- HyH/(HyH + HyI + HyHy + HyB)
  HyI2 <- HyI/(HyH + HyI + HyHy + HyB)
  HyHy2 <- HyHy/(HyH + HyI + HyHy + HyB)
  HyH <- HyH2
  HyI <- HyI2
  HyHy <- HyHy2
```

```
   M<-matrix(c(HH, HI, HHy, IH, II, IHy, HyH, HyI, HyHy), nrow = 3, ncol = 3)
  }
  final_tableH[1:51,j]<-t(proj)[1:51, 1]
  final_tableI[1:51,j]<-t(proj)[1:51, 2]
  final_tableHy[1:51,j]<-t(proj)[1:51, 3]
  print(j)
}

# Run the same code for all the other transitions making sure each time to decrease the
appropriate transition probability by 0.1%

# Sensitivity of time to visible recovery to changes in transition probabilities
# Back to the 10% decrease in the healthy to healthy transition probability example
# Create an empty table that will contain the projected proportion of healthy branches when there
is a 0.1% decrease in the healthy to healthy transition probability
# These proportions will be calculated without taking branch loss into consideration
propH_HH <- data.frame(matrix(ncol = 5151, nrow = 51))
colnames(propH_HH) <- colnames(sim_table)
row.names(propH_HH) <-seq(0,50, by=1)

# Re-name the projection tables
numbH<-final_tableH_HH
numbI<-final_tableI_HH
numbHy<-final_tableHy_HH

# Calculate all proportions
for (i in 1:5151){
  propH_HH[,i]<-
(as.numeric(numbH[,i])/(as.numeric(numbH[,i])+as.numeric(numbI[,i])+as.numeric(numbHy[,i]
)))
}

# Calculate the time to visible recovery
# Create an empty table that will store all these values
sens_table_HH <- data.frame(matrix(ncol = 5151, nrow = 2))
colnames(sens_table_HH) <- colnames(sim_table)

# Fill the table
for (i in 1:5151){
  Hsim <- propH_HH
  Hsim<-droplevels(Hsim[Hsim[,i]<=0.95,])
  teq<-dim(Hsim)[1] # Calculate the time to visible recovery
  # Add these values to the table
  sens_table_HH[1,i]<-teq
  print(i)
}
```

```
# Create a table that contains the difference between the times to recovery estimated after and before decreasing the healthy to healthy transition probability by 10%
sens_table_10_HH <- sens_table_HH - sens_table_nochange

# Create a matrix
# Empty matrix
MHH<-matrix(,nrow=101, ncol=101)

# Initialize
start <- 1

# Fill the matrix
sens_m<-as.matrix(sens_table_10_HH)
for (i in 1:101){
  start = start
  end = start + (101-i)
  MHH[1:(102-i),i]<-as.numeric(sens_m[1,start:end])
  start = end + 1
  print(i)
}

# Plot the sensitivity matrix
# Define the x and y axes
X<-seq(0, 1, 0.01)
Y<-seq(0, 1, 0.01)
# Define a color palette
r.palette= colorRampPalette(c("#2c7bb6","#abd9e9", "#ffffbf","#fdae61","#d7191c"))(100)
r.breaks<- seq(0, 1, length = 101)

# Time to visible recovery sensitivity
par(mar=c(5.5,5.5,5.5,5.5))
image.plot(X, Y, MHH, xlab="Proportion of unhealthy branches", ylab="", col=r.palette, las=1, cex.lab=3, cex.axis=2, main="Time to visible recovery", cex.main= 4, zlim=c(-1,1)) # The difference in time to visible recovery was never higher than 1 or lower than -1
title(ylab="Proportion of branches colonized by hydroids", line=3.5, cex.lab=3, cex.axis=2)

# Repeat the same steps for all the other transition probabilities

##############################################################################
```

VITA

Fanny Girard

Prior Education

- **M.S** - University of Western Brittany, Brest, France
- **Bachelor (Major: Biology)** - Pierre et Marie Curie University, Paris, France

Research and Teaching Experience

- Lab instructor - Penn State (2014 and 2015)
- Master's project - Dalhousie University, Halifax, Canada (2013)
- Research assistant - MICS, Longue Pointe de Mingan, Canada (2012)
- Master's project - IFREMER, Plouzané, France (2012)
- Intern - MICS, Longue Pointe de Mingan, Canada (2011)

Presentations

- **Gulf of Mexico Oil Spill and Ecosystem Science Conference** – Invited talk (2017)
- **Ecological Restoration of Deep-sea Coral Populations workshop** – Talk (2016)
- **6th International Symposium on Deep-Sea Corals** – Plenary talk (2016)
- **Gulf of Mexico Oil Spill and Ecosystem Science Conference** – Poster (2016)
- **Deep-Sea Biology Symposium** – Poster (2015)
- **Gulf of Mexico Oil Spill and Ecosystem Science Conference** – Talk (2015)
- **Deep-C student research symposium** - Talk (2014)
- **Marine Imaging Workshop** – Poster (2014)
- **Marine Science Society** – Talk (2014)
- **ECOGIG_GoMRI site visit presentation** - Talk (2014)
- **Conference of Dalhousie Oceanography Graduate Students** - Talk (2013)

Publications

- **Fanny Girard,** Charles R. Fisher (in review). Long-term impact of the Deepwater Horizon oil spill on deep-sea corals detected after seven years of monitoring.
- Stephanie K. Archer, Amanda S. Kahn, Sally P. Leys, Tammy Norgard, **Fanny Girard**, Cherisse Du Preez, Anya Dunham (2018). Pyrosome consumption by benthic organisms during blooms in the NE Pacific and Gulf of Mexico. *Ecology, 0(0): 1-4*
- **Fanny Girard,** Katriona Shea, Charles R. Fisher (in press). Projecting the recovery of a long-lived deep-sea coral species after the Deepwater Horizon oil spill using state-structured models. *Journal of Applied Ecology*.
- **Fanny Girard**, Bo Fu, Charles R. Fisher (2016). Mutualistic symbiosis with ophiuroids limited the impact of the *Deepwater Horizon* oil spill on deep-sea octocorals. *Marine Ecology Progress Series*, 549: 89-98.
- **Fanny Girard**, Myriam Lacharité, Anna Metaxas (2016). Colonization of benthic invertebrates in a submarine canyon in the NW Atlantic. *Marine Ecology Progress Series*, 544: 53-64.